

Fall 2018

Tissue Specificity of Sex-biased Gene Expression and the Development of Sexual Dimorphism

Albert K. Chung

Follow this and additional works at: <https://digitalcommons.georgiasouthern.edu/etd>



Part of the [Bioinformatics Commons](#), and the [Other Genetics and Genomics Commons](#)

Recommended Citation

Chung, Albert K., "Tissue Specificity of Sex-biased Gene Expression and the Development of Sexual Dimorphism" (2018). *Electronic Theses and Dissertations*. 1851.
<https://digitalcommons.georgiasouthern.edu/etd/1851>

This thesis (open access) is brought to you for free and open access by the Graduate Studies, Jack N. Averitt College of at Digital Commons@Georgia Southern. It has been accepted for inclusion in Electronic Theses and Dissertations by an authorized administrator of Digital Commons@Georgia Southern. For more information, please contact digitalcommons@georgiasouthern.edu.

TISSUE SPECIFICITY OF SEX-BIASED GENE EXPRESSION AND THE DEVELOPMENT
OF SEXUAL DIMORPHISM

by

ALBERT K. CHUNG

(Under the Direction of Christian L. Cox)

ABSTRACT

One prominent form of phenotypic diversity in nature is the dramatic difference between males and females within a single species. A central genetic obstacle which must be overcome is that two distinct phenotypes must be produced from a single, shared genome. One genetic mechanism that is of particular import that would allow sexes to overcome the limitation of a shared genome is sex-specific regulation of gene expression. Although sex-biased gene expression is generally predicted to increase over ontogeny as male and female phenotypes diverge, this pattern should be most pronounced in tissues that contribute to the most extreme aspects of sexual dimorphism. However, few studies have simultaneously examined multiple tissues throughout development to quantify sex-biased gene expression, which is crucial as sexual dimorphism occurs as a complex developmental process and sex-biased gene expression changes over time and differs among various tissues. We used the brown anole (*Anolis sagrei*), a lizard that exhibits extreme sexual size dimorphism, to examine sex-, age-, and tissue-specificity of gene expression. Using high-throughput RNA-Seq, we analyzed liver, muscle, and brain transcriptomes at one, four, eight, and twelve months of age. We predicted that (1) sex-biased gene expression would increase during ontogeny as phenotypes diverge between the sexes, (2) ontogenetic increases in sex-biased expression would differ among tissues because of different

contributions to sexual dimorphism, and (3) growth-regulatory gene networks would be more sex-biased in liver and muscle than the brain as key contributors to extreme size dimorphism. We also predicted that sex-biased expression of upstream components of growth regulatory (e.g., hormones) networks in the liver would be higher compared to the muscle where there would be higher sex-biased expression of downstream components (e.g., hormone receptors and downstream effectors) in muscle. We determined that sex-biased gene expression increased during development, but that the trajectory of sex-biased expression varied between tissues. The liver had the greatest number of sex-biased growth genes, but the muscle had the greatest divergence of growth gene expression. We also found that while sex-biased expression of growth genes increased sharply during development in the liver and muscle, the brain showed no sex-bias in any growth gene at any point. Our results confirm that sex-biased gene expression increases throughout ontogeny, but also demonstrate tissue-specific trajectories. Our results also suggest that different components of growth-regulatory networks are activated in different tissues. More broadly, our work implies that sex-biased gene expression across the whole transcriptome and within specific regulatory pathways produces sexually dimorphic phenotypes.

INDEX WORDS: Sexual dimorphism, Ontogeny, *Anolis*, Differential gene expression, RNA-Seq, Transcriptomics

TISSUE SPECIFICITY OF SEX-BIASED GENE EXPRESSION AND THE DEVELOPMENT
OF SEXUAL DIMORPHISM

by

ALBERT K. CHUNG

B.S., University of Virginia, 2013

A Thesis Submitted to the Graduate Faculty of Georgia Southern University
in Partial Fulfillment of the Requirements for the Degree

MASTER OF SCIENCE

STATESBORO, GEORGIA

© 2018

ALBERT K. CHUNG

All Rights Reserved

TISSUE SPECIFICITY OF SEX-BIASED GENE EXPRESSION AND THE DEVELOPMENT
OF SEXUAL DIMORPHISM

by

ALBERT K. CHUNG

Major Professor: Christian L. Cox
Committee: Christine N. Bedore
John J. Schenk

Electronic Version Approved:
December 2018

TABLE OF CONTENTS

	Page
LIST OF TABLES	3
LIST OF FIGURES	5
GENERAL INTRODUCTION.....	7
REFERENCES	13
CHAPTER 1	18
ABSTRACT.....	18
INTRODUCTION	18
MATERIALS AND METHODS.....	21
RESULTS	26
DISCUSSION.....	30
REFERENCES	35
CHAPTER 2	51
ABSTRACT.....	51
INTRODUCTION	51
MATERIALS AND METHODS.....	57
RESULTS	59
DISCUSSION.....	64
REFERENCES	70

LIST OF TABLES

	Page
Table 1.1: The number of sex-biased genes per sex at one, four, eight, and twelve months of age in liver, femoral muscle, and brain	39
Table 1.2: Pairwise comparisons of overlap of genes exhibiting sex-biased expression between tissues at one, four, eight, and twelve months of age	40
Table 1.3: Pairwise comparisons of overlap of genes exhibiting sex-biased expression between ages within the liver, femoral muscle, and brain	41
Table 1.4: The results of a general linear model testing for sex, age, and tissue effects on expression levels of all genes exhibiting sex-biased expression	42
Table 2.1: A list of all 114 a priori growth genes found in the growth hormone/insulin-like growth factor (GH/IGF), insulin-signaling, and mechanistic target of rapamycin (mTOR) networks	78
Table 2.2: A priori growth genes in the growth hormone/insulin-like factor 1 pathway	83
Table 2.3: A priori growth genes in the insulin-signaling pathway.....	84
Table 2.4: A priori growth genes in mechanistic target of rapamycin pathway	88
Table 2.5: A priori growth genes that exhibit sex-biased expression in the liver at one, four, eight, and twelve months of age	90
Table 2.6 A priori growth genes that exhibit sex-biased expression in femoral muscle at ages one, four, eight, and twelve months	92
Table 2.7: The results of general linear models testing for sex, age, and tissue effects on mean expression level of the growth hormone/insulin-like growth factor (GH/IGF), insulin, and	

mechanistic target of rapamycin (mTOR) growth networks within liver, femoral muscle,
and brain of brown anoles.....93

Table 2.8: The results of general linear models testing for sex and age effects on mean
expression level of target growth genes within liver, femoral muscle, and brain of brown
anoles94

LIST OF FIGURES

	Page
Figure 1.1: As the sexes age, they increasingly diverge in size in both length and body mass.....	43
Figure 1.2: The number of genes that exhibit sex-biased expression increases for both sexes and diverges between sexes within the liver, muscle, and brain across ontogeny	44
Figure 1.3: The sexes show similar mean expression of all genes to each other within tissues and across ontogeny.....	45
Figure 1.4: The sexes diverge in their expression levels of genes that exhibit sex-biased expression both between tissues and across ontogeny.....	46
Figure 1.5: Genes that exhibit sex-biased expression in one tissue exhibit the same direction of sex-bias in other tissues	47
Figure 1.6: Genes that exhibit sex-biased expression at one age exhibit the same direction of sex-bias in adjacent ages within each tissue	49
Figure 2.1: A flow chart of the growth hormone/insulin-like factor, insulin signaling, and mechanistic target of rapamycin growth regulatory signaling pathways interact to direct growth in vertebrates, specifically in the liver.....	98
Figure 2.2: Male and female brown anoles increase and diverge in number of growth genes that exhibit sex-biased expression in the (A) liver and (B) femoral muscle across ontogeny.....	99
Figure 2.3: Male and female brown anoles express growth genes at similar levels across ontogeny within tissues.....	100
Figure 2.4: Male and female brown anoles diverge in growth gene sex-biased gene expression in the liver and muscle across ontogeny	101

Figure 2.5: Expression of growth hormone receptor (GHR) increases in the liver and muscle for both male and female brown anoles across ontogeny.....	102
Figure 2.6: Male and female brown anoles diverge in expression of insulin-like growth factor 1 (IGF1) and insulin-like growth factor 2 (IGF2) in the liver across ontogeny	103
Figure 2.7: Male and female brown anole expression of the insulin growth factor binding proteins varies across tissues and ontogeny.....	104
Figure 2.8: Male and female brown anoles diverge in their expression of the insulin-like growth factor 1 receptor across tissues and ontogeny.....	106
Figure 2.9: Male and female brown anoles diverge in their expression of insulin receptor substrate 1 (IRS1) and insulin receptor substrate 4 (IRS4) across tissues and ontogeny.....	107
Figure 2.10: Male and female brown anoles express the mechanistic target of rapamycin (mTOR) at similar levels across tissues and ontogeny.....	108
Figure 2.11: Male and female brown anoles have similar levels of expression of all growth genes in the growth hormone/insulin-like growth factor 1 signaling network within tissues across ontogeny.....	109
Figure 2.12: Male and female brown anoles have similar levels of expression of growth genes in the insulin-signaling network across tissues and ontogeny	110
Figure 2.13: Male and female brown anoles have similar levels of expression of growth genes in the mechanistic target of rapamycin network across tissues and ontogeny.....	111

GENERAL INTRODUCTION

Sexual Dimorphism

Sexual dimorphism, which is the physiological or behavioral differences between the sexes of one species, is one of the most conspicuous sources of phenotypic diversity in nature. From the brightly colored plumage of the peacock to paternal care of offspring in stickleback fish, sexual dimorphism is ubiquitous among animals and has long been studied by evolutionary biologists who seek to understand its evolution (Darwin 1888). There are three main hypotheses that explain the evolution of sexual dimorphism (Hedrick & Temeles 1989): ecological divergence between the sexes (Selander 1966; Shine 1989), natural selection (Darwin 1888), and sexual selection (Darwin 1888).

Ecological hypotheses regarding the evolution of sexual dimorphism posit that ecological factors drive the evolution of sexual dimorphism (Selander 1966; Shine 1989). Under an ecological causation model (Shine 1989), male and female competition (i.e., intersexual competition) for ecological resources (e.g., prey items) leads to disruptive selection (i.e., sexual dimorphism) and evolution of phenotypic characters such that the sexes occupy separate ecological niches (i.e., ecological niche partitioning). Ecological niche partitioning between the sexes has been observed across several lineages of snakes (Mushinsky, Hebrard & Vodopich 1982; Shine 1991b; Shine 1991a; Houston & Shine 1993; Shetty & Shine 2002; Shine *et al.* 2002) where species have developed sexual size dimorphism and consume different sized prey items.

Natural selection is thought to drive the evolution of sexual dimorphism by acting differently on the sexes based on their differing reproductive roles (Darwin 1888) (i.e., fecundity advantage hypothesis). In sexually dimorphic species, natural selection is thought to act mainly

on females by selecting for larger body sizes. Under the fecundity advantage hypothesis, females with larger body sizes are more capable of allocating energy to reproduction, producing more and/or higher quality offspring, and are better able to provide resources to their offspring compared to females with smaller bodies. Larger female body size, therefore, provides a reproductive advantage and is selected for, driving the evolution of larger females and causing sexual size dimorphism. The fecundity advantage hypothesis has been used to explain the occurrence of female-biased sexual size dimorphism across a range of taxa including invertebrates (Bateman 1948; Head 1995), amphibians (Shine 1979), reptiles (Berry & Shine 1980), birds (Summers & Underhill 1991; Sandercock 1998), and mammals (Ralls 1976).

Sexual selection promotes differential mating success, which can drive phenotypic divergence between the sexes (Darwin 1888). Sexual selection acts through two separate processes: intrasexual selection (e.g., male-male competition) and intersexual selection (e.g., female choice). Intrasexual selection occurs when differential mating success is determined by individuals of one sex competing with each other to mate with the other sex. This competition causes selection to act on the competing sex, often favoring the evolution of larger male body size and other traits that may confer an advantage when competing for mates (Darwin 1888; Andersson 1994). Thus, intrasexual selection drives phenotypic divergence between the sexes through selective pressures imposed by a sex on itself.

Intersexual selection, which commonly occurs as female choice although it may also occur as male choice, occurs when differential mating success is determined by the choice of females to mate with males that possess attractive phenotypic traits (Darwin 1888; Kirkpatrick 1982; Andersson 1994; Fisher 1999). Female choice is able to drive sexual dimorphism as only

males with attractive traits will reproduce and these attractive traits are able to rapidly increase in frequency across generations causing male phenotypes to diverge from female phenotypes.

Sexual Dimorphism and Differential Gene Expression

A central paradox of the development of sexual dimorphism is that a species must produce two distinct phenotypes from a single, shared genome (Lande 1980). Many sexually dimorphic species possess sex chromosomes, non-autosomal chromosomes that contain genes which determine sex and make it possible for one sex to possess genes that the other does not (Rice 1984; Mank 2009). However, the number of genes limited to sex chromosomes relative to genes on autosomal chromosomes is quite small and there are sexually dimorphic species that do not possess sex chromosomes at all (Bachtrog *et al.* 2014). This implies that the majority of sexually dimorphic traits result from shared genes. Male and female differential expression of shared genes, sex-biased gene expression, is one genetic mechanism that may allow sexual dimorphism to develop from a shared genome (Ellegren & Parsch 2007; Mank 2009; Williams & Carroll 2009; Mank *et al.* 2010; Grath & Parsch 2016; Mank 2017).

Study System

Brown anoles (*Anolis sagrei*) are small lizards that are native to Cuba and The Bahamas and exhibit male-biased extreme sexual size dimorphism with males attaining more than double the body mass of females (Cox & Calsbeek 2010; Reedy *et al.* 2016). Brown anoles typically live for just one year and exhibit a territorial social structure with both sexes engaging in non-monogamous mating (Schoener & Schoener 1980; Calsbeek *et al.* 2007). Anole species often fall into specific ecological niches referred to as ecomorphs, an ecomorph being, “species with the same structural habitat/niche, similar in morphology and behavior, but not necessarily close phylogenetically” (Williams 1972). Brown anoles belong to the trunk-ground *Anolis* ecomorph

(Losos 2011) and are often found on broad surfaces (e.g., tree trunks, walls) within two meters of the ground. Males and females experience different selective pressures which likely drive the evolution of sexual size dimorphism in this species.

In *Anolis* species, patterns of sexual size dimorphism are strongly tied to ecomorph class (Butler, Schoener & Losos 2000). The brown anole belongs to the trunk-ground ecomorph, which exhibits male-biased sexual size dimorphism, providing support for ecological forces driving the evolution of sexual size dimorphism in brown anoles. Body size is a critical factor that affects male combat outcomes in brown anoles (Tokarz 1985) and is likely subject to sexual selection as larger males are able to occupy higher quality territories (Schoener & Schoener 1980) although the lack of a strict territorial polygynous social structure (Kamath & Losos 2017) may undercut the strength of sexual selection in brown anoles. Support for the fecundity advantage hypothesis is only weakly supported among reptiles (Cox, Butler & John-Alder 2007), although increases in clutch size are generally associated with increases in female-biased sexual size dimorphism in lizards (Cox, Skelly & John-Alder 2003), thus natural selection for larger female body size might be a relatively weak driving force of sexual size dimorphism in brown anoles. We sought to understand how differential gene expression between the sexes within several tissues and across ontogeny facilitates the development of sexual dimorphism in an organism that is subject to these evolutionary pressures.

Previous work on sex-biased gene expression, which is expression of a gene that is exclusive to or at a higher level for one sex, has shown that large proportions of expressed genes exhibit sex-biased expression, in both adult gonadal and whole organism tissue preparations (Zhang *et al.* 2007; Mank *et al.* 2010), and have linked the magnitude of sex-bias in gene expression to the magnitude of sexual dimorphism (Pointer *et al.* 2013; Harrison *et al.* 2015). We

also know that sex-biased gene expression patterns change over ontogeny (Perry, Harrison & Mank 2014) and exhibit tissue-specificity (Yang *et al.* 2006). However, few, if any, studies have integrated these approaches to examine how sex-biased gene expression patterns of several tissues across ontogeny are linked to the development of sexual dimorphism.

Experimental Design

We sought to examine the relationship between the amount of sex-biased expression, in both number of sex-biased genes and the degree to which a gene's expression is biased towards one sex, and phenotypic dimorphism across tissues and over time. We collected liver, femoral muscle, and brain tissue from male and female brown anoles at ages one month, four months, eight months, and twelve months to examine age-, sex-, and tissue-specificity of sex-biased gene expression in the brown anole across ontogeny. We hypothesize that as phenotypic divergence increases between male and female brown anoles, sex-biased gene expression should as well as a general pattern across ontogeny to facilitate the development of sexual dimorphism from a single genome. Furthermore, we hypothesize that tissues should exhibit different patterns of sex-biased gene expression, both over time and from other tissues, as they contribute different amounts to sexual dimorphism at different developmental stages with tissues that contribute more to expression of phenotypic differences having higher levels of sex-biased gene expression. In addition, we hypothesize that signaling pathways that control the development of growth, and therefore sexual size dimorphism, exhibit sex-biased expression as well, specifically downstream elements that are the effectors of phenotypic divergence. In particular, we examined the expression of the growth hormone/insulin-like growth factor, insulin signaling, and mechanistic target of rapamycin growth regulatory gene networks. We utilized our experimental design, that sampled multiple tissues over an ontogenetic time-series from male and female brown anoles, to

perform differential gene expression analysis to test our hypotheses and answer these questions:

(1) Does sex-biased gene expression increase during ontogeny as phenotypes diverge between the sexes? (2) Do ontogenetic increases in sex-biased expression differ among tissues that differ in function and therefore contribute different amounts to sexual dimorphism? (3) Are growth-regulatory gene networks more sex-biased in liver and muscle than the brain as they are key contributors to extreme size dimorphism in brown anoles.

REFERENCES

- Andersson, M.B. (1994) *Sexual selection*. Princeton University Press, Princeton, New Jersey.
- Bachtrog, D., Mank, J.E., Peichel, C.L., Kirkpatrick, M., Otto, S.P., Ashman, T.-L., Hahn, M.W., Kitano, J., Mayrose, I., Ming, R., Perrin, N., Ross, L., Valenzuela, N. & Vamosi, J.C. (2014) Sex Determination: Why So Many Ways of Doing It? *PLoS biology*, **12**, e1001899.
- Bateman, A.J. (1948) Intra-sexual selection in *Drosophila*. *Heredity*, **2**, 349-368.
- Berry, J.F. & Shine, R. (1980) Sexual size dimorphism and sexual selection in turtles (Order Testudines). *Oecologia*, **44**, 185-191.
- Butler, M.A., Schoener, T.W. & Losos, J.B. (2000) The relationship between sexual size dimorphism and habitat use in Greater Antillean *Anolis* lizards. *Evolution*, **54**, 259-272.
- Calsbeek, R., Bonneaud, C., Prabhu, S., Manoukis, N. & Smith, T.B. (2007) Multiple paternity and sperm storage lead to increased genetic diversity in *Anolis* lizards. *Evolutionary Ecology Research*, **9**, 495-503.
- Cox, R.M., Butler, M.A. & John-Alder, H.B. (2007) The evolution of sexual size dimorphism in reptiles. *Sex, Size and Gender Roles: Evolutionary Studies of Sexual Size Dimorphism* (eds D.J. Fairbairn, T. Szekely & W.U. Blanckenhorn). Oxford University Press, Oxford, United Kingdom.
- Cox, R.M. & Calsbeek, R. (2010) SEX-SPECIFIC SELECTION AND INTRASPECIFIC VARIATION IN SEXUAL SIZE DIMORPHISM. *Evolution*, **64**, 798-809.
- Cox, R.M., Skelly, S.L. & John-Alder, H.B.J.E. (2003) A comparative test of adaptive hypotheses for sexual size dimorphism in lizards. **57**, 1653-1669.
- Darwin, C. (1888) *The descent of man and selection in relation to sex*. Murray.

- Ellegren, H. & Parsch, J. (2007) The evolution of sex-biased genes and sex-biased gene expression. *Nature Reviews Genetics*, **8**, 689-698.
- Fisher, R.A. (1999) *The genetical theory of natural selection: a complete variorum edition*. Oxford University Press, Oxford, United Kingdom.
- Grath, S. & Parsch, J. (2016) Sex-biased gene expression. *Annual Review of Genetics*, **50**, 29-44.
- Harrison, P.W., Wright, A.E., Zimmer, F., Dean, R., Montgomery, S.H., Pointer, M.A. & Mank, J.E. (2015) Sexual selection drives evolution and rapid turnover of male gene expression. *Proceedings of the National Academy of Sciences*, 201501339.
- Head, G. (1995) Selection on fecundity and variation in the degree of sexual size dimorphism among spider species (class Araneae). *Evolution*, **49**, 776-781.
- Hedrick, A.V. & Temeles, E.J. (1989) The Evolution of Sexual Dimorphism in Animals: Hypotheses and Tests. *Trends in Ecology & Evolution*, **4**, 136-138.
- Houston, D. & Shine, R. (1993) Sexual Dimorphism and Niche Divergence: Feeding Habits of the Arafura Filesnake. *Journal of Animal Ecology*, 737-748.
- Kamath, A. & Losos, J. (2017) The erratic and contingent progression of research on territoriality: a case study. *Behavioral Ecology and Sociobiology*, **71**, 89.
- Kirkpatrick, M. (1982) Sexual selection and the evolution of female choice. *Evolution*, **36**, 1-12.
- Lande, R. (1980) Sexual dimorphism, sexual selection, and adaptation in polygenic characters. *Evolution*, 292-305.
- Losos, J.B. (2011) *Lizards in an evolutionary tree: ecology and adaptive radiation of anoles*. University of California Press, Berkeley, California.
- Mank, J.E. (2009) Sex chromosomes and the evolution of sexual dimorphism: lessons from the genome. *The American Naturalist*, **173**, 141-150.

- Mank, J.E. (2017) The transcriptional architecture of phenotypic dimorphism. *Nature Ecology & Evolution*, **1**, 0006.
- Mank, J.E., Nam, K., Brunström, B. & Ellegren, H. (2010) Ontogenetic complexity of sexual dimorphism and sex-specific selection. *Molecular biology and evolution*, **27**, 1570-1578.
- Mushinsky, H.R., Hebrard, J.J. & Vodopich, D.S. (1982) Ontogeny of water snake foraging ecology. *Ecology*, **63**, 1624-1629.
- Perry, J.C., Harrison, P.W. & Mank, J.E. (2014) The ontogeny and evolution of sex-biased gene expression in *Drosophila melanogaster*. *Molecular biology and evolution*, **31**, 1206-1219.
- Pointer, M.A., Harrison, P.W., Wright, A.E. & Mank, J.E. (2013) Masculinization of gene expression is associated with exaggeration of male sexual dimorphism. *PLoS genetics*, **9**, e1003697.
- Ralls, K. (1976) Mammals in which females are larger than males. *The Quarterly Review of Biology*, **51**, 245-276.
- Reedy, A.M., Cox, C.L., Chung, A.K., Evans, W.J. & Cox, R.M. (2016) Both sexes suffer increased parasitism and reduced energy storage as costs of reproduction in the brown anole, *Anolis sagrei*. *Biological Journal of the Linnean Society*, **117**, 516-527.
- Rice, W.R. (1984) Sex chromosomes and the evolution of sexual dimorphism. *Evolution*, **38**, 735-742.
- Sandercock, B.K. (1998) Assortative mating and sexual size dimorphism in Western and Semipalmated Sandpipers. *The Auk*, **115**, 786-791.
- Schoener, T.W. & Schoener, A. (1980) Densities, sex ratios, and population structure in four species of Bahamian *Anolis* lizards. *The Journal of Animal Ecology*, 19-53.

- Selander, R.K. (1966) Sexual dimorphism and differential niche utilization in birds. *The Condor*, **68**, 113-151.
- Shetty, S. & Shine, R. (2002) Sexual divergence in diets and morphology in Fijian sea snakes *Laticauda colubrina* (Laticaudinae). *Austral Ecology*, **27**, 77-84.
- Shine, R. (1979) Sexual selection and sexual dimorphism in the Amphibia. *Copeia*, 297-306.
- Shine, R. (1989) Ecological causes for the evolution of sexual dimorphism: a review of the evidence. *The Quarterly Review of Biology*, **64**, 419-461.
- Shine, R. (1991a) Intersexual dietary divergence and the evolution of sexual dimorphism in snakes. *The American Naturalist*, **138**, 103-122.
- Shine, R. (1991b) Why do larger snakes eat larger prey items? *Functional Ecology*, 493-502.
- Shine, R., Reed, R.N., Shetty, S. & Cogger, H.G. (2002) Relationships between sexual dimorphism and niche partitioning within a clade of sea-snakes (Laticaudinae). *Oecologia*, **133**, 45-53.
- Summers, R.W. & Underhill, L.G. (1991) The relationship between body size and time of breeding in Icelandic Redshanks *Tringa t. robusta*. *Ibis*, **133**, 134-139.
- Tokarz, R.R. (1985) Body size as a factor determining dominance in staged agonistic encounters between male brown anoles (*Anolis sagrei*). *Animal Behaviour*, **33**, 746-753.
- Williams, E.E. (1972) The origin of faunas. Evolution of lizard congeners in a complex island fauna: a trial analysis. *Evolutionary Biology*, pp. 47-89. Springer, Boston, Massachusetts.
- Williams, T.M. & Carroll, S.B. (2009) Genetic and molecular insights into the development and evolution of sexual dimorphism. *Nature Reviews Genetics*, **10**, 797.

- Yang, X., Schadt, E.E., Wang, S., Wang, H., Arnold, A.P., Ingram-Drake, L., Drake, T.A. & Lusk, A.J. (2006) Tissue-specific expression and regulation of sexually dimorphic genes in mice. *Genome research*, **16**, 995-1004.
- Zhang, Y., Sturgill, D., Parisi, M., Kumar, S. & Oliver, B. (2007) Constraint and turnover in sex-biased gene expression in the genus *Drosophila*. *Nature*, **450**, 233.

CHAPTER 1

SEX-BIASED GENE EXPRESSION AND THE DEVELOPMENT OF SEXUAL SIZE

DIMORPHISM

ABSTRACT

Sexual dimorphism is a fundamental source of phenotypic diversity in nature, but the evolution of sexual dimorphism is expected to be constrained due to the sexes sharing a single genome. However, differential expression of shared genes between the sexes may be a genetic mechanism that allows species to develop sexual dimorphism despite the genomic constraint of shared genome. Because sexual dimorphism occurs as a developmental process, patterns of differential gene expression between the sexes should change over time and also differ within tissues that contribute differently to the development of sexual dimorphism. We performed an RNA-Seq experiment to examine the differential gene expression basis of sexual dimorphism and found that sex-, age-, and tissue-specific patterns of differential gene expression underlie the development of sexual dimorphism.

INTRODUCTION

Sexual dimorphism is a fundamental source of phenotypic diversity in nature. Sexual dimorphism has long been of interest to evolutionary biologists, because it can affect many aspects of a species' evolutionary trajectory, including physiology, behavior, and life history (Andersson 1994). Despite the importance of sexual dimorphism in evolutionary biology, we know relatively little about how the development of sexual dimorphism is regulated on the genetic level.

Sexual dimorphism presents a genomic paradox: two phenotypes are produced from a single genome. Even in species with genetic sex determination, where genes on sex

chromosomes direct the development of phenotypic divergence, only a few genes are truly sex-limited (Koerich *et al.* 2008; Hughes *et al.* 2012; Moghadam *et al.* 2012) and the majority of genes responsible for sexual-dimorphic traits lie on autosomes (Mank 2009). Thus, male and female phenotypes must be produced from the shared autosomal genome. Resolving this apparent genetic paradox will allow us to understand how the sexes produce dimorphic phenotypes despite sharing a genome, giving us insight into the evolution and development of sexual dimorphism, a fundamental source of phenotypic variation and diversity in nature.

Due to the sexes sharing a largely, and often completely, identical genome, sexual dimorphism is expected to be produced from differential expression between the sexes (i.e., sex-biased expression) of shared autosomal genes (Ellegren & Parsch 2007; Mank 2009; Williams & Carroll 2009; Mank *et al.* 2010; Grath & Parsch 2016; Mank 2017). As phenotype is ultimately determined by genotype, it is predicted that as phenotypic divergence between the sexes increases over ontogeny, there should be an accompanying divergence in gene expression between the sexes. However, because tissues differ in their contribution to phenotypic sexual dimorphism, gene expression patterns will not be uniform across tissues (Mank *et al.* 2008). Thus, not only should there be differing patterns of gene expression during ontogeny within each sex, but there must be also tissue-specific patterns of sex-biased gene expression that change during ontogeny.

With the advent of high-throughput sequencing, several studies examining gene expression patterns between the sexes have been published in recent years. Some studies of sexual dimorphism have characterized gene expression patterns of multiple tissues at a single time point (Mank *et al.* 2008; Pointer *et al.* 2013; Stuglik *et al.* 2014). Other studies have characterized gene expression profiles at multiple time points using single-tissue or whole-body

RNA preparations (Mank *et al.* 2010; Perry, Harrison & Mank 2014; Shi, Zhang & Su 2016; Cox *et al.* 2017). Few studies have examined gene expression patterns of multiple tissues that contribute to sexual dimorphism at multiple age points.

We studied the ontogeny of sex-biased gene expression patterns in several tissues that contribute to sexual dimorphism in the brown anole, *Anolis sagrei*. This sexually dimorphic lizard exhibits male-biased extreme sexual size dimorphism, with males exceeding two to three times the mass of females (Cox & Calsbeek 2010; Reedy *et al.* 2016). We performed an RNA-Seq experiment and constructed whole transcriptomes for the liver, muscle, and brain tissues of males and females at one, four, eight, and twelve months of age. We chose these ages to sample changing gene expression patterns as males and females develop from monomorphic phenotypes at one month to full dimorphism at twelve months. We focused on liver because it regulates metabolism and growth and is, therefore, important to the development of size dimorphism. Muscle is a dimorphic tissue, being larger in males than in females, and is a component in the extreme sexual size dimorphism of anoles with males possessing larger muscles. The brain is not dimorphic in size between the sexes so it can act as a control for growth gene activity and it serves an important role functionally as an integral component in the endocrine system that regulates growth. We conducted differential gene expression analyses to examine sex-biased gene expression patterns within each tissue and sex across the brown anole's ontogeny.

We predicted that as the sexes increase in phenotypical divergence, gene expression divergence in both number of genes with sex-biased expression and amount of expression of those sex-biased genes would increase over ontogeny and across tissues. We predicted that tissue-specific patterns in both numbers of sex-biased genes and levels of sex-biased gene expression would differ from each other. In the brain, we predicted low numbers of sex-biased

genes and low levels of sex-biased gene expression with little divergence between the sexes in both number of sex-biased genes and level of expression of sex-biased genes, relative to the other tissues, across ontogeny as it is an upstream regulator of growth and is not a target tissue for growth regulatory signals. In the liver, which exhibits expression of both upstream and downstream growth regulators and signaling targets, we predicted higher numbers of genes with male-biased expression (i.e., male-biased genes), relative to genes with female-biased expression (i.e., female-biased genes), and higher expression of male-biased genes relative to female-biased genes. We also expected, in the liver, that gene expression would show increasing sexual divergence as the sexes diverge in size over time. In muscle, we had the same predictions as in the liver, however, we expected that sex-biased gene expression would be lower in both number of sex-biased genes and amount of sex-biased expression relative to the liver as muscle is a downstream target of signaling pathways that regulate growth. We found that tissues vary in the extent and magnitude of sex-biased gene expression over time, implying that complex regulation of gene expression throughout ontogeny orchestrates the development of sexual size dimorphism.

MATERIALS AND METHODS

Study System

The brown anole is a small lizard native to Cuba and The Bahamas that exhibits male-biased extreme sexual size dimorphism. As hatchlings and juveniles, male and female brown anoles are sexually monomorphic, often distinguishable only by back pattern and size of post-anal scales. Throughout their ontogeny, anoles diverge in size until reaching sexual maturity at one year of age, when males are much larger, up to two to three times the mass of females, and possess a brightly colored dewlap. The animals used in this study were descendants of wild adult

Anolis sagrei lizards collected in January 2012 from the island of Great Exuma, near George Town, in The Bahamas. These lizards were transported to a breeding facility at the University of Virginia and were bred in a common garden design for several generations.

Animal husbandry

The animals used in this study hatched from June 2015 to January 2017. Animals were housed individually in plastic cages (30 × 20 × 20 cm; Lee's Kritter Keeper, San Marcos, California, U.S.A.) with a carpet substrate, a strip of fiberglass screening for basking, and a piece of PVC pipe (2.5 cm diameter, 30 cm length) for hiding in and perching on. Animals were maintained at constant humidity (65%), temperature (29°C diurnal, 25°C nocturnal), and photoperiod (13L:11D during spring, summer, and fall; 12L:12D during winter) and cages were placed underneath two ReptiSun 10.0 UVB bulbs (ZooMed; San Luis Obispo, California, U.S.A.). Cage walls and potted plants were sprayed with deionized water twice per day. Three times per week, juvenile and adult animals were fed crickets (*Gryllus assimilis* and *Gryllus sigillatus*; Ghann's Cricket Farm, Augusta, Georgia, U.S.A.); juveniles were fed 10–15 1/4-inch crickets, adult females were fed three to five 3/8-inch crickets, and adult males were fed five to seven 1/2-inch crickets. Hatchling animals were fed 10–15 pinhead crickets (*Acheta domestica*) daily. Crickets were dusted weekly with Fluker's Reptile Vitamin and Calcium Supplements (Fluker's Cricket Farms; Port Allen, Louisiana, U.S.A.).

Tissue Collection

Liver, muscle, and brain tissue were collected from lizards of one, four, eight, and twelve months of age. Tissues from age groups four, eight, and twelve months were collected between May 19 and June 10, 2016; one-month tissues were collected in February 2017. All tissues were collected from 10:00-14:00 (EST) to avoid potential circadian rhythm confounding factors. For

ages four, eight, and twelve months, tissues were collected from five males and five females, selected to minimize deviation from mean mass within each sex and age group; for age one month, tissues were collected from four males and four females as that was the maximum equal number of individuals per sex available. Immediately prior to tissue collection, individuals were euthanized by decapitation, approved by the University of Virginia Animal Care and Use Committee (Protocol 3896), and then immediately dissected. The entire liver, femoral muscle, and whole brain were collected and immediately placed in 2 mL screw cap centrifuge tubes filled with *RNAlater*TM RNA Stabilization Solution (Thermo Fisher Scientific; Waltham, Massachusetts, U.S.A.) to prevent RNA degradation. Tissue samples were then stored at 4°C overnight to allow the solution to thoroughly penetrate the tissue, as suggested by the manual, before being stored at -80°C until RNA was isolated.

RNA Isolation and Sequencing

Tissues were thawed, removed from *RNAlater* solution, and placed into new RNase-free centrifuge tubes filled with 1 mL of TRIZOL reagent (Invitrogen; Waltham, Massachusetts, U.S.A.) per 100 mg of tissue and four 2.4 mm stainless steel beads. Tissues were then lysed using a TissueLyser II (Qiagen; Hilden, Germany) at 20 Hz for 12 minutes, with the tubes rotated at six minutes, and incubated at room temperature for five minutes following lysing. One hundred μ L of 1-Bromo-3-chloropropane were then added to each tube, tubes were vortexed for 15 seconds, allowed to incubate at room temperature for five minutes, and then centrifuged at 12,000 g for five minutes to extract RNA from lysed tissues. The RNA-containing upper aqueous phase of each tube was then transferred to a fresh tube and 500 μ L of isopropanol was added before storing at -80° C overnight to precipitate isolated RNA from solution. Tubes were then incubated at room temperature for 5 minutes and centrifuged at 12,000 g for eight minutes to

produce an RNA pellet before discarding the supernatant. One mL of 75% ethanol, prepared with nuclease-free water, was then added, tubes were gently mixed, and then allowed to sit for 30 seconds before centrifuging at 12,000 g for five minutes and discarding supernatant. The isolated RNA was then allowed to air-dry for 30 minutes, centrifuged at 12,000 g for four minutes, and any remaining ethanol was discarded. RNA was then re-suspended in 50 µl of nuclease-free water. Quality and concentration of each RNA sample was evaluated using a Qubit Fluorometer (Qubit 2.0; Invitrogen; Waltham, MA) and an Agilent 2100 Bioanalyzer (Agilent Technologies, Inc.; Waldbronn, Germany).

The RNA samples of the one-month age group were pooled to meet minimum RNA concentration requirements for sequencing such that there was only one replicate per tissue per sex in contrast with the other three age groups, which had five replicates per tissue per sex. Thus, individual effects could not be examined within the one-month age class.

RNA samples were submitted to the Georgia Genomics Facility at the University of Georgia where cDNA libraries were assembled using Kapa Biosystems RNA library preparation (Kapa Biosystems; Boston, Massachusetts, U.S.A.) and sequenced on the Illumina NextSeq 500 platform (Illumina; San Diego, California, U.S.A.) using two High-Output flow cells to generate paired end transcripts of 150 base pair length.

Transcriptome Assembly and RNA-Seq Analysis

We mapped RNA-Seq data to the *Anolis carolinensis* genome (AnoCar2.0 assembly; Accessed September 4, 2018). RNA data was trimmed for Illumina adapter sequences and quality filtered using Trimmomatic version 0.36 (Bolger, Lohse & Usadel 2014). Our settings for Trimmomatic were to remove leading and trailing low quality bases below Phred33 quality of 10, scan reads with a 4-base wide sliding window that cut when the average quality per base

dropped below Phred33 15, and drop reads that were less than 36 bases long. We discarded unpaired reads and aligned RNA data to the *Anolis carolinensis* genome using BWA version 0.7.13 (Bolger, Lohse & Usadel 2014) using the MEM algorithm. Samtools version 1.8 (Li *et al.* 2009) was used to convert file formats, sort alignments, index sorted files for fast random access, merge files belonging to the same sample, and output gene names and mapped transcript count for each sample. Gene expression was normalized across all samples using the trimmed mean of M-values normalization method (Robinson & Oshlack 2010) within edgeR (Robinson, McCarthy & Smyth 2010). EdgeR was then used to perform differential gene expression analysis between the sexes within each tissue and each age group, using a false discovery rate (Benjamini & Hochberg 1995) of 0.05.

Statistical Methods

We performed linear regressions of pairwise comparisons between the sexes, using normalized gene expression values, within liver, muscle, and brain of their \log_2 fold changes of all genes that exhibit sex-biased expression, in any tissue and any age, across ontogeny. We performed 12 regressions and used a Bonferroni adjusted alpha level of 0.0042 to assess whether genes with sex-biased expression exhibited the same pattern of sex-biased expression across all tissues. In addition, we estimated linear regressions between adjacent ages of the \log_2 fold changes of all genes that exhibit sex-biased expression, in any tissue and any age, within the liver, muscle, and brain. We performed nine regressions and used a Bonferroni adjusted alpha level of 0.0056 to assess whether genes with sex-biased expression exhibit the same pattern of sex-biased expression across ontogeny within tissues. In addition, we used general linear models to test for differences in expression of all genes with sex-biased expression between sexes, ages, and tissues.

RESULTS

Number of Genes Exhibiting Sex-biased Expression

Transcriptome assembly and differential gene expression analysis resulted in detection of expression of a total of 19,214 genes and 5,051 sex-biased genes across all tissues and ages with an average proportion of 61.5% mapped to unmapped reads across all samples. The number of genes with sex-biased expression generally increased over time for both sexes within each tissue mirroring the increase in body size that both sexes exhibit over ontogeny (Figure 1.1). The liver, muscle, and brain had divergent patterns in both numbers of genes with sex-biased expression and which sex had more sex-biased genes (Figure 1.2; Table 1.1). In general, we found more genes with female-biased expression than male-biased across all tissues and most age points, however the number of genes with sex-biased expression did not simply increase across all age points within each tissue. For all tissues, we found that there were much fewer sex-biased genes for the one-month age group compared to other ages in the one replicate for the one-month age group for each sex.

In the liver (Figure 1.2A), females had the greater number of genes with sex-biased expression across all age points. While the number of genes with male-biased expression continued to increase across all age points, the number of genes with female-biased expression only increased from one to eight months and slightly decreased from eight to twelve months. The greatest increase in number of sex-biased genes occurred between four months and eight months for both sexes. In the muscle (Figure 1.2B), females had the greater number of genes with sex-biased expression at all age points except at four months. While the number of genes with female-biased expression continuously increased across ontogeny, the number of male-biased genes only increased between one and four months and between eight and twelve months,

slightly decreasing between four and eight months in an almost sigmoidal fashion. The greatest increase in number of genes with sex-biased expression occurred between one month and four months for males and between eight months and twelve months in females. In the brain (Figure 1.2C), the number of genes with female-biased expression continuously increased across all ages while the number of genes with male-biased expression increased from one to eight months before decreasing between eight and twelve months, which is the most decrease in the data. The numbers of genes with sex-biased expression were generally an order of magnitude less in the brain than in the liver and muscle (Table 1.1), reaching a maximum of 25 genes with male-biased expression and 13 genes with female-biased expression at any age compared to 614 male-biased and 1,013 female-biased genes in the liver and 622 male-biased and 1,139 female-biased genes in the muscle (see also Figure 1.2).

Magnitude of Gene Expression

The mean expression of all genes was much higher in the liver and muscle than in the brain (Figure 1.3). The liver (Figure 1.3A) had a slight increasing trend in mean gene expression for both sexes over ontogeny which were approximately equal to each other. However, the muscle (Figure 1.3B) and brain (Figure 1.3C) both exhibited more constant mean levels of expression across ontogeny that was equal between the sexes.

The mean expression of all genes with sex-biased expression within each tissue was much higher in the liver than in the muscle or brain (Figure 1.4). In the liver (Figure 1.4A), both sexes slightly increased in mean expression of genes with sex-biased expression, however female-biased expression was much higher than male-biased expression in the latter three ages compared to one month, but note that females have a parabolic relationship. In the muscle (Figure 1.4B), both sexes exhibited somewhat constant levels of mean expression of genes with

sex-biased expression over ontogeny relative to the liver, however mean male-biased expression was higher than mean female-biased expression at only one and four months. At eight and twelve months, mean female-biased gene expression was greater than mean male-biased expression. In the brain (Figure 1.4C), mean expression of genes with sex-biased expression was constant and approximately equal between the sexes over ontogeny.

Overlap of Genes with Sex-Biased Expression Between Tissues Across Ontogeny

We performed pairwise comparisons of sex-biased genes between each tissue to determine the level of overlap of sex-biased genes between tissues across ontogeny (Table 1.2). Between the brain and either muscle or liver there were very few shared genes with sex-biased expression at any age. There was a maximum of 1.1% of genes with sex-biased expression at eight months exhibiting sex-biased expression in both the brain and muscle. The liver and muscle exhibited a similar pattern of non-overlap throughout ontogeny with the number of shared genes with sex-biased expression only reaching a maximum of 6.3% of total unique genes with sex-biased genes exhibiting sex-biased expression in both the liver and muscle at twelve months. These results indicate that the sexes exhibited sex-biased expression of different genes among tissues throughout ontogeny.

Overlap of Sex-biased Genes Within Tissues Across Ontogeny

We performed pairwise comparisons between adjacent age points within each tissue to determine the level of overlap of genes with sex-biased expression within tissues across ontogeny (Table 1.3). Within the liver, the percentage of shared genes with sex-biased expression increased from 0.3% of total genes between one and four months exhibiting sex-biased expression at both ages to 23.1% of total genes between eight and twelve months exhibiting sex-biased expression at both ages. Within the muscle, the percentage of shared genes

with sex-biased expression did increase across ontogeny but only to a maximum of 8.1% of total genes with sex-biased expression between eight and twelve months exhibiting sex-biased expression at both ages. Within the brain, the percentage of shared genes with sex-biased expression between ages increased from 0% between one and four months to 23.1% between four and eight months but then decreased to 13.7% between eight months and twelve months. These results indicate that even within the same tissue, the genes that exhibit sex-biased expression did not remain constant.

Relationship of Expression of Sex-biased Genes Between Tissues Across Ontogeny

We found significant positive correlations across all pairwise tissue comparisons and all ages except for in the one-month muscle and brain comparison (Figure 1.5). These results indicate that genes with sex-biased expression exhibited similar patterns of expression across tissues (e.g., if a gene with sex-biased expression gene exhibits female sex-biased gene expression in the liver, then the gene is likely to exhibit higher female expression than male expression in the muscle and brain as well).

Relationship of Expression of Sex-biased Genes Between Ages Within Tissues

We found significant positive correlations across all age comparisons and tissues except for the one and four month muscle comparison (Figure 1.6). These results indicate that genes that exhibit sex-biased expression exhibited the same pattern of expression from age to age (e.g., if a gene exhibits male-biased expression at four months, then it is likely to exhibit higher male expression than female expression at one month and eight months as well within tissues).

Sex-biased Gene Expression Levels

The expression levels of genes that exhibit sex-biased expression across the whole transcriptome only differed between tissues (Figure 1.3). Expression of sex-biased genes

significantly differed between the liver, muscle, and brain ($F_{(2,484872)} = 86.833, P < 0.0001$). Expression of sex-biased genes did not differ between the sexes ($F_{(1,484872)} = 0.301, P = 0.58324$) or between ages ($F_{(3,484872)} = 1.260, P = 0.28626$). Furthermore, there were no significant interactions (all p-values > 0.05). Full results are available in Table 1.4.

DISCUSSION

The relationship between sexual dimorphism and sex-biased gene expression has historically been unclear considering that not all genetic loci contribute equally or even show a direct impact on phenotype. Sexual dimorphism occurs as a developmental process (Mackay, Stone & Ayroles 2009; Emlen *et al.* 2012; Khila, Abouheif & Rowe 2012; Sanger *et al.* 2013), indicating the importance of ontogenetic patterns of sex-biased gene expression. In addition, rate of gene expression evolution varies among tissues (Brawand *et al.* 2011), indicating the importance of tissue-specific patterns of sex-biased gene expression. Indeed, sex-biased gene expression changes across ontogeny (Mank *et al.* 2010; Perry, Harrison & Mank 2014) and differs among tissues (Yang *et al.* 2006). Thus, to understand the complex relationship between sexual dimorphism and sex-biased gene expression, sex-biased gene expression must be examined across tissues and ontogeny. We determined that as brown anoles phenotypically diverge in size from monomorphic juveniles to sexually dimorphic adults (Figure 1.1), gene expression between the sexes diverged as well. As predicted, the number of male and female sex-biased genes increased over time (Figure 1.2; Table 1.1) in all tissues, mirroring the phenotypic divergence of the sexes. However, the changes in magnitude of gene expression between the sexes over time did not show clear patterns that correlate to phenotypic divergence.

In the liver and muscle, the number of sex-biased genes was two to three orders of magnitude greater than in the brain for both male-biased and female-biased genes in the four,

eight, and twelve month age groups. Although the brain is an important component of the endocrine system which regulates sexual development, sexual dimorphism may not require as many differentially expressed genes in the brain to develop compared to liver and muscle. The brain is an upstream component of the endocrine system, meaning that fewer numbers of sex-biased genes may be required in the brain to have large downstream effects that direct the development of sexual dimorphism. For example, expression of the two primary sex hormones, testosterone and oestrogen, which are regulators of sexual differentiation and sexual dimorphism (Owens & Short 1995; Lange, Hartel & Meyer 2002; Hau 2007; Cox, Stenquist & Calsbeek 2009), are both regulated by gonadotropin-releasing hormone, follicle-stimulating hormone, and luteinizing hormone (Schally *et al.* 1971; Pierce & Parsons 1981), which are both expressed and released by the brain. However, it is important to note that due to the difficulty of extracting brain tissue, it is quite possible that regions from the base of the brain were not collected and this might be why we did not detect as many sex-biased genes in the brain. These results, in conjunction with the finding that magnitude of sex-biased gene expression does not differ with age among any tissues, indicate that differences in RNA abundance may not have a direct relationship to phenotypic dimorphism.

For females, our results suggest that there are biological processes in the liver that occur during development that do not continue into sexual maturity. In the liver (Figure 1.2A; Table 1.1), the number of genes with female-biased expression peaked at eight months but in twelve months for genes with males-biased expression, although the increase in genes with male-biased expression from eight to twelve months is less than 25% of the increase from four months to eight months. These results may indicate that the liver's contribution to the development of sexual dimorphism is greatest around eight months of age, when brown anoles are between

juvenile and adult phenotypes for both sexes. Given that the number of genes with female-biased expression decreased between eight and twelve months, despite still growing during that time frame, sex-biased gene expression may contribute the most to sexual dimorphism before the sexes reach maturity and are most phenotypically dimorphic.

The high number of genes with female-biased expression in muscle at twelve months may relate to changes in female behavior that includes increased foraging to support reproductive efforts, copulation, and oviposition. In the muscle, we found that the number of genes with female-biased expression steadily increased across all age groups to peak at 12 months (Figure 1.2B), but the number of genes with male-biased expression actually decreased between four and eight months, but then increased and peaked at twelve months. The number of genes with male-biased expression remained relatively constant from four to twelve months, peaking at 622 genes at twelve months, compared to increasing increases in the number of genes with female-biased expression that peaked at 1,139 at twelve months (Figure 1.2B). These results might indicate that male muscle development is extended and begins earlier than female muscle development, corresponding to the development of the brown anole's extreme sexual size dimorphism.

In the brain, there are fewer numbers of genes with sex-biased expression. Female brains peaked in the number of genes with sex-biased expression at 12 months while male brains peaked at 8 months (Figure 1.2C). This spike in genes with male-biased expression at eight months could correspond to how the greatest increase in phenotypic divergence between the sexes occurs between eight and twelve months of age. Between eight and twelve months, males not only attain doubled the mass of females (Figure 1.1). In contrast, females reached

approximate full size at eight months and may not require large changes in brain gene expression from eight to twelve months of age to support their development.

Tissues are distinct in their patterns of sex-biased gene expression, potentially revealing a physiological mechanism that allows for reduction of between-sex genetic correlations. Despite being closely linked by regulatory pathways and showing similar patterns of expression of genes with sex-biased expression both between tissues across ages (Figure 1.5) and between ages within tissues (Figure 1.6), we observed little to no overlap in sex-biased genes between tissues across ontogeny (Table 1.2). Even within tissues (Table 1.3), tissues largely exhibited sex-biased expression of different genes over time. In other words, tissue-specific patterns of gene expression were separate from each other and exhibit temporal trajectories that exhibit sex-biased expression of largely different genes over time. Given this compartmentalization of sex-biased gene expression between tissues that changed temporally and how rates of sex-biased gene expression evolution differ among tissues (Brawand *et al.* 2011), tissue-specific sex-biased gene expression may be a mechanism that reduces the build-up of between-sex genetic correlations. Given that rates of gene expression within tissues are able to evolve separately from each other, perhaps tissue-specific gene expression patterns allow sexes to circumvent the obstacle of a shared genome by allowing tissues that contribute to different aspects of sexual dimorphism develop their own gene expression patterns separate from sex.

The evolutionary drivers of sexual dimorphism, and sexual size dimorphism in particular, are highly debated (Hedrick & Temeles 1989). Regardless of why sexual dimorphism evolves, sexes need to overcome the genetic obstacle of a shared genome that should make it difficult for the sexes to evolve independently (Lande 1980). Differential gene expression between the sexes is expected to allow species to overcome the genetic obstacle and evolve sexual dimorphism. We

found that phenotypic divergence between the sexes of the brown anole were accompanied by increases in sex-biased gene expression. However, this relationship is complex and there was no direct relationship between amount of sex-biased gene expression, in both number of genes with sex-biased expression and expression levels of those genes, across ages and tissues and amount of phenotypic dimorphism. In fact, sex-biased gene expression was highly age- and tissue-specific with little overlap between ages and tissues and within tissues over time. This differential expression of genes between tissues and ages may provide the sexes the utility from a single genome to reduce between-sex genetic correlations by allowing the sexes to enact separate gene expression developmental programs that utilize different genes across tissues and ages to facilitate the development of sexual dimorphism. Furthermore, our results have broader implications for the evolution of phenotypic diversity. Because sexual dimorphism is essentially a form of polyphenism, conclusions from this study can be directly applied to other forms of intraspecific variation.

REFERENCES

- Andersson, M.B. (1994) *Sexual selection*. Princeton University Press, Princeton, New Jersey.
- Benjamini, Y. & Hochberg, Y. (1995) Controlling the false discovery rate: a practical and powerful approach to multiple testing. *Journal of the royal statistical society. Series B (Methodological)*, 289-300.
- Bolger, A.M., Lohse, M. & Usadel, B. (2014) Trimmomatic: a flexible trimmer for Illumina sequence data. *Bioinformatics*, **30**, 2114-2120.
- Brawand, D., Soumillon, M., Necsulea, A., Julien, P., Csárdi, G., Harrigan, P., Weier, M., Liechti, A., Aximu-Petri, A. & Kircher, M. (2011) The evolution of gene expression levels in mammalian organs. *Nature*, **478**, 343.
- Cox, R.M. & Calsbeek, R. (2010) SEX-SPECIFIC SELECTION AND INTRASPECIFIC VARIATION IN SEXUAL SIZE DIMORPHISM. *Evolution*, **64**, 798-809.
- Cox, R.M., Cox, C.L., McGlothlin, J.W., Card, D.C., Andrew, A.L. & Castoe, T.A. (2017) Hormonally Mediated Increases in Sex-Biased Gene Expression Accompany the Breakdown of Between-Sex Genetic Correlations in a Sexually Dimorphic Lizard. *The American Naturalist*, **189**, 315-332.
- Cox, R.M., Stenquist, D.S. & Calsbeek, R. (2009) Testosterone, growth and the evolution of sexual size dimorphism. *Journal of evolutionary biology*, **22**, 1586-1598.
- Ellegren, H. & Parsch, J. (2007) The evolution of sex-biased genes and sex-biased gene expression. *Nature Reviews Genetics*, **8**, 689-698.
- Emlen, D.J., Warren, I.A., Johns, A., Dworkin, I. & Lavine, L.C. (2012) A mechanism of extreme growth and reliable signaling in sexually selected ornaments and weapons. *Science*, **337**, 860-864.

- Grath, S. & Parsch, J. (2016) Sex-biased gene expression. *Annual Review of Genetics*, **50**, 29-44.
- Hau, M. (2007) Regulation of male traits by testosterone: implications for the evolution of vertebrate life histories. *Bioessays*, **29**, 133-144.
- Hedrick, A.V. & Temeles, E.J. (1989) The Evolution of Sexual Dimorphism in Animals: Hypotheses and Tests. *Trends in Ecology & Evolution*, **4**, 136-138.
- Hughes, J.F., Skaletsky, H., Brown, L.G., Pyntikova, T., Graves, T., Fulton, R.S., Dugan, S., Ding, Y., Buhay, C.J. & Kremitzki, C. (2012) Strict evolutionary conservation followed rapid gene loss on human and rhesus Y chromosomes. *Nature*, **483**, 82.
- Khila, A., Abouheif, E. & Rowe, L. (2012) Function, developmental genetics, and fitness consequences of a sexually antagonistic trait. *Science*, **336**, 585-589.
- Koerich, L.B., Wang, X., Clark, A.G. & Carvalho, A.B. (2008) Low conservation of gene content in the *Drosophila* Y chromosome. *Nature*, **456**, 949.
- Lande, R. (1980) Sexual dimorphism, sexual selection, and adaptation in polygenic characters. *Evolution*, 292-305.
- Lange, I.G., Hartel, A. & Meyer, H.H.D. (2002) Evolution of oestrogen functions in vertebrates. *The Journal of Steroid Biochemistry & Molecular Biology*, **83**, 219-226.
- Li, H., Handsaker, B., Wysoker, A., Fennell, T., Ruan, J., Homer, N., Marth, G., Abecasis, G. & Durbin, R. (2009) The sequence alignment/map format and SAMtools. *Bioinformatics*, **25**, 2078-2079.
- Mackay, T.F., Stone, E.A. & Ayroles, J.F. (2009) The genetics of quantitative traits: challenges and prospects. *Nature Reviews Genetics*, **10**, 565.
- Mank, J.E. (2009) Sex chromosomes and the evolution of sexual dimorphism: lessons from the genome. *The American Naturalist*, **173**, 141-150.

- Mank, J.E. (2017) The transcriptional architecture of phenotypic dimorphism. *Nature Ecology & Evolution*, **1**, 0006.
- Mank, J.E., Hultin-Rosenberg, L., Webster, M.T. & Ellegren, H. (2008) The unique genomic properties of sex-biased genes: insights from avian microarray data. *BMC genomics*, **9**, 148.
- Mank, J.E., Nam, K., Brunström, B. & Ellegren, H. (2010) Ontogenetic complexity of sexual dimorphism and sex-specific selection. *Molecular biology and evolution*, **27**, 1570-1578.
- Moghadam, H.K., Pointer, M.A., Wright, A.E., Berlin, S. & Mank, J.E. (2012) W chromosome expression responds to female-specific selection. *Proceedings of the National Academy of Sciences*, **109**, 8207-8211.
- Owens, I.P.F. & Short, R.V. (1995) Hormonal basis of sexual dimorphism in birds: implications for new theories of sexual selection. *Trends in Ecology & Evolution*, **10**, 44-47.
- Perry, J.C., Harrison, P.W. & Mank, J.E. (2014) The ontogeny and evolution of sex-biased gene expression in *Drosophila melanogaster*. *Molecular biology and evolution*, **31**, 1206-1219.
- Pierce, J.G. & Parsons, T.F. (1981) Glycoprotein hormones: structure and function. *Annual review of biochemistry*, **50**, 465-495.
- Pointer, M.A., Harrison, P.W., Wright, A.E. & Mank, J.E. (2013) Masculinization of gene expression is associated with exaggeration of male sexual dimorphism. *PLoS genetics*, **9**, e1003697.
- Reedy, A.M., Cox, C.L., Chung, A.K., Evans, W.J. & Cox, R.M. (2016) Both sexes suffer increased parasitism and reduced energy storage as costs of reproduction in the brown anole, *Anolis sagrei*. *Biological Journal of the Linnean Society*, **117**, 516-527.

- Robinson, M.D., McCarthy, D.J. & Smyth, G.K. (2010) edgeR: a Bioconductor package for differential expression analysis of digital gene expression data. *Bioinformatics*, **26**, 139-140.
- Robinson, M.D. & Oshlack, A. (2010) A scaling normalization method for differential expression analysis of RNA-seq data. *Genome Biology*, **11**, R25.
- Sanger, T.J., Sherratt, E., McGlothlin, J.W., Brodie, E.D., Losos, J.B. & Abzhanov, A. (2013) Convergent evolution of sexual dimorphism in skull shape using distinct developmental strategies. *Evolution*, **67**, 2180-2193.
- Schally, A.V., Arimura, A., Kastin, A.J., Matsuo, H., Baba, Y., Redding, T., Nair, R., Debeljuk, L. & White, W. (1971) Gonadotropin-releasing hormone: one polypeptide regulates secretion of luteinizing and follicle-stimulating hormones. *Science*, **173**, 1036-1038.
- Shi, L., Zhang, Z. & Su, B. (2016) Sex biased gene expression profiling of human brains at major developmental stages. *Scientific Reports*, **6**, 21181.
- Stuglik, M.T., Babik, W., Prokop, Z. & Radwan, J. (2014) Alternative reproductive tactics and sex-biased gene expression: the study of the bulb mite transcriptome. *Ecology & Evolution*, **4**, 623-632.
- Williams, T.M. & Carroll, S.B. (2009) Genetic and molecular insights into the development and evolution of sexual dimorphism. *Nature Reviews Genetics*, **10**, 797.
- Yang, X., Schadt, E.E., Wang, S., Wang, H., Arnold, A.P., Ingram-Drake, L., Drake, T.A. & Lusis, A.J. (2006) Tissue-specific expression and regulation of sexually dimorphic genes in mice. *Genome research*, **16**, 995-1004.

Table 1.1 The number of genes exhibiting sex-biased expression per sex at one, four, eight, and twelve months of age in liver, femoral muscle, and brain.

Tissue	Age (months)	Female-biased genes	Male-biased genes	Total sex-biased genes
Liver	1	6	1	7
	4	256	131	387
	8	1013	531	1544
	12	917	614	1531
Muscle	1	9	3	12
	4	103	455	558
	8	459	436	895
	12	1139	622	1761
Brain	1	0	0	0
	4	4	9	13
	8	25	10	35
	12	10	13	23

Table 1.2 Pairwise comparisons of overlap of genes exhibiting sex-biased expression between tissues at one, four, eight, and twelve months of age.

Age (months)	Pairwise Comparison of Tissues	Total Number of Unique Sex-biased genes	Number of Sex-biased Genes Unique to Tissue A (%)	Number of Sex-biased Genes Unique to Tissue B (%)	Number of Shared Sex-biased genes
1	(A) Brain & (B) Muscle	12	0 (0%)	12 (100%)	0 (0%)
4		566	8 (1.4%)	553 (97.7%)	5 (0.9%)
8		920	25 (2.7%)	885 (96.2%)	10 (1.1%)
12		1776	15 (0.8%)	1753 (98.7%)	8 (0.5%)
1	(A) Muscle & (B) Liver	18	11 (61.1%)	6 (33.3%)	1 (5.6%)
4		932	545 (58.5%)	374 (40.1%)	13 (1.4%)
8		2326	782 (33.6%)	1431 (61.5%)	113 (4.9%)
12		3096	1565 (50.5%)	1335 (43.1%)	196 (6.3%)
1	(A) Liver & (B) Brain	7	7 (100%)	0 (0%)	0 (0%)
4		396	383 (96.7%)	9 (2.3%)	4 (1.0%)
8		1569	1534 (97.8%)	25 (1.6%)	10 (0.6%)
12		1544	1521 (98.5%)	13 (0.8%)	10 (0.7%)

Table 1.3 Pairwise comparisons of overlap of genes exhibiting sex-biased expression between ages within the liver, femoral muscle, and brain.

Tissue	Pairwise Comparison of Ages	Total Number of Unique Sex-biased genes	Number of Sex-biased Genes Unique to Age A	Number of Sex-biased Genes Unique to Age B	Number of Shared Sex-biased genes
Liver	(A) 1 month & (B) 4 months	393	6 (1.5%)	386 (98.2%)	1 (0.3%)
	(A) 4 Months & (B) 8 months	1733	189 (10.9%)	1346 (77.7%)	198 (11.4%)
	(A) 8 months & (B) 12 months	2497	966 (38.7%)	953 (38.2%)	578 (23.1%)
Muscle	(A) 1 month & (B) 4 months	570	12 (2.1%)	558 (97.9%)	0 (0%)
	(A) 4 Months & (B) 8 months	1354	459 (33.9%)	796 (58.8%)	99 (7.3%)
	(A) 8 months & (B) 12 months	2458	697 (28.4%)	1563 (63.6%)	198 (8.1%)
Brain	(A) 1 month & (B) 4 months	13	0 (0%)	13 (100%)	0 (0%)
	(A) 4 Months & (B) 8 months	39	4 (10.3%)	26 (66.7%)	9 (23.1%)
	(A) 8 months & (B) 12 months	51	28 (54.9%)	16 (31.4%)	7 (13.7%)

Table 1.4 The results of a general linear model testing for sex, age, and tissue effects on expression levels of all genes exhibiting sex-biased expression. Factors with significant p-values are bolded.

Factor	Degrees of freedom	F-value	P-value
Sex	1, 72	0.301019311	0.583244361
Age	3, 72	1.259907315	0.286254905
Tissue	2, 72	86.8325545	< 0.0001
Sex:Age	3, 72	0.413555117	0.743268576
Sex:Tissue	2, 72	0.601006427	0.548259983
Age:Tissue	6, 72	1.827559699	0.089455459
Sex:Age:Tissue	6, 72	0.511992897	0.799762388
Residuals	72		

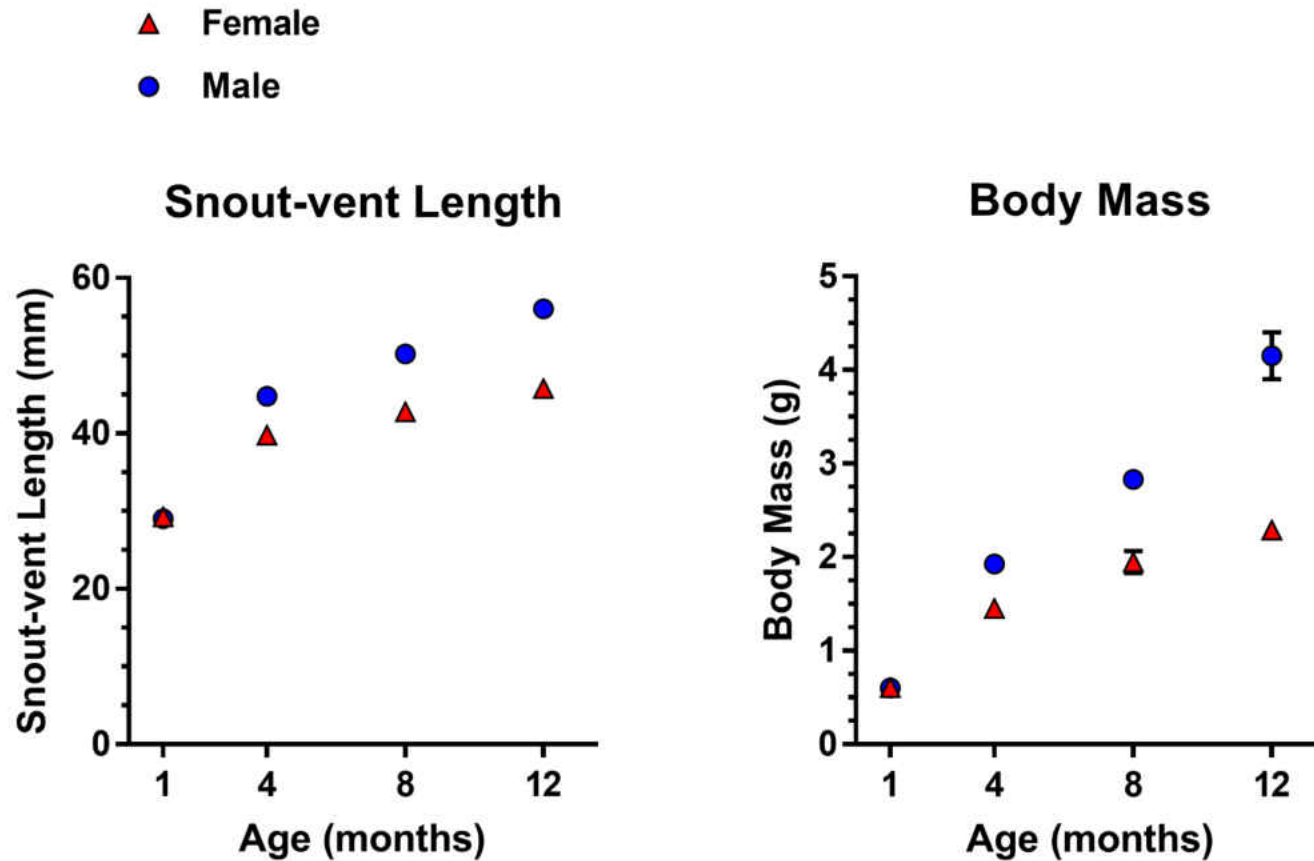


Figure 1.1 As the sexes age, they increasingly diverge in size in both length and body mass. Data are the mean snout-vent length, in millimeters, and body mass, in grams, plotted against age of male and female brown anoles used in this RNA-Seq experiment. Data are expressed as means (symbols) with standard error bars (error bars shorter than the height of the symbol are not depicted).

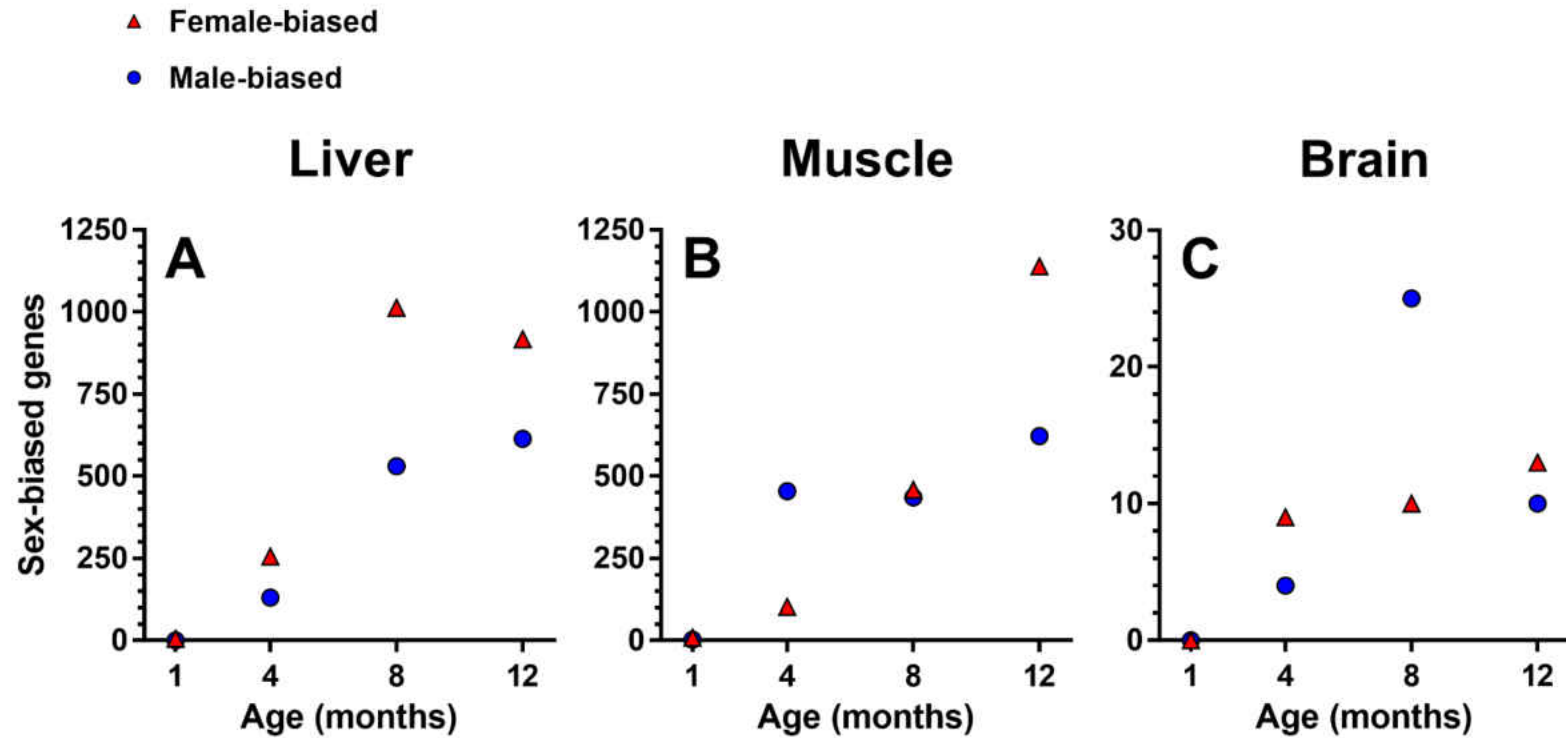


Figure 1.2 The number of genes that exhibit sex-biased expression increases for both sexes and diverges between sexes within the liver, muscle, and brain across ontogeny. Data are numbers of genes that exhibit sex-biased expression, across all detected genes, plotted against age for male and female brown anoles in the liver, muscle, and brain. Note that the y-axis scale for the C) brain is much lower than for the A) liver and B) femoral muscle.

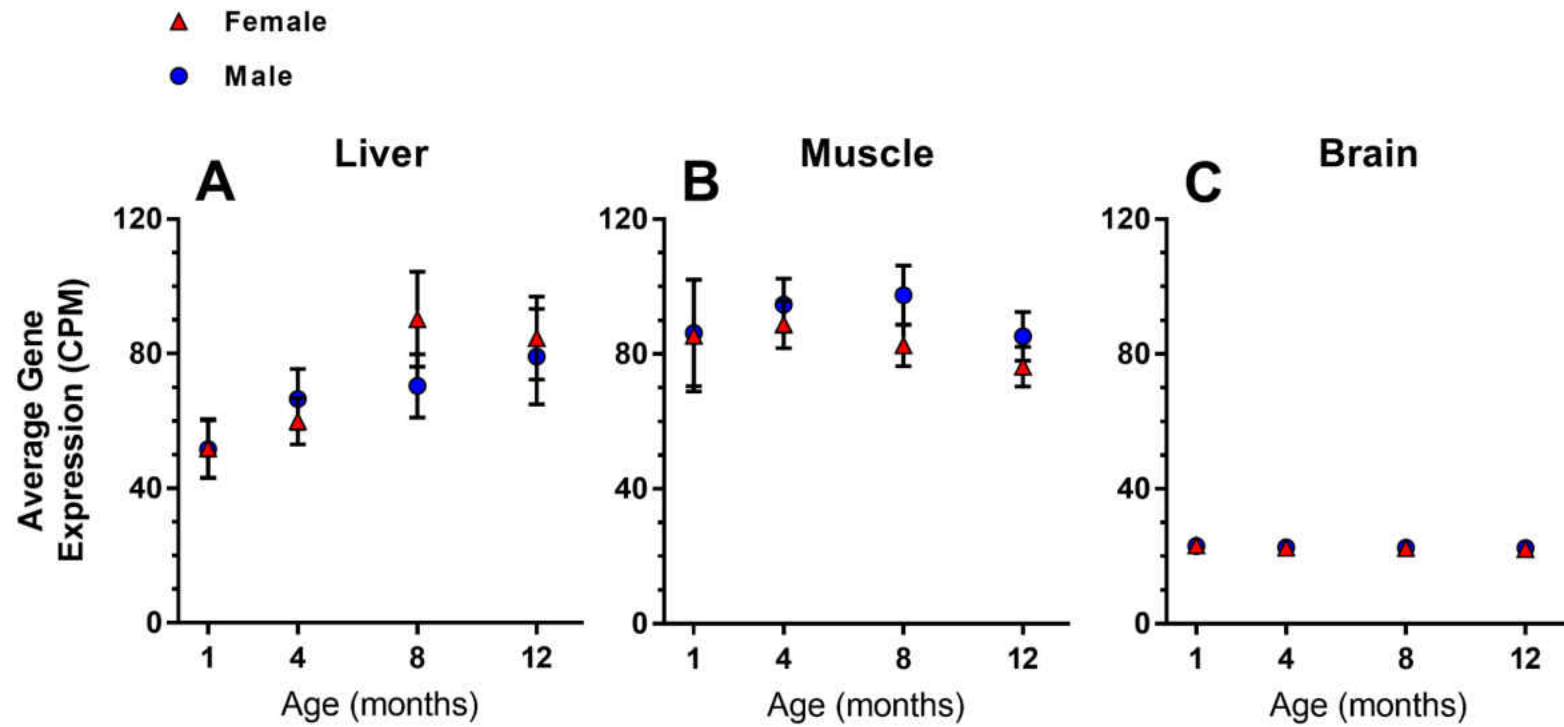


Figure 1.3 The sexes show similar mean expression of all genes to each other within tissues and across ontogeny. Data are the expression of all detected genes plotted against age for male and female brown anoles in the liver, muscle, and brain. Data are expressed as means (symbols) with standard error bars (error bars shorter than the height of the symbol are not depicted).

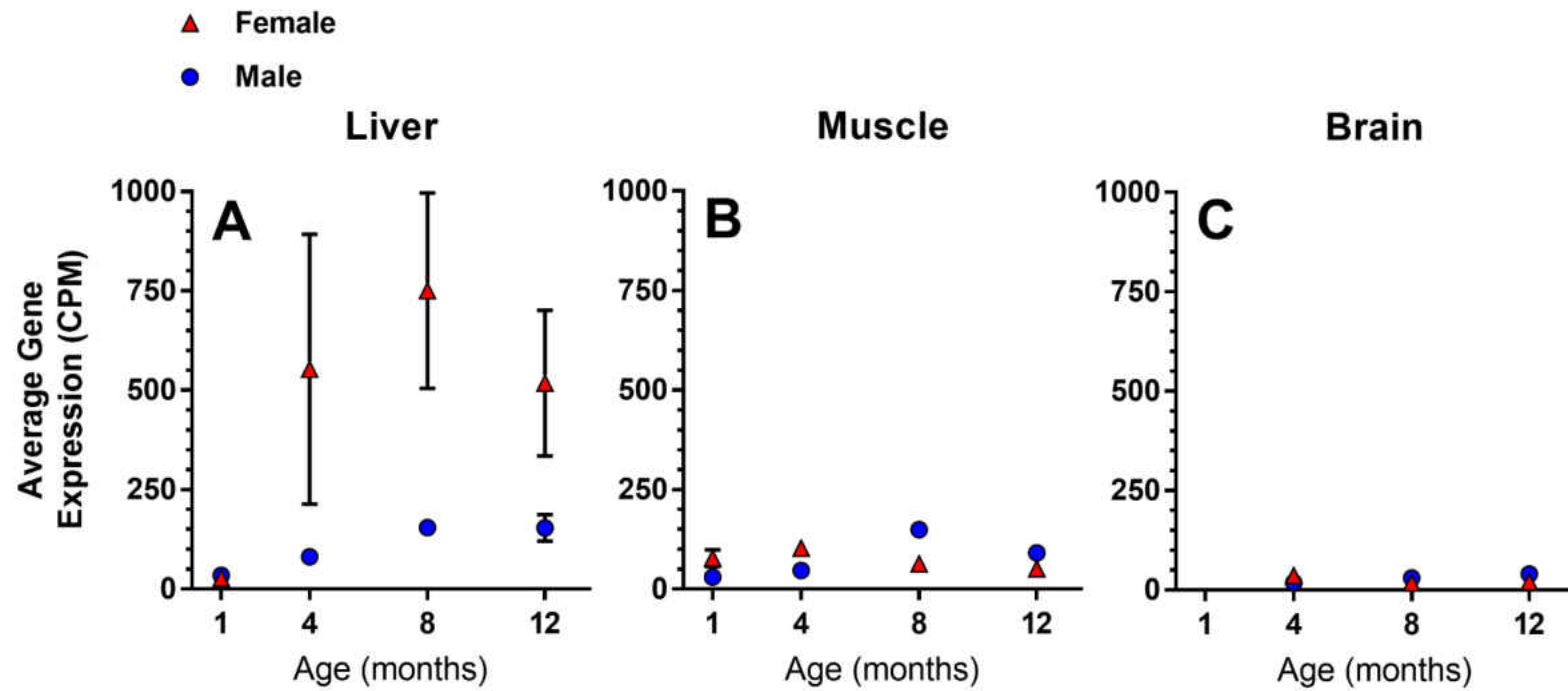


Figure 1.4 The sexes diverge in their expression levels of genes that exhibit sex-biased expression both between tissues and across ontogeny. Data are mean expression of genes with sex-biased expression plotted against age for male and female brown anoles in the liver, muscle, and brain. Data are expressed as means (symbols) with standard error bars (error bars shorter than the height of the symbol are not depicted).

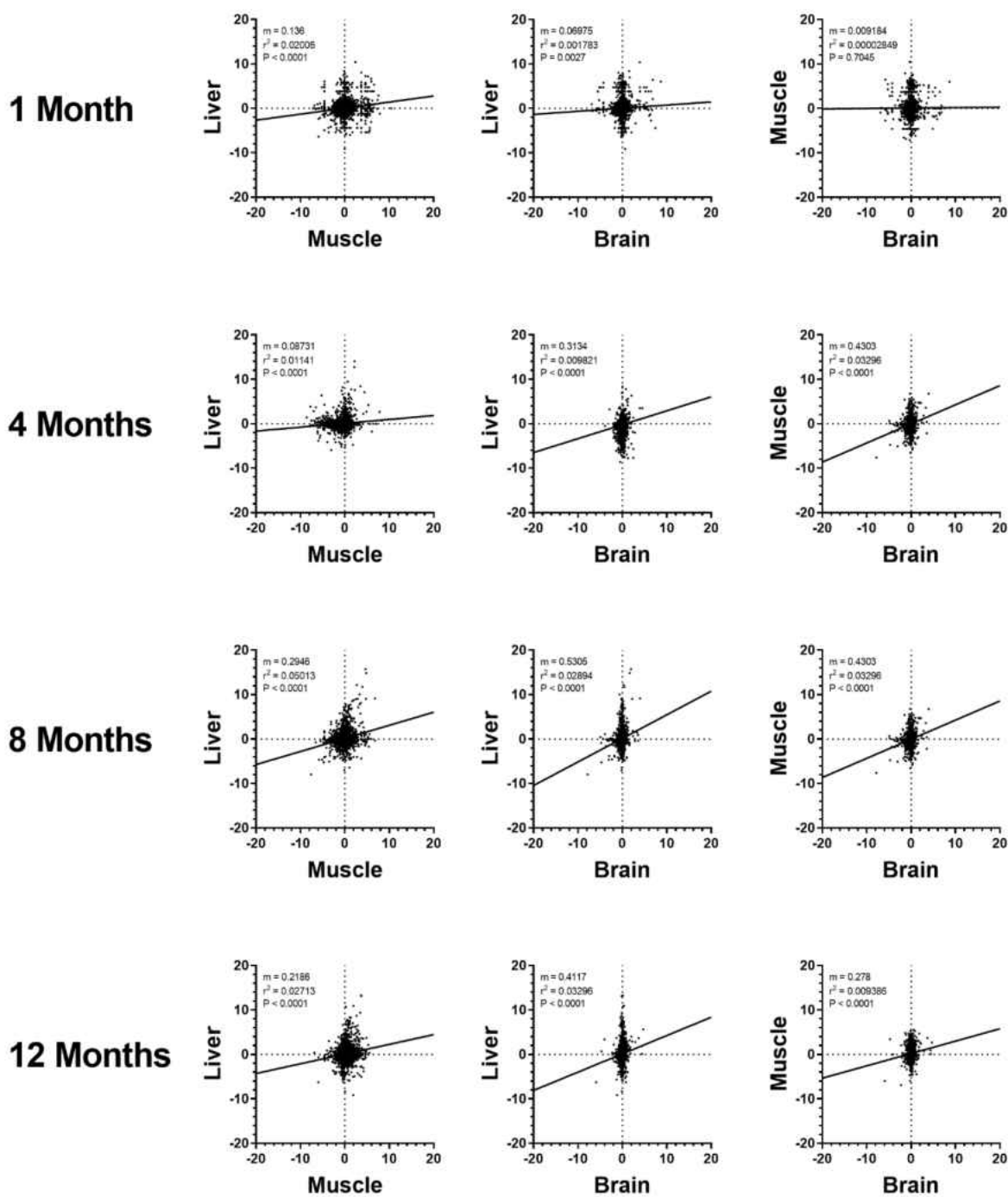
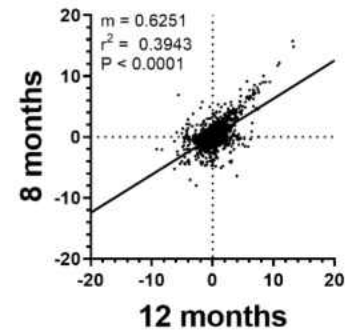
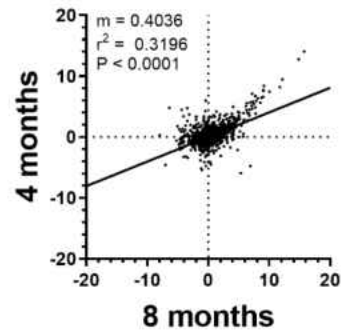
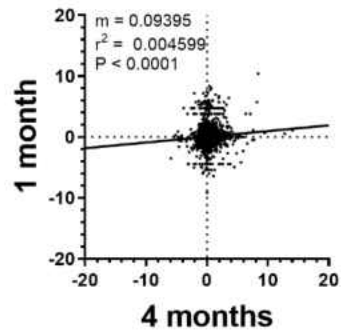


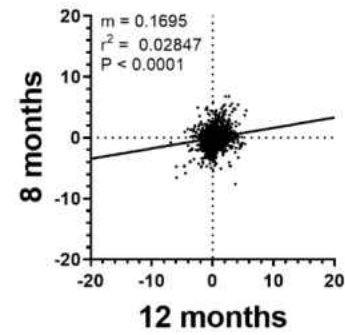
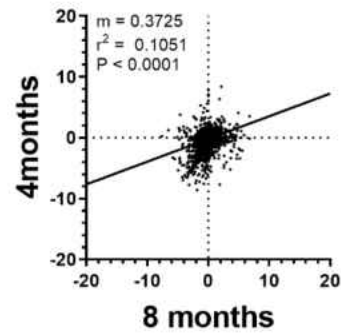
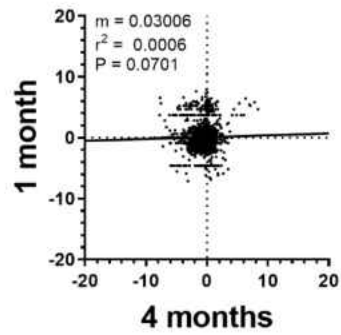
Figure 1.5 Genes that exhibit sex-biased expression in one tissue exhibit the same direction of sex-bias in other tissues. Graphs are pairwise comparisons with linear regressions between tissues of the \log_2 fold changes of all genes that exhibited sex-biased expression, in any tissue

and any age, at each age. Both axes are in units of \log_2 fold change of the ratio of female to male gene expression. Positive \log_2 fold changes indicate greater female expression compared to male expression while negative \log_2 fold changes indicate greater male expression. Quadrant I contains genes that have exhibited sex-biased expression that have higher female expression than male expression in both tissues indicated by the axes. Quadrant II contains genes that have exhibited sex-biased expression that have higher female expression in the tissue on the y-axis and higher male expression in the tissue on the x-axis. Quadrant III contains genes that have exhibited sex-biased expression that have higher male expression in both tissues. Quadrant IV contains genes that have exhibited sex-biased expression with higher male expression in the y-axis tissue and higher female expression in the x-axis tissue. Positive slopes of regression lines indicate that genes in one tissue with greater expression in one sex will have greater expression of the same sex in the other tissue. Note that all slopes, except for the comparison between muscle and brain at one month, are significant.

Liver



Muscle



Brain

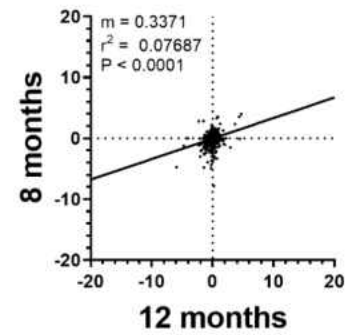
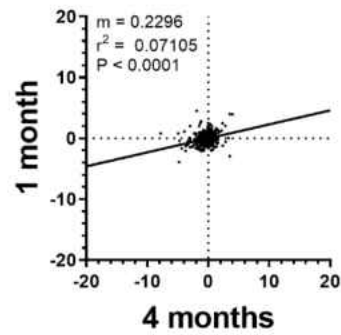
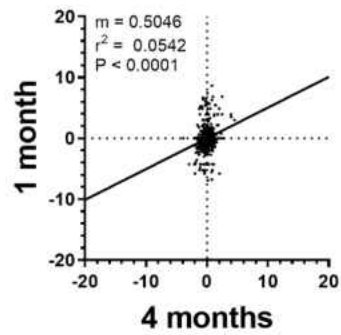


Figure 1.6 Genes that exhibit sex-biased expression at one age exhibit the same direction of sex-bias in adjacent ages within each tissue. Graphs are pairwise comparisons with linear regressions between adjacent ages of the \log_2 fold changes of all genes that have exhibited sex-biased expression, in any tissue and any age, within each tissue. Both axes are in units of \log_2 fold change of the ratio of female to male gene expression. Positive \log_2 fold changes indicate greater female expression compared to male expression while negative \log_2 fold changes indicate greater male expression. Quadrant I contains genes that have exhibited sex-biased expression that have higher female expression than male expression in both ages indicated by the axes. Quadrant II contains genes that have exhibited sex-biased expression that have higher female expression in the age on the y-axis and higher male expression in the age on the x-axis. Quadrant III contains genes that have exhibited sex-biased expression that have higher male expression in both ages. Quadrant IV contains genes that have exhibited sex-biased expression with higher male expression in the y-axis age and higher female expression in the x-axis age. Positive slopes of regression lines indicate that genes in one age with greater expression in one sex will have greater expression of the same sex in the other age. Note that all slopes, except for the comparison between one-month and four-months in muscle, are significant.

CHAPTER 2

SEX-BIASED GENE EXPRESSION OF GROWTH REGULATORY NETWORKS AND THE
DEVELOPMENT OF SEXUAL SIZE DIMORPHISM

ABSTRACT

Sexual size dimorphism is a form of phenotypic diversity that affects many aspects of a species' evolutionary trajectory including physiology, ecology, and behavior among other life-history traits. While sexual size dimorphism is common in nature, it should be difficult to evolve given that the sexes share an autosomal genome. One solution to this paradox is differential expression of shared genes between the sexes that could allow sexual dimorphism to evolve and, in particular, differential expression of growth-regulatory genes may be important for the evolution and development of sexual size dimorphism. We identified genes crucial to the growth hormone/insulin-like growth factor, insulin-signaling, and mechanistic target of rapamycin regulatory networks that regulate growth in vertebrates. Differential gene expression analysis of these growth regulatory networks revealed that tissue-specificity of differential expression of growth-regulatory genes drives the development of sexual size dimorphism.

INTRODUCTION

One of the most common types of sexual dimorphism is sexual size dimorphism, whereby the sexes differ in adult body size. Given the role of body size as a fundamental determinant of physiological processes and ultimately fitness, understanding the evolution of sexual size dimorphism has been a major goal of evolutionary biology. Research has tended to focus on the evolutionary drivers of sexual size dimorphism. The evolution of sexual size dimorphism is likely driven by a combination of ecological evolutionary forces (Selander 1966; Shine 1989; Butler, Schoener & Losos 2000), natural selection (Darwin 1888; Cox, Skelly &

John-Alder 2003), and sexual selection (Darwin 1888; Cox, Skelly & John-Alder 2003).

However, the repeated evolution of sexual size dimorphism is paradoxical, as the sexes share the constraint of a common genome.

An obstacle to evolving sexual size dimorphism is the central paradox of the development of sexual dimorphism: two distinct phenotypes must be produced from one shared genome (Lande 1980; Rice 1984; Fisher 1999; Badyaev 2002). In a sexually dimorphic species, genomic conflict will arise if selection promotes separate phenotypic optima for each sex (i.e., sexually antagonistic selection) but the genetic loci for divergent traits are the same for both sexes (i.e., intralocus sexual conflict) (Chippindale, Gibson & Rice 2001; Rice & Chippindale 2001; Bonduriansky, Rowe & Tregenza 2005; Bonduriansky & Chenoweth 2009; Cox & Calsbeek 2009). Intralocus sexual conflict is expected to impede the divergence of the sexes to their phenotypic optima as the genetic influence on traits shared between the sexes (i.e., between-sex genetic correlations) is high, and for that reason, the sexes should be unable to diverge when selection for the female and male optima point in different directions resulting in a genomic tug-of-war (Lande 1980; Lande 1987; Fisher 1999; Bonduriansky & Chenoweth 2009; Poissant, Wilson & Coltman 2010). Given that sexual dimorphism and sexual size dimorphism are common in nature, there must be genetic mechanisms that reduce between sex genetic correlations for shared phenotypic traits to resolve genomic conflict and allow sexual dimorphism and sexual size dimorphism to evolve (Lande 1980; Lande 1987; Fairbairn & Roff 2006).

The development of sexual size dimorphism must arise from sex-specific differences in regulatory processes that direct an individual's growth (Sanger *et al.* 2013). One common mechanism that regulates the development of sexual size dimorphism in vertebrates is

differential production of systemic hormones. Oestrogen and testosterone, the two main sex hormones, are prominent regulators of the amount of growth and rate of growth is attained within each sex across vertebrate lineages (Badyaev 2002; Cox, Stenquist & Calsbeek 2009; Adkins-Regan 2012). Although physiological mechanisms that regulate sexual size dimorphism, including hormonal mediation, are well understood, it is unclear how sexual size dimorphism is regulated by genetic mechanisms, enabling species to evolve sexual size dimorphism (Badyaev 2002).

Several genetic mechanisms might facilitate the evolution and development of sexual dimorphism and sexual size dimorphism by resolving intralocus sexual conflict. Sex chromosomes, DNA molecules that determine the sex of an individual, can facilitate the evolution of sexual dimorphism when sexually antagonistic traits (traits beneficial to one sex and detrimental to the other) become sex-linked or sex-limited to the sex it benefits, thereby reducing or removing a genetic constraint on the impeded sex (Rice 1984; Van Doorn & Kirkpatrick 2007; Roberts, Ser & Kocher 2009). Sex-specific transcript splicing can reduce intralocus sexual conflict by allowing a single locus to produce sex-specific gene products (Stewart, Pischedda & Rice 2010; Kijimoto, Moczek & Andrews 2012). Genomic imprinting is able to reduce between-sex genetic correlations and intralocus sexual conflict by altering or silencing the expression of genes inherited from the parent of the opposite sex to allow independent selection on a locus for each sex (Day & Bonduriansky 2004; Bonduriansky 2007). Gene duplication, a genomic event where additional copies of genes are produced, may also reduce intrasexual conflict by generating copies of genes that gain sex-specific functions, thus becoming able to evolve independently and facilitate divergence between the sexes (Connallon & Clark 2011; Gallach & Betrán 2011). While all of these genetic mechanisms may be utilized to reduce between-sex

genetic correlations and intrasexual conflict, one mechanism is predicted to be particularly important to the reduction of intralocus sexual conflict: differential gene expression.

Because males and females are essentially genetically identical, with most sexes differing in a few genes on sex chromosomes or actually being genetically identical in systems with environmental sex-determination, it is expected that sexual dimorphism results mainly from differential expression of shared genes between the sexes (Ellegren & Parsch 2007; Mank 2009; Williams & Carroll 2009; Mank *et al.* 2010; Grath & Parsch 2016; Mank 2017). Differential expression of shared genes between the sexes (i.e., sex-biased gene expression) is predicted to reduce intralocus sexual conflict by allowing the sexes to produce distinct phenotypes through sex-specific expression patterns under the assumption that male-biased genes produce male traits and female-biased genes produce female traits (Ellegren & Parsch 2007; Mank 2009; Innocenti & Morrow 2010; Mank *et al.* 2010; Ingleby, Flis & Morrow 2015; Grath & Parsch 2016).

Large proportions of genes exhibit sex-biased expression (Zhang *et al.* 2007; Mank *et al.* 2010), and the magnitude of sex-bias in gene expression has been linked to the magnitude of phenotypic sexual dimorphism (Pointer *et al.* 2013; Harrison *et al.* 2015). However, it is unclear what proportion of sex-biased genes are ultimately responsible for the development of sexual dimorphism and sexual size dimorphism. In vertebrates, the growth hormone/insulin-like growth factor (GH/IGF), insulin-signaling, and mechanistic target of rapamycin (mTOR) gene networks regulate growth, energetics, and cell proliferation and, therefore, are likely to contain genes whose differential expression between the sexes might be of particular importance in the brown anole's development of sexual size dimorphism (Cox *et al.* 2017).

The growth hormone/insulin-like growth factor (GH/IGF) axis is a signaling pathway that regulates postnatal muscle and bone growth in vertebrates through a complex system of direct

influences and feedback interactions between growth hormone, insulin-like growth factors, and tissues that they act on (Giustina, Mazziotti & Canalis 2008; Perrini *et al.* 2010). The insulin-signaling network is a crucial biological pathway that regulates glucose and lipid metabolism. Insulin regulates metabolism by stimulating glucose, fatty acid, and amino acid uptake into cells as well as promoting their synthesis and inhibiting their degradation (Saltiel & Kahn 2001). Insulin also stimulates protein synthesis and inhibits protein degradation by activating mTOR (Raught, Gingras & Sonenberg 2001). The mechanistic (formerly “mammalian”) target of rapamycin (mTOR) signaling network revolves around the protein kinase mTOR which promotes cell growth and proliferation in eukaryotes through a large number of downstream targets (Hay & Sonenberg 2004; Saxton & Sabatini 2017).

Previous work examining ontogenetic changes in hepatic sex-biased gene expression in brown anoles has found that all three of these signaling pathways exhibit ontogenetic increases in the liver from subadult to adult life stages (Cox *et al.* 2017). In particular, the GH/IGF and mTOR pathways exhibit higher ontogenetic increases in sex-biased expression relative to the general trend of sex-biased expression (Cox *et al.* 2017). Differential expression of genes in these pathways in target tissues (e.g., expression of hormone receptors in musculoskeletal tissue) might be a key genetic mechanism that allows sexual size dimorphism to evolve (Ranz *et al.* 2003; Emlen *et al.* 2006; McGlothlin & Ketterson 2008; Williams & Carroll 2009), however it is unknown how these pathways are differentially utilized between the sexes over ontogeny and across tissues important to the development of sexual size dimorphism.

We selected three a priori signaling pathways that regulate growth, metabolism, and cell proliferation in vertebrates to examine (1) the growth hormone/insulin-like growth factor (GH/IGF) axis, (2) insulin-signaling network, and (3) the mechanistic target of rapamycin

(mTOR) gene networks. An illustration of how these pathways interact in the liver is provided in Figure 2.1. Exploring sex-biased gene expression patterns of these pathways will uncover how complex physiological traits like growth are regulated over time and coordinated among tissues to avoid intralocus sexual conflict and directly connect sex-biased gene expression to sexually dimorphic phenotypes.

We used a targeted approach to characterize the differential gene expression basis of sexual size dimorphism and examined the expression of the GH/IGF axis, insulin-signaling, and mTOR growth regulatory signaling pathways. We sought to answer these questions: (1) How do the sexes differ in expression of growth regulatory signaling pathways important to the regulation of growth? (2) How do sex-specific expression patterns of growth regulatory signaling pathways change over time? (3) How do tissues important to the development of sexual dimorphism differ in expression of growth regulatory signaling pathways? (4) How does expression of growth regulatory signaling pathways within tissues change over time? We predicted: (1) Sex-biased expression of growth regulatory signaling pathways would generally be male-biased in direction as male brown anoles experience higher rates of growth and attain larger body size relative to female brown anoles. (2) Expression levels of growth regulatory signaling pathways would increase over time for both sexes as they develop from juveniles to adults, but male expression levels would increase more over time as they grow larger than females. (3) As an upstream regulator of these networks, the brain should exhibit more expression of upstream components of growth regulatory signaling pathways relative to the liver and muscle, which should exhibit expression of downstream components of growth regulatory signaling pathways. In addition, the brain should not exhibit as much sex-biased gene expression relative to the liver and muscle as small amounts of upstream component expression can enact large downstream

effects and, therefore, the brain may not require sex-biased expression of growth regulatory signaling pathways to regulate development of sexual size dimorphism. 4) The brain should exhibit relatively constant levels of expression of growth regulatory signaling pathways over time as an upstream regulator, and we expect that liver and muscle expression of growth regulatory signaling pathways will increase over time as the sexes grow. In addition, the liver and muscle and should show the greatest increases in expression at eight and twelve months, the two ages with the greatest amount of growth for both sexes.

MATERIALS AND METHODS

Study System

We focused on the brown anole, which exhibits male-biased extreme sexual size dimorphism. We used laboratory-raised brown anoles, descended from a wild population in The Bahamas, to collect tissues important to growth and assess gene expression patterns. For additional information see Materials and Methods of Chapter 1.

Animal husbandry

Animals were cared for in a vivarium at the University of Virginia in Charlottesville, Virginia. Animals were housed separately, watered twice daily, and fed a diet of crickets, amount and frequency depending on age and sex of the individual. Environmental conditions were kept at levels meant to replicate natural conditions. For additional information see Materials and Methods of Chapter 1.

Tissue Collection

Liver, femoral muscle, and brain were collected from male and female brown anoles of ages one, four, eight, and twelve months. Animals were euthanized by decapitation, a method approved by the University of Virginia Animal Care and Use Committee (Protocol 3896).

Following euthanasia, animals were dissected and tissues of interest were placed in RNAlater solution to preserve RNA integrity. For additional information see Materials and Methods of Chapter 1.

RNA Isolation and Sequencing

Tissue samples were transported, on dry ice, to Georgia Southern University in Statesboro, Georgia. Total RNA was extracted from all samples utilizing a TRIzol reagent protocol. RNA from one-month-old anoles were pooled to meet minimum RNA concentrations required for sequencing. RNA samples were submitted to the Georgia Genomics Facility at the University of Georgia and sequenced on the Illumina NextSeq 500 platform. For additional information see Materials and Methods of Chapter 1.

Transcriptome Assembly and RNA-Seq Analysis

RNA-Seq data were quality filtered, mapped to the *Anolis carolinensis* genome, and analyzed for differential expression of genes predicted to be important to the development of sexual size dimorphism in brown anoles using several bioinformatic programs. For additional information see Materials and Methods of Chapter 1.

Assembly of Growth Gene Networks.

In this targeted approach, we a priori selected the growth hormone/insulin-like growth factor (GH/IGF) network, the mechanistic target of rapamycin (mTOR) network, and the insulin-signaling network to examine for differential gene expression between the liver, muscle, and brain tissues of male and female brown anoles across their development. These signaling pathways regulate growth, energetics, and cell proliferation in vertebrates and are likely to be differentially utilized in brown anoles, a system that exhibits extreme sexual size dimorphism. We used the KEGG database (Kanehisa & Goto 2000; Kanehisa *et al.* 2004) and WikiPathways

(Kelder *et al.* 2011) to identify and assemble genes annotated to belong to these networks and developed an a priori list of 114 genes (hereafter “growth genes”; Table 2.1), five of which that had two splice variants. Tables 2.2 through 2.4 contain the individual networks and the growth genes that belong to them.

Statistical Methods

In addition to differential gene expression analysis, we used general linear models to test for differences in mean expression of the GH/IGF, insulin-signaling, and mTOR growth networks between sexes, ages, and tissues. We also tested for differences in mean expression levels of several growth genes crucial to our a priori selected growth networks between sexes, between ages, and between tissues.

RESULTS

The liver and muscle exhibited sex-biased expression of growth genes while the brain exhibited no sex-biased expression of any growth gene belonging to the GH/IGF, mTOR, and insulin-signaling networks a priori selected as being important to the development of sexual size dimorphism in the brown anole. The exact growth genes, broken down by age, that exhibited sex-biased expression in liver and muscle can be found in Table 2.5 and Table 2.6, respectively.

Amount of Sex-biased Growth Genes

In the liver (Figure 2.2A), the number of growth genes that exhibited sex-biased expression increased for both sexes over time. Neither sex exhibited sex-biased expression of growth genes at the one-month age point, but the number of growth genes with sex-biased expression continually increased to reach 14 in male livers and six in female livers at the twelve-month age point. The number of growth genes with sex-biased expression per sex was equal in the one- and four-month age points, but in the eight- and twelve-month age points the number of

growth genes with male sex-biased expression was more than double the number of growth genes with female-biased expression.

In the femoral muscle, the number of growth genes that exhibit sex-biased expression increased for both sexes over time (Figure 2.2B). Neither sex exhibited sex-biased expression of growth genes at the one-month age point, but the number of growth genes that exhibited sex-biased expression continually increased to reach nine in female femoral muscle and five in male femoral muscle at the twelve-month age point. The femoral muscle had a different pattern of sex-biased growth gene expression from the liver in that the difference in number of growth genes that exhibited sex-biased expression between the sexes was not as extreme and there were more growth genes with female-biased expression than growth genes with male-biased expression across ontogeny (Figure 2.2).

Tissue-specific Growth Gene Patterns

The liver and femoral muscle both exhibited divergent patterns of sex-biased growth gene expression. In the liver (Table 2.5), approximately half of the growth genes that exhibited sex-biased expression were growth genes that exhibited sex-biased expression over multiple age points. In the muscle (Table 2.6), only 4 out of 25 growth genes that exhibited sex-biased expression were genes that exhibited sex-bias at multiple age points. Additionally, the insulin-like growth factor pathway was disproportionately represented in the liver compared to the muscle. In the liver, insulin-like growth factors 1 and 2 both experienced male-biased expression across the four-, eight-, and twelve-month age points as well as several of their binding proteins. In the muscle, insulin-like growth factor 1 only exhibited sex-biased expression in eight-month-old males and insulin-like growth factor 2 exhibited no sex-biased expression for either sex at any age point. However, there was male sex-biased expression of insulin-like growth factor 2

binding protein 2 at eight months and female-biased expression of insulin-like growth factor binding proteins 4 and 7 at twelve months.

Growth Gene Expression Levels

The expression levels of all growth genes were similar between males and females within all tissues and that expression remained consistent across each age point within each tissue. In the liver (Figure 2.3A), mean growth gene expression did not differ between the sexes ($F_{(1,3800)} = 0.136$, $P = 0.713$) or ages ($F_{(3,3800)} = 0.836$, $P = 0.474$) and there was no interaction between sex or age ($F_{(3,3800)} = 0.148$, $P = 0.931$). In the muscle (Figure 2.3B), mean growth gene expression did not differ between the sexes ($F_{(1,3800)} = 0.093$, $P = 0.760$) or ages ($F_{(3,3800)} = 1.305$, $P = 0.271$) and there was no interaction between sex or age ($F_{(3,3800)} = 0.472$, $P = 0.702$). In the brain (Figure 2.3C), mean growth gene expression did not differ between the sexes ($F_{(1,3800)} = 0.037$, $P = 0.848$) or ages ($F_{(3,3800)} = 0.076$, $P = 0.973$) and there was no interaction between sex or age ($F_{(3,3800)} = 0.025$, $P = 0.995$). Although sexes and ages did not differ in mean growth gene expression levels within tissues, the tissues did differ in mean growth gene expression level between each other ($F_{(2,11421)} = 83.68$, $P < 0.0001$). These results indicate that while there were no sex- or age-specific patterns of mean growth gene expression there were tissue-specific patterns that differ from each other.

Sex-biased Growth Gene Expression Levels

The expression levels of growth genes that were sex-biased in expression exhibit divergent patterns in the liver and muscle (Figure 2.4). Due to both liver and muscle gene expression data violating the assumption of homogeneity of variance (Brown-Forsythe test statistics all less than 0.05), before and after log transformation, we adjusted our alpha level to 0.01 to compensate and further adjusted the alpha level to 0.005 using a Bonferroni correction (n

= 2). In the liver (Figure 2.4A), mean expression of growth genes exhibiting sex-biased expression differed between ages ($F_{(2,494)} = 7.325$, $P < 0.0001$) but did not differ between the sexes ($F_{(1,494)} = 5.169$, $P = 0.02342$) and there was no an interaction between sex and age ($F_{(2,494)} = 0.001$, $P = 0.99881$). In the muscle (Figure 2.4B), mean expression of growth genes exhibiting sex-biased expression differed between ages ($F_{(2,264)} = 8.257$, $P = 0.00033$) with a significant interaction between sex and age ($F_{(2,264)} = 5.770$, $P = 0.00353$) but did not differ between sexes ($F_{(1,264)} = 0.002$, $P = 0.96096$). These results may be indicative of a temporal trajectory of sex-biased growth gene expression within tissues as ages significantly differed in mean sex-biased growth gene expression while the sexes did not.

Growth Gene Network Expression

For all three networks, there were differences in mean expression among tissues (all p-values < 0.0001), however there were no significant differences in mean expression of any these networks between the sexes or between ages with no significant interactions between. Full results are available in Table 2.7.

Expression of Growth Hormone Receptor and Growth Factors

The expression of growth hormone receptor (GHR; Figure 2.5) increased in both the liver and muscle across ontogeny, but not the brain. GHR significantly differed in mean expression between ages ($F_{(3,72)} = 14.694$, $P < 0.0001$) and between tissues ($F_{(2,72)} = 307.124$, $P < 0.0001$) and had a significant interaction between age and tissue ($F_{(6,72)} = 4.89$, $P < 0.0001$). GHR did not significantly differ in mean expression between sexes or have other significant interactions (all p-values > 0.05 ; Table 2.7). The expression of insulin-like growth factor 1 (IGF1; Figure 2.6) increasingly diverged between the sexes throughout ontogeny and was heavily male-biased through ages four, eight, and twelve months. IGF1 significantly differed in mean expression

between the sexes ($F_{(1,72)} = 66.810$, $P < 0.0001$) and between tissues ($F_{(2,72)} = 85.173$, $P < 0.0001$) with a significant interaction between sex and tissue ($F_{(2,72)} = 62.225$, $P < 0.0001$). The expression of insulin-like growth factor 2 (IGF2; Figure 2.6) had a similar pattern to IGF1, being highly divergent in the liver relative to muscle and brain. IGF2 significantly differed in mean expression between sexes ($F_{(1,72)} = 33.250$, $P < 0.0001$), between ages ($F_{(3,72)} = 6.049$, $P < 0.0010$), and between tissues ($F_{(2,72)} = 66.810$, $P < 0.0001$). The interactions between sex and tissue ($F_{(2,72)} = 33.117$, $P < 0.0001$) and age and tissue ($F_{(6,72)} = 6.079$, $P < 0.0001$) were also significant while interactions involving both sex and age are not.

Expression of Growth Factor Binding Proteins and Receptor

The insulin-like growth factor binding proteins one through seven (IGFBP1-7) varied in their sex-, age-, and tissue-specific patterns (Figure 2.7; Table 2.8). All IGFBPs had significant differences in mean expression between tissues, while IGFBP2, IGFBP4, and IGFBP5 also had significant differences between sexes. IGFBP2 and IGFBP4 additionally both had significant differences in mean expression between ages while the other IGFBPs did not. All possible interactions had at least one IGFBP where they were significant except for the sex and age interaction that was not significant in any IGFBP. The *Anolis carolinensis* genome has two splice variants for the insulin-like growth factor 1 receptor (IGF1R): IGF1R-201 and IGF1R-202. Overall expression of IGF1R was much lower compared to other target growth genes (Figure 2.8). Both splice variants significantly differed in mean gene expression between tissues (Table 2.8) but did not significantly differ between sexes or between ages with no significant interactions between factors.

Expression of Insulin-signaling and mTOR

The *Anolis carolinensis* genome did not have an annotated insulin receptor ortholog at the time of transcriptome assembly, so we examined the expression of insulin receptor substrate 1 (IRS1) and insulin receptor substrate 4 (IRS4; Figure 2.9) which both bind to insulin receptor. IRS1 only significantly differed in mean expression between tissues ($F_{(2,72)} = 439.672$, $P < 0.0001$) with no significant differences between sexes or ages and no significant interactions. IRS4 significantly differed in mean expression between ages ($F_{(3,72)} = 6.465$, $P = 0.00062$) and tissues ($F_{(2,72)} = 62.057$, $P < 0.0001$) with significant interactions between sex and age ($F_{(3,72)} = 5.030$, $P = 0.00320$), age and tissue ($F_{(6,72)} = 5.387$, $P = 0.00012$), and between sex, age, and tissue ($F_{(6,72)} = 3.684$, $P = 0.00301$). The mechanistic target of rapamycin (mTOR) was expressed at a similar level within the muscle and brain but not the liver across age points for both sexes (Figure 2.10). mTOR only significantly differed in mean expression between ages ($F_{(3,72)} = 8.929$, $P < 0.0001$) and between tissues ($F_{(2,72)} = 63.052$, $P < 0.0001$) with a significant interaction between age and tissue ($F_{(6,72)} = 6.936$, $P < 0.0001$; Table 2.3).

DISCUSSION

Determining the relationship between differences in gene expression and differences in phenotype is one of the outstanding questions in the study of the molecular basis of sexual dimorphism (Mank 2017). As sexual dimorphism is essentially a form of polyphenism, the relationship between gene expression and phenotype is also fundamental to understanding the evolution of phenotypic diversity and speciation (Nijhout 2003; West-Eberhard 2003). Crucially, the role of genes that are sex-biased in expression in the development and evolution of sexual dimorphism is unclear. Large proportions of the genome are genes that exhibit sex-biased expression (Zhang *et al.* 2007; Mank *et al.* 2010) and while there are relationships between the magnitude of sex-biased gene expression and phenotypic dimorphism (Pointer *et al.* 2013;

Harrison *et al.* 2015), we found no causal relationships between total number of genes with sex-biased expression and phenotypic dimorphism. Given that there is significant variation in amount of sex-biased gene expression and impact of individual loci, it is likely that there are subsets of genes that contribute more to sexual dimorphism.

We found that many genes in the growth hormone/insulin-like growth factor (GH/IGF) axis increased in sex-biased expression during development. The GH/IGF axis is a signaling pathway that regulates postnatal muscle and bone growth in vertebrates through a complex system of direct influences and feedback interactions between growth hormone, insulin-like growth factors, and tissues that they act on (Giustina, Mazziotti & Canalis 2008; Perrini *et al.* 2010). Growth hormone (GH) is a peptide hormone synthesized in and secreted from the anterior pituitary gland in the brain. Its binding to growth hormone receptor (GHR), which is highly expressed in the liver and skeletal muscle as well as the heart, lungs, kidneys, pancreas, intestine, and cartilage, initiates signal transduction and GH's primary method of action: synthesis of insulin-like growth factor 1 (IGF1). IGF1 is a complex growth-promoting hormone that has a similar structure to insulin and acts as both a systemic hormone and as a localized growth factor (Melmed 1999). Systemic IGF1 is synthesized in the liver as an endocrine hormone and is GH dependent while localized synthesis of IGF1 outside of the liver is regulated by a variety of other hormones (Melmed 1999). IGF1 binds to IGF1 binding proteins which alter IGF1's interaction with cell surface receptors, and then binds to the IGF1 receptor, a transmembrane cell surface receptor that mediates IGF1's effects to promote growth and cell proliferation across somatic tissues (Ohlsson *et al.* 2009). Insulin-like growth factor 2 (IGF2) is a similar peptide hormone to IGF1 and is thought to primarily promote prenatal growth (Giustina, Mazziotti & Canalis 2008) but may more generally promote growth across ontogeny in reptiles (McGaugh *et al.* 2015; Cox

et al. 2017). Surprisingly, ontogenetic increases in size (Figure 1.1) were not accompanied by ontogenetic increases in expression of the GH/IGF network (Figure 2.11). Across the whole GH/IGF network, the only significant difference in mean gene expression was between tissues with no significant interactions between any factors (Table 2.3). These results suggest that the whole GH/IGF network may be regulated by tissue-specific patterns that are constant between the sexes throughout ontogeny. However, the number of genes with sex-biased expression in this network increased in the liver (Table 2.1) and muscle (Table 2.2) across ontogeny, which suggests that sex-biased expression of only a subset of genes in the GH/IGF network may be required to direct the GH/IGF pathway's involvement in development of sexual size dimorphism. Additionally, we found that IGF2 expression increased throughout ontogeny in both sexes, providing support for IGF2's role in reptilian growth across ontogeny (McGaugh *et al.* 2015).

The insulin-signaling network is a crucial biological pathway that regulates glucose and lipid metabolism. Insulin regulates metabolism by stimulating glucose, fatty acid, and amino acid uptake into cells as well as promoting their synthesis and inhibiting their degradation (as reviewed in (Saltiel & Kahn 2001)). Insulin also stimulates protein synthesis and inhibits protein degradation by activating mTOR (Raught, Gingras & Sonenberg 2001). We found that mean expression of the whole insulin-signaling network (Figure 2.12) only significantly differed between tissues (Table 2.3) and not between the sexes or between ages. Similar to the GH/IGF pathway, this may indicate that expression of the insulin-signaling network is directed by tissue-specific and not sex- or age-specific trajectories to direct growth of sexual size dimorphism. However, there was sex-biased expression of genes in the insulin-signaling pathway throughout ontogeny in both the liver and muscle (Table 2.)

The mechanistic (formerly “mammalian”) target of rapamycin (mTOR) signaling network revolves around the protein kinase mTOR which promotes cell growth and proliferation in eukaryotes through a large number of downstream targets (Hay & Sonenberg 2004; Saxton & Sabatini 2017). mTOR is able to regulate protein synthesis by phosphorylating/inactivating the mRNA translation inhibitor 4E-BP1 (Brunn *et al.* 1996) and phosphorylating/activating S6 Kinase which promotes mRNA translation initiation and cell proliferation (Brown *et al.* 1995). mTOR further facilitates cell growth by promoting lipid synthesis for cell membrane formation and expansion (Porstmann *et al.* 2008), nucleotide synthesis for DNA replication and ribosome generation (Ben-Sahra *et al.* 2013; Robitaille *et al.* 2013; Ben-Sahra *et al.* 2016), and glucose metabolism (Düvel *et al.* 2010; Saxton & Sabatini 2017). In addition to numerous other roles in regulating cell growth and proliferation (reviewed in (Hay & Sonenberg 2004; Saxton & Sabatini 2017), mTOR is associated with muscle hypertrophy (Anthony *et al.* 2000; Bodine *et al.* 2001) and may promote muscle growth as a downstream target of IGF1 (Rommel *et al.* 2001). We found that mean expression of the whole mTOR network (Figure 2.13) only differed between tissues and not between the sexes or between ages (Table 2.3). However, elements of the mTOR network experienced sex-biased expression in the liver and muscle throughout ontogeny. These results may indicate that tissue-specific patterns of expression of the whole network and sex-biased expression of key genes over ontogeny in the pathway coordinate the mTOR network’s contribution to the development of sexual size dimorphism in the brown anole.

Sexual dimorphism is predicted to be difficult to evolve due to the buildup of between-sex genetic correlations due to a shared genome between the sexes. However differential expression of shared genes can reduce between-sex genetic correlations and allow sexual dimorphism to evolve. Large proportions of the genome exhibit sex-biased gene expression but it

is unclear what proportion of sex-biased genes are actually important to the development of sexual dimorphism. We examined the expression of 114 growth genes in the GH/IGF, insulin, and mTOR signaling pathways, that we predicted to be important to growth and development of sexual size dimorphism in the brown anole, in liver, muscle, and brain to uncover sex-, age-, and tissue-specific patterns. We predicted the sexes to exhibit high levels of sex-biased expression of these genes that increase over ontogeny in order to facilitate the development of their sexual size dimorphism. Indeed, we found that male and female brown anoles differentially expressed genes in these pathways in the liver and muscle, but not the brain, throughout ontogeny. We found that only 43.7% of the growth genes we examined exhibit sex-biased expression in at least one of three functionally diverse tissues important to growth. However, we chose to examine genes known to be strong effectors of growth, thus the sexes may not require a larger proportion of growth genes to be sex-biased in expression to develop sexual size dimorphism. Furthermore, when we tested for sex-, age-, and tissue-specific effects on gene expression of entire growth networks, we only found significant differences between tissues. Although these networks are crucial to the development of sexual size dimorphism, the sexes did not differ in expression levels of these growth networks. Combined with the low number of growth genes that exhibit sex-biased expression, these results suggest that sex-biased expression of only relatively few growth genes across three signaling pathways important to growth are required to develop sexual size dimorphism in brown anoles. More broadly, these results suggest that, despite large proportions of the genome exhibiting sex-biased gene expression, sex-biased expression of relatively few genes, albeit genes that exert strong effects, are enough to reduce between-sex genetic correlations and allow sexual dimorphism to develop. Thus, the genetic constraint of a

shared genome might be relatively easy to overcome, explaining the ubiquity of sexual dimorphism despite the genomic paradox of producing two phenotypes from a single genome.

REFERENCES

- Adkins-Regan, E. (2012) Hormonal organization and activation: evolutionary implications and questions. *General and Comparative Endocrinology*, **176**, 279-285.
- Anthony, J.C., Yoshizawa, F., Anthony, T.G., Vary, T.C., Jefferson, L.S. & Kimball, S.R. (2000) Leucine stimulates translation initiation in skeletal muscle of postabsorptive rats via a rapamycin-sensitive pathway. *The Journal of Nutrition*, **130**, 2413-2419.
- Badyaev, A.V. (2002) Growing apart: an ontogenetic perspective on the evolution of sexual size dimorphism. *Trends in Ecology & Evolution*, **17**, 369-378.
- Ben-Sahra, I., Howell, J.J., Asara, J.M. & Manning, B.D. (2013) Stimulation of de novo pyrimidine synthesis by growth signaling through mTOR and S6K1. *Science*, 1228792.
- Ben-Sahra, I., Hoxhaj, G., Ricoult, S.J.H., Asara, J.M. & Manning, B.D. (2016) mTORC1 induces purine synthesis through control of the mitochondrial tetrahydrofolate cycle. *Science*, **351**, 728-733.
- Bodine, S.C., Stitt, T.N., Gonzalez, M., Kline, W.O., Stover, G.L., Bauerlein, R., Zlotchenko, E., Scrimgeour, A., Lawrence, J.C. & Glass, D.J.J.N.c.b. (2001) Akt/mTOR pathway is a crucial regulator of skeletal muscle hypertrophy and can prevent muscle atrophy in vivo. *Nature Cell Biology*, **3**, 1014.
- Bonduriansky, R. (2007) The genetic architecture of sexual dimorphism: the potential roles of genomic imprinting and condition dependence. *Sex, size and gender roles: evolutionary studies of sexual size dimorphism* (eds D.J. Fairbairn, W.U. Blanckenhorn & T. Székely), pp. 176-184. Oxford University Press, Oxford, United Kingdom.
- Bonduriansky, R. & Chenoweth, S.F. (2009) Intralocus sexual conflict. *Trends in Ecology & Evolution*, **24**, 280-288.

- Bonduriansky, R., Rowe, L. & Tregenza, T. (2005) Intralocus sexual conflict and the genetic architecture of sexually dimorphic traits in *Prochyliza xanthostoma* (Diptera: Piophilidae). *Evolution*, **59**, 1965-1975.
- Brown, E.J., Beal, P.A., Keith, C.T., Chen, J., Shin, T.B. & Schreiber, S.L. (1995) Control of p70 s6 kinase by kinase activity of FRAP in vivo. *Nature*, **377**, 441.
- Brunn, G.J., Williams, J., Sabers, C., Wiederrecht, G., Lawrence Jr, J. & Abraham, R.T. (1996) Direct inhibition of the signaling functions of the mammalian target of rapamycin by the phosphoinositide 3-kinase inhibitors, wortmannin and LY294002. *The EMBO Journal*, **15**, 5256-5267.
- Butler, M.A., Schoener, T.W. & Losos, J.B. (2000) The relationship between sexual size dimorphism and habitat use in Greater Antillean *Anolis* lizards. *Evolution*, **54**, 259-272.
- Chippindale, A.K., Gibson, J.R. & Rice, W.R. (2001) Negative genetic correlation for adult fitness between sexes reveals ontogenetic conflict in *Drosophila*. *Proceedings of the National Academy of Sciences*, **98**, 1671-1675.
- Connallon, T. & Clark, A.G. (2011) The resolution of sexual antagonism by gene duplication. *Genetics*, genetics. 110.123729.
- Cox, R.M. & Calsbeek, R. (2009) Sexually antagonistic selection, sexual dimorphism, and the resolution of intralocus sexual conflict. *The American Naturalist*, **173**, 176-187.
- Cox, R.M., Cox, C.L., McGlothlin, J.W., Card, D.C., Andrew, A.L. & Castoe, T.A. (2017) Hormonally Mediated Increases in Sex-Biased Gene Expression Accompany the Breakdown of Between-Sex Genetic Correlations in a Sexually Dimorphic Lizard. *The American Naturalist*, **189**, 315-332.

- Cox, R.M., Skelly, S.L. & John-Alder, H.B.J.E. (2003) A comparative test of adaptive hypotheses for sexual size dimorphism in lizards. **57**, 1653-1669.
- Cox, R.M., Stenquist, D.S. & Calsbeek, R. (2009) Testosterone, growth and the evolution of sexual size dimorphism. *Journal of evolutionary biology*, **22**, 1586-1598.
- Darwin, C. (1888) *The descent of man and selection in relation to sex*. Murray.
- Day, T. & Bonduriansky, R. (2004) Intralocus sexual conflict can drive the evolution of genomic imprinting. *Genetics*, **167**, 1537-1546.
- Düvel, K., Yecies, J.L., Menon, S., Raman, P., Lipovsky, A.I., Souza, A.L., Triantafellow, E., Ma, Q., Gorski, R. & Cleaver, S. (2010) Activation of a metabolic gene regulatory network downstream of mTOR complex 1. *Molecular Cell*, **39**, 171-183.
- Ellegren, H. & Parsch, J. (2007) The evolution of sex-biased genes and sex-biased gene expression. *Nature Reviews Genetics*, **8**, 689-698.
- Emlen, D., Szafran, Q., Corley, L. & Dworkin, I.J.H. (2006) Insulin signaling and limb-patterning: candidate pathways for the origin and evolutionary diversification of beetle 'horns'. **97**, 179.
- Fairbairn, D.J. & Roff, D.A. (2006) The quantitative genetics of sexual dimorphism: assessing the importance of sex-linkage. *Heredity*, **97**, 319.
- Fisher, R.A. (1999) *The genetical theory of natural selection: a complete variorum edition*. Oxford University Press, Oxford, United Kingdom.
- Gallach, M. & Betrán, E. (2011) Intralocus sexual conflict resolved through gene duplication. *Trends in Ecology & Evolution*, **26**, 222-228.
- Giustina, A., Mazziotti, G. & Canalis, E. (2008) Growth hormone, insulin-like growth factors, and the skeleton. *Endocrine reviews*, **29**, 535-559.

- Grath, S. & Parsch, J. (2016) Sex-biased gene expression. *Annual Review of Genetics*, **50**, 29-44.
- Harrison, P.W., Wright, A.E., Zimmer, F., Dean, R., Montgomery, S.H., Pointer, M.A. & Mank, J.E. (2015) Sexual selection drives evolution and rapid turnover of male gene expression. *Proceedings of the National Academy of Sciences*, 201501339.
- Hay, N. & Sonenberg, N. (2004) Upstream and downstream of mTOR. *Genes & Development*, **18**, 1926-1945.
- Ingleby, F.C., Flis, I. & Morrow, E.H. (2015) Sex-biased gene expression and sexual conflict throughout development. *Cold Spring Harbor perspectives in biology*, **7**, a017632.
- Innocenti, P. & Morrow, E.H. (2010) The sexually antagonistic genes of *Drosophila melanogaster*. *PLoS biology*, **8**, e1000335.
- Kanehisa, M. & Goto, S. (2000) KEGG: kyoto encyclopedia of genes and genomes. *Nucleic acids research*, **28**, 27-30.
- Kanehisa, M., Goto, S., Kawashima, S., Okuno, Y. & Hattori, M. (2004) The KEGG resource for deciphering the genome. *Nucleic acids research*, **32**, D277-D280.
- Kelder, T., van Iersel, M.P., Hanspers, K., Kutmon, M., Conklin, B.R., Evelo, C.T. & Pico, A.R. (2011) WikiPathways: building research communities on biological pathways. *Nucleic acids research*, **40**, D1301-D1307.
- Kijimoto, T., Moczek, A.P. & Andrews, J. (2012) Diversification of doublesex function underlies morph-, sex-, and species-specific development of beetle horns. *Proceedings of the National Academy of Sciences*, **109**, 20526-20531.
- Lande, R. (1980) Sexual dimorphism, sexual selection, and adaptation in polygenic characters. *Evolution*, 292-305.

- Lande, R. (1987) Genetic correlations between the sexes in the evolution of sexual dimorphism and mating preferences. *Sexual Selection: Testing the Alternatives* (eds J.W. Bradbury & M.B. Andersson), pp. 83-94. Wiley, Chichester, United Kingdom.
- Mank, J.E. (2009) Sex chromosomes and the evolution of sexual dimorphism: lessons from the genome. *The American Naturalist*, **173**, 141-150.
- Mank, J.E. (2017) The transcriptional architecture of phenotypic dimorphism. *Nature Ecology & Evolution*, **1**, 0006.
- Mank, J.E., Nam, K., Brunström, B. & Ellegren, H. (2010) Ontogenetic complexity of sexual dimorphism and sex-specific selection. *Molecular biology and evolution*, **27**, 1570-1578.
- McGaugh, S.E., Bronikowski, A.M., Kuo, C.-H., Reding, D.M., Addis, E.A., Fligel, L.E., Janzen, F.J. & Schwartz, T.S. (2015) Rapid molecular evolution across amniotes of the IIS/TOR network. *Proceedings of the National Academy of Sciences*, 201419659.
- McGlothlin, J.W. & Ketterson, E.D. (2008) Hormone-mediated suites as adaptations and evolutionary constraints. *Philosophical Transactions of the Royal Society of London B: Biological Sciences*, **363**, 1611-1620.
- Melmed, S. (1999) Insulin-Like Growth Factor I—A Prototypic Peripheral-Paracrine Hormone? *Endocrinology*, **140**, 3879-3880.
- Nijhout, H.F. (2003) Development and evolution of adaptive polyphenisms. *Evolution & development*, **5**, 9-18.
- Ohlsson, C., Mohan, S., Sjogren, K., Tivesten, A., Isgaard, J., Isaksson, O., Jansson, J.-O. & Svensson, J. (2009) The role of liver-derived insulin-like growth factor-I. *Endocrine reviews*, **30**, 494-535.

- Perrini, S., Laviola, L., Carreira, M.C., Cignarelli, A., Natalicchio, A. & Giorgino, F. (2010) The GH/IGF1 axis and signaling pathways in the muscle and bone: mechanisms underlying age-related skeletal muscle wasting and osteoporosis. *Journal of Endocrinology*, **205**, 201-210.
- Pointer, M.A., Harrison, P.W., Wright, A.E. & Mank, J.E. (2013) Masculinization of gene expression is associated with exaggeration of male sexual dimorphism. *PLoS genetics*, **9**, e1003697.
- Poissant, J., Wilson, A.J. & Coltman, D.W. (2010) Sex-specific genetic variance and the evolution of sexual dimorphism: a systematic review of cross-sex genetic correlations. *Evolution*, **64**, 97-107.
- Porstmann, T., Santos, C.R., Griffiths, B., Cully, M., Wu, M., Leever, S., Griffiths, J.R., Chung, Y.-L. & Schulze, A. (2008) SREBP activity is regulated by mTORC1 and contributes to Akt-dependent cell growth. *Cell metabolism*, **8**, 224-236.
- Ranz, J.M., Castillo-Davis, C.I., Meiklejohn, C.D. & Hartl, D.L. (2003) Sex-dependent gene expression and evolution of the Drosophila transcriptome. *Science*, **300**, 1742-1745.
- Raught, B., Gingras, A.-C. & Sonenberg, N. (2001) The target of rapamycin (TOR) proteins. *Proceedings of the National Academy of Sciences*, **98**, 7037-7044.
- Rice, W. & Chippindale, A. (2001) Intersexual ontogenetic conflict. *Journal of evolutionary biology*, **14**, 685-693.
- Rice, W.R. (1984) Sex chromosomes and the evolution of sexual dimorphism. *Evolution*, **38**, 735-742.
- Roberts, R.B., Ser, J.R. & Kocher, T.D. (2009) Sexual conflict resolved by invasion of a novel sex determiner in Lake Malawi cichlid fishes. *Science*, **326**, 998-1001.

- Robitaille, A.M., Christen, S., Shimobayashi, M., Cornu, M., Fava, L.L., Moes, S., Prescianotto-Baschong, C., Sauer, U., Jenoe, P. & Hall, M.N. (2013) Quantitative phosphoproteomics reveal mTORC1 activates de novo pyrimidine synthesis. *Science*, **339**, 1320-1323.
- Rommel, C., Bodine, S.C., Clarke, B.A., Rossman, R., Nunez, L., Stitt, T.N., Yancopoulos, G.D. & Glass, D.J. (2001) Mediation of IGF-1-induced skeletal myotube hypertrophy by PI (3) K/Akt/mTOR and PI (3) K/Akt/GSK3 pathways. *Nature Cell Biology*, **3**, 1009.
- Saltiel, A.R. & Kahn, C.R. (2001) Insulin signalling and the regulation of glucose and lipid metabolism. *Nature*, **414**, 799.
- Sanger, T.J., Sherratt, E., McGlothlin, J.W., Brodie, E.D., Losos, J.B. & Abzhanov, A. (2013) Convergent evolution of sexual dimorphism in skull shape using distinct developmental strategies. *Evolution*, **67**, 2180-2193.
- Saxton, R.A. & Sabatini, D.M. (2017) mTOR signaling in growth, metabolism, and disease. *Cell*, **168**, 960-976.
- Selander, R.K. (1966) Sexual dimorphism and differential niche utilization in birds. *The Condor*, **68**, 113-151.
- Shine, R. (1989) Ecological causes for the evolution of sexual dimorphism: a review of the evidence. *The Quarterly Review of Biology*, **64**, 419-461.
- Stewart, A.D., Pischedda, A. & Rice, W.R. (2010) Resolving intralocus sexual conflict: genetic mechanisms and time frame. *Journal of Heredity*, **101**, S94-S99.
- Van Doorn, G.S. & Kirkpatrick, M. (2007) Turnover of sex chromosomes induced by sexual conflict. *Nature*, **449**, 909.
- West-Eberhard, M.J. (2003) *Developmental plasticity and evolution*. Oxford University Press, Oxford, United Kingdom.

- Williams, T.M. & Carroll, S.B. (2009) Genetic and molecular insights into the development and evolution of sexual dimorphism. *Nature Reviews Genetics*, **10**, 797.
- Zhang, Y., Sturgill, D., Parisi, M., Kumar, S. & Oliver, B. (2007) Constraint and turnover in sex-biased gene expression in the genus *Drosophila*. *Nature*, **450**, 233.

Table 2.1 A list of all 114 a priori growth genes found in the growth hormone/insulin-like growth factor (GH/IGF), insulin-signaling, and mechanistic target of rapamycin (mTOR) networks. Gene IDs ending in “.1” and “.2” reflect the 201 splice variant and 202 splice variant of the gene, respectively.

Ensembl transcript ID	Gene ID	Ensembl description
ENSACAT00000010700	GHR	Growth Hormone Receptor [Source:Hgnc Symbol;Acc:4263]
ENSACAT00000006111	GHRRH	Growth Hormone Releasing Hormone Receptor [Source:Hgnc Symbol;Acc:4266]
ENSACAT00000016563	IGF1	Insulin-Like Growth Factor 1 (Somatomedin C) [Source:Hgnc Symbol;Acc:5464]
ENSACAT00000008062	IGFBP1	Insulin-Like Growth Factor Binding Protein 1 [Source:Hgnc Symbol;Acc:5469]
ENSACAT00000004558	IGFBP2	Insulin-Like Growth Factor Binding Protein 2, 36Kda [Source:Hgnc Symbol;Acc:5471]
ENSACAT00000008083	IGFBP3	Insulin-Like Growth Factor Binding Protein 3 [Source:Hgnc Symbol;Acc:5472]
ENSACAT00000016203	IGFBP4	Insulin-Like Growth Factor Binding Protein 4 [Source:Hgnc Symbol;Acc:5473]
ENSACAT00000000083	IGFBP5	Insulin-Like Growth Factor Binding Protein 5 [Source:Hgnc Symbol;Acc:5474]
ENSACAT00000029049	IGFBP6	Insulin-Like Growth Factor Binding Protein 6 [Source:Hgnc Symbol;Acc:5475]
ENSACAT00000002051	IGFBP7	Insulin-Like Growth Factor Binding Protein 7 [Source:Hgnc Symbol;Acc:5476]
ENSACAT00000029347	IGF1R.1	Insulin-Like Growth Factor 1 Receptor [Source:Hgnc Symbol;Acc:5465]
ENSACAT00000008235	IGF1R.2	Insulin-Like Growth Factor 1 Receptor [Source:Hgnc Symbol;Acc:5465]
ENSACAT00000009701	IGF2	Insulin-Like Growth Factor 2 (Somatomedin A) [Source:Hgnc Symbol;Acc:5466]
ENSACAT00000006271	IGF2BP1	Insulin-Like Growth Factor 2 Mrna Binding Protein 1 [Source:Hgnc Symbol;Acc:28866]
ENSACAT00000008070	IGF2BP2	Insulin-Like Growth Factor 2 Mrna Binding Protein 2 [Source:Hgnc Symbol;Acc:28867]
ENSACAT00000013612	IGF2BP3	Insulin-Like Growth Factor 2 Mrna Binding Protein 3 [Source:Hgnc Symbol;Acc:28868]
ENSACAT00000011634	AKT1	Akt Serine/Threonine Kinase 1 [Source:Hgnc Symbol;Acc:Hgnc:391]
ENSACAT00000002209	Cbl	Cbl Proto-Oncogene [Source:Hgnc Symbol;Acc:Hgnc:1541]
ENSACAT00000004315	CDKN1B	Cyclin-Dependent Kinase Inhibitor 1B (P27, Kip1) [Source:Hgnc Symbol;Acc:1785]
ENSACAT00000029358	EIF4EBP1	Eukaryotic Translation Initiation Factor 4E Binding Protein 1 [Source:Hgnc Symbol;Acc:3288]
ENSACAT00000014236	EIF4E	Eukaryotic Translation Initiation Factor 4E [Source:Hgnc Symbol;Acc:3287]
ENSACAT00000017135	GYS2	Glycogen Synthase 2 [Source:Hgnc Symbol;Acc:Hgnc:4707]
ENSACAT00000004836	GYS1	Glycogen Synthase 1 [Source:Hgnc Symbol;Acc:Hgnc:4706]

ENSACAT00000004723	ELK1	Ets Transcription Factor [Source:Hgnc Symbol;Acc:Hgnc:3321]
ENSACAT00000009932	FASN	Fatty Acid Synthase [Source:Hgnc Symbol;Acc:Hgnc:3594]
ENSACAT00000013303	FBP1	Fructose-Bisphosphatase 1 [Source:Hgnc Symbol;Acc:Hgnc:3606]
ENSACAT00000008015	FLOT2	Flotillin 2 [Source:Ncbi Gene;Acc:100563055]
ENSACAT00000017291	FLOT1	Flotillin 1 [Source:Hgnc Symbol;Acc:Hgnc:3757]
ENSACAT00000001070	G6PC2	Glucose-6-Phosphatase Catalytic Subunit 2 [Source:Hgnc Symbol;Acc:Hgnc:28906]
ENSACAT00000007397	GNL3.1	G Protein Nucleolar 3 [Source:Hgnc Symbol;Acc:Hgnc:29931]
ENSACAT00000026449	GNL3.2	G Protein Nucleolar 3 [Source:Hgnc Symbol;Acc:Hgnc:29931]
ENSACAT00000006564	GRB2	Growth Factor Receptor-Bound Protein 2 [Source:Hgnc Symbol;Acc:4566]
ENSACAT00000016466	RAPGEF2	Rap Guanine Nucleotide Exchange Factor 2 [Source:Hgnc Symbol;Acc:Hgnc:16854]
ENSACAT00000013894	RAPGEF1	Rap Guanine Nucleotide Exchange Factor 1 [Source:Ncbi Gene;Acc:100558908]
ENSACAT00000029738	GSK3B.1	Glycogen Synthase Kinase 3 Beta [Source:Hgnc Symbol;Acc:Hgnc:4617] 201 Splice Variant
ENSACAT00000003712	GSK3B.2	Glycogen Synthase Kinase 3 Beta [Source:Hgnc Symbol;Acc:Hgnc:4617] 202 Splice Variant
ENSACAT00000007957	HSL	Hormone Sensitive Lipase
ENSACAT00000003820	IRS1	Insulin Receptor Substrate 1 [Source:Hgnc Symbol;Acc:6125]
ENSACAT00000012637	IRS4	Insulin Receptor Substrate 4 [Source:Hgnc Symbol;Acc:6128]
ENSACAT00000000408	MAP2K2	Mitogen-Activated Protein Kinase Kinase 2 [Source:Hgnc Symbol;Acc:6842]
ENSACAT00000001764	MAP2K3	Mitogen-Activated Protein Kinase Kinase 3 [Source:Hgnc Symbol;Acc:6843]
ENSACAT00000017532	MAP2K4	Mitogen-Activated Protein Kinase Kinase 4 [Source:Hgnc Symbol;Acc:6844]
ENSACAT00000010177	MAP2K5	Mitogen-Activated Protein Kinase Kinase 5 [Source:Hgnc Symbol;Acc:6845]
ENSACAT00000030866	MAP2K6	Mitogen-Activated Protein Kinase Kinase 6 [Source:Hgnc Symbol;Acc:6846]
ENSACAT00000009956	MAP2K7	Mitogen-Activated Protein Kinase Kinase 7 [Source:Hgnc Symbol;Acc:6847]
ENSACAT00000013773	MLST8	Mtor Associated Protein, Lst8 Homolog (S. Cerevisiae) [Source:Hgnc Symbol;Acc:24825]
ENSACAT00000010374	MYC	Myc Proto-Oncogene, Bhlh Transcription Factor [Source:Hgnc Symbol;Acc:Hgnc:7553]
ENSACAT00000013790	NR3C1	Nuclear Receptor Subfamily 3, Group C, Member 1 (Glucocorticoid Receptor) [Source:Hgnc Symbol;Acc:7978]
ENSACAT00000017591	PDE3A	Phosphodiesterase 3A [Source:Hgnc Symbol;Acc:Hgnc:8778]
ENSACAT00000003554	PDPK1	3-Phosphoinositide Dependent Protein Kinase-1 [Source:Hgnc Symbol;Acc:8816]
ENSACAT00000016391	PCK1	Phosphoenolpyruvate Carboxykinase 1 [Source:Hgnc Symbol;Acc:Hgnc:8724]
ENSACAT00000001275	PCK2	Phosphoenolpyruvate Carboxykinase 2, Mitochondrial [Source:Hgnc Symbol;Acc:Hgnc:8725]
ENSACAT00000004827	PPARA	Peroxisome Proliferator Activated Receptor Alpha [Source:Hgnc Symbol;Acc:Hgnc:9232]
ENSACAT00000011918	PHKA2	Phosphorylase Kinase Regulatory Subunit Alpha 2 [Source:Hgnc Symbol;Acc:Hgnc:8926]

ENSACAT00000014131	PHKB	Phosphorylase Kinase Regulatory Subunit Beta [Source:Hgnc Symbol;Acc:Hgnc:8927]
ENSACAT00000004979	PIK3CA	Phosphatidylinositol-4,5-Bisphosphate 3-Kinase, Catalytic Subunit Alpha [Source:Hgnc Symbol;Acc:8975]
ENSACAT00000017770	PIK3R5.1	Phosphoinositide-3-Kinase, Regulatory Subunit 5 [Source:Hgnc Symbol;Acc:30035]
ENSACAT00000029838	PIK3R5.2	Phosphoinositide-3-Kinase, Regulatory Subunit 5 [Source:Hgnc Symbol;Acc:30035]
ENSACAT00000006498	PRKCH	Protein Kinase C, Eta [Source:Hgnc Symbol;Acc:9403]
ENSACAT00000015152	PTEN	Phosphatase And Tensin Homolog [Source:Hgnc Symbol;Acc:9588]
ENSACAT00000014006	PYG	Glycogen Phosphorylase
ENSACAT00000012973	RAC1	Rac Family Small Gtpase 1 [Source:Hgnc Symbol;Acc:Hgnc:9801]
ENSACAT00000016135	RAC2	Rac Family Small Gtpase 2 [Source:Hgnc Symbol;Acc:Hgnc:9802]
ENSACAT00000029270	RAF1.1	Raf-1 Proto-Oncogene, Serine/Threonine Kinase [Source:Hgnc Symbol;Acc:Hgnc:9829]
ENSACAT00000013316	RAF1.2	Raf-1 Proto-Oncogene, Serine/Threonine Kinase [Source:Hgnc Symbol;Acc:Hgnc:9829]
ENSACAT00000004483	RASD1	Ras, Dexamethasone-Induced 1 [Source:Hgnc Symbol;Acc:15828]
ENSACAT00000002273	Rheb	Ras Homolog, Mtorc1 Binding [Source:Hgnc Symbol;Acc:Hgnc:10011]
ENSACAT00000014310	RHO	Rhodopsin [Source:Hgnc Symbol;Acc:10012]
ENSACAT00000010084	RICTOR	Rptor Independent Companion Of Mtor, Complex 2 [Source:Hgnc Symbol;Acc:28611]
ENSACAT00000013049	RPS6KB1	Ribosomal Protein S6 Kinase B1 [Source:Hgnc Symbol;Acc:Hgnc:10436]
ENSACAT00000016838	RPS6KL1	Ribosomal Protein S6 Kinase-Like 1 [Source:Hgnc Symbol;Acc:20222]
ENSACAT00000015640	RPTOR	Regulatory Associated Protein Of Mtor, Complex 1 [Source:Hgnc Symbol;Acc:30287]
ENSACAT00000014553	SHBG	Sex Hormone-Binding Globulin [Source:Hgnc Symbol;Acc:10839]
ENSACAT00000015879	SHC1	Shc Adaptor Protein 1 [Source:Hgnc Symbol;Acc:Hgnc:10840]
ENSACAT00000012679	SHC2	Shc Adaptor Protein 2 [Source:Ncbi Gene;Acc:100553545]
ENSACAT00000005997	SHC4	Shc Adaptor Protein 4 [Source:Hgnc Symbol;Acc:Hgnc:16743]
ENSACAT00000014599	SOCS1	Suppressor Of Cytokine Signaling 1 [Source:Hgnc Symbol;Acc:Hgnc:19383]
ENSACAT00000012617	SOCS2	Suppressor Of Cytokine Signaling 2 [Source:Hgnc Symbol;Acc:Hgnc:19382]
ENSACAT00000016743	SOCS3	Suppressor Of Cytokine Signaling 3 [Source:Hgnc Symbol;Acc:Hgnc:19391]
ENSACAT00000016330	SOCS4	Suppressor Of Cytokine Signaling 4 [Source:Hgnc Symbol;Acc:Hgnc:19392]
ENSACAT00000004217	SOCS5	Suppressor Of Cytokine Signaling 5 [Source:Hgnc Symbol;Acc:Hgnc:16852]
ENSACAT00000011543	SOCS6	Suppressor Of Cytokine Signaling 6 [Source:Hgnc Symbol;Acc:Hgnc:16833]
ENSACAT00000007427	SOCS7	Suppressor Of Cytokine Signaling 7 [Source:Hgnc Symbol;Acc:Hgnc:29846]
ENSACAT00000006394	SOS1	Sos Ras/Rac Guanine Nucleotide Exchange Factor 1 [Source:Hgnc Symbol;Acc:Hgnc:11187]
ENSACAT00000001643	SOS2	Sos Ras/Rho Guanine Nucleotide Exchange Factor 2 [Source:Hgnc Symbol;Acc:Hgnc:11188]

ENSACAT00000006298	STAT1	Signal Transducer And Activator Of Transcription 1, 91Kda [Source:Hgnc Symbol;Acc:11362]
ENSACAT00000025425	STAT2	Signal Transducer And Activator Of Transcription 2, 113Kda [Source:Hgnc Symbol;Acc:11363]
ENSACAT00000018021	STAT3	Signal Transducer And Activator Of Transcription 3 (Acute-Phase Response Factor) [Source:Hgnc Symbol;Acc:11364]
ENSACAT00000009792	STAT6	Signal Transducer And Activator Of Transcription 6, Interleukin-4 Induced [Source:Hgnc Symbol;Acc:11368]
ENSACAT00000014051	STK11	Serine/Threonine Kinase 11 [Source:Hgnc Symbol;Acc:11389]
ENSACAT0000001057	TGFB1	Transforming Growth Factor, Beta-Induced, 68Kda [Source:Hgnc Symbol;Acc:11771]
ENSACAT0000001108	TGFB2	Transforming Growth Factor, Beta 2 [Source:Hgnc Symbol;Acc:11768]
ENSACAT00000017101	TGFB3	Transforming Growth Factor, Beta 3 [Source:Hgnc Symbol;Acc:11769]
ENSACAT00000025616	TGFBP3L	Transforming Growth Factor, Beta Receptor Iii-Like [Source:Hgnc Symbol;Acc:44152]
ENSACAT00000009230	TGFBR1	Transforming Growth Factor, Beta Receptor 1 [Source:Hgnc Symbol;Acc:11772]
ENSACAT00000014316	TGFBR2	Transforming Growth Factor, Beta Receptor Ii (70/80Kda) [Source:Hgnc Symbol;Acc:11773]
ENSACAT0000001424	TGFBR3	Transforming Growth Factor, Beta Receptor Iii [Source:Hgnc Symbol;Acc:11774]
ENSACAT00000004260	TSC1	Tuberous Sclerosis 1 [Source:Hgnc Symbol;Acc:12362]
ENSACAT00000008992	TSC2	Tuberous Sclerosis 2 [Source:Hgnc Symbol;Acc:12363]
ENSACAT00000013230	PRKAB2	Protein Kinase Amp-Activated Non-Catalytic Subunit Beta 2 [Source:Hgnc Symbol;Acc:Hgnc:9379]
ENSACAT00000006834	PRKAA2	Protein Kinase Amp-Activated Catalytic Subunit Alpha 2 [Source:Hgnc Symbol;Acc:Hgnc:9377]
ENSACAT00000002435	PRKAG2	Protein Kinase Amp-Activated Non-Catalytic Subunit Gamma 2 [Source:Hgnc Symbol;Acc:Hgnc:9386]
ENSACAT00000010286	PRKAA1	Protein Kinase Amp-Activated Catalytic Subunit Alpha 1 [Source:Hgnc Symbol;Acc:Hgnc:9376]
ENSACAT00000012952	PRKAG3	Protein Kinase Amp-Activated Non-Catalytic Subunit Gamma 3 [Source:Ncbi Gene;Acc:100564629]
ENSACAT00000008189	PRKAG1	Protein Kinase Amp-Activated Non-Catalytic Subunit Gamma 1 [Source:Hgnc Symbol;Acc:Hgnc:9385]
ENSACAT00000003404	PRKAB1	Protein Kinase Amp-Activated Non-Catalytic Subunit Beta 1 [Source:Hgnc Symbol;Acc:Hgnc:9378]
ENSACAT00000000480	MTOR	Mechanistic Target Of Rapamycin (Serine/Threonine Kinase) [Source:Hgnc Symbol;Acc:3942]
ENSACAT00000015594	RPS6KA2	Ribosomal Protein S6 Kinase A2 [Source:Hgnc Symbol;Acc:Hgnc:10431]
ENSACAT00000006193	RPS6KC1	Ribosomal Protein S6 Kinase C1 [Source:Hgnc Symbol;Acc:Hgnc:10439]
ENSACAT00000008356	RPS6KB2	Ribosomal Protein S6 Kinase B2 [Source:Hgnc Symbol;Acc:Hgnc:10437]
ENSACAT00000012470	STRADA	Ste20-Related Kinase Adaptor Alpha [Source:Hgnc Symbol;Acc:Hgnc:30172]
ENSACAT00000001329	STRADB	Ste20-Related Kinase Adaptor Beta [Source:Hgnc Symbol;Acc:Hgnc:13205]
ENSACAT00000005087	RAG1	Recombination Activating 1 [Source:Hgnc Symbol;Acc:Hgnc:9831]
ENSACAT00000005084	RAG2	Recombination Activating 2 [Source:Hgnc Symbol;Acc:Hgnc:9832]

ENSACAT00000011317	BRAF	B-Raf Proto-Oncogene, Serine/Threonine Kinase [Source:Hgnc Symbol;Acc:Hgnc:1097]
ENSACAT00000011021	HIF1AN	Hypoxia Inducible Factor 1 Subunit Alpha Inhibitor [Source:Hgnc Symbol;Acc:Hgnc:17113]
ENSACAT00000005963	VEGFC	Vascular Endothelial Growth Factor C [Source:Hgnc Symbol;Acc:Hgnc:12682]
ENSACAT00000001649	VEGFA	Vascular Endothelial Growth Factor A [Source:Hgnc Symbol;Acc:Hgnc:12680]
ENSACAT000000012033	EIF4B	Eukaryotic Translation Initiation Factor 4B [Source:Hgnc Symbol;Acc:Hgnc:3285]

Table 2.2 A priori growth genes in the growth hormone/insulin-like factor 1 pathway. Gene IDs ending in “.1” and “.2” reflect the 201 splice variant and 202 splice variant of the gene, respectively.

Ensembl transcript ID	Gene ID	Ensembl description
ENSACAT00000010700	GHR	Growth Hormone Receptor [Source:Hgnc Symbol;Acc:4263]
ENSACAT00000006111	GHRRH	Growth Hormone Releasing Hormone Receptor [Source:Hgnc Symbol;Acc:4266]
ENSACAT00000016563	IGF1	Insulin-Like Growth Factor 1 (Somatomedin C) [Source:Hgnc Symbol;Acc:5464]
ENSACAT00000008062	IGFBP1	Insulin-Like Growth Factor Binding Protein 1 [Source:Hgnc Symbol;Acc:5469]
ENSACAT00000004558	IGFBP2	Insulin-Like Growth Factor Binding Protein 2, 36Kda [Source:Hgnc Symbol;Acc:5471]
ENSACAT00000008083	IGFBP3	Insulin-Like Growth Factor Binding Protein 3 [Source:Hgnc Symbol;Acc:5472]
ENSACAT00000016203	IGFBP4	Insulin-Like Growth Factor Binding Protein 4 [Source:Hgnc Symbol;Acc:5473]
ENSACAT00000000083	IGFBP5	Insulin-Like Growth Factor Binding Protein 5 [Source:Hgnc Symbol;Acc:5474]
ENSACAT00000029049	IGFBP6	Insulin-Like Growth Factor Binding Protein 6 [Source:Hgnc Symbol;Acc:5475]
ENSACAT00000002051	IGFBP7	Insulin-Like Growth Factor Binding Protein 7 [Source:Hgnc Symbol;Acc:5476]
ENSACAT00000029347	IGF1R.1	Insulin-Like Growth Factor 1 Receptor [Source:Hgnc Symbol;Acc:5465]
ENSACAT00000008235	IGF1R.2	Insulin-Like Growth Factor 1 Receptor [Source:Hgnc Symbol;Acc:5465]
ENSACAT00000009701	IGF2	Insulin-Like Growth Factor 2 (Somatomedin A) [Source:Hgnc Symbol;Acc:5466]
ENSACAT00000006271	IGF2BP1	Insulin-Like Growth Factor 2 Mrna Binding Protein 1 [Source:Hgnc Symbol;Acc:28866]
ENSACAT00000008070	IGF2BP2	Insulin-Like Growth Factor 2 Mrna Binding Protein 2 [Source:Hgnc Symbol;Acc:28867]
ENSACAT00000013612	IGF2BP3	Insulin-Like Growth Factor 2 Mrna Binding Protein 3 [Source:Hgnc Symbol;Acc:28868]

Table 2.3 A priori growth genes in the insulin-signaling pathway. Gene IDs ending in “.1” and “.2” reflect the 201 splice variant and 202 splice variant of the gene, respectively.

Ensembl ID	Gene	Ensembl description
ENSACAT00000011634	AKT1	Akt Serine/Threonine Kinase 1 [Source:Hgnc Symbol;Acc:Hgnc:391]
ENSACAT00000002209	Cbl	Cbl Proto-Oncogene [Source:Hgnc Symbol;Acc:Hgnc:1541]
ENSACAT00000004315	CDKN1B	Cyclin-Dependent Kinase Inhibitor 1B (P27, Kip1) [Source:Hgnc Symbol;Acc:1785]
ENSACAT00000029358	EIF4EBP1	Eukaryotic Translation Initiation Factor 4E Binding Protein 1 [Source:Hgnc Symbol;Acc:3288]
ENSACAT00000014236	EIF4E	Eukaryotic Translation Initiation Factor 4E [Source:Hgnc Symbol;Acc:3287]
ENSACAT00000017135	GYS2	Glycogen Synthase 2 [Source:Hgnc Symbol;Acc:Hgnc:4707]
ENSACAT00000004836	GYS1	Glycogen Synthase 1 [Source:Hgnc Symbol;Acc:Hgnc:4706]
ENSACAT00000004723	ELK1	Ets Transcription Factor [Source:Hgnc Symbol;Acc:Hgnc:3321]
ENSACAT00000009932	FASN	Fatty Acid Synthase [Source:Hgnc Symbol;Acc:Hgnc:3594]
ENSACAT00000013303	FBP1	Fructose-Bisphosphatase 1 [Source:Hgnc Symbol;Acc:Hgnc:3606]
ENSACAT00000008015	FLOT2	Flotillin 2 [Source:Ncbi Gene;Acc:100563055]
ENSACAT00000017291	FLOT1	Flotillin 1 [Source:Hgnc Symbol;Acc:Hgnc:3757]
ENSACAT00000001070	G6PC2	Glucose-6-Phosphatase Catalytic Subunit 2 [Source:Hgnc Symbol;Acc:Hgnc:28906]
ENSACAT00000007397	GNL3.1	G Protein Nucleolar 3 [Source:Hgnc Symbol;Acc:Hgnc:29931]
ENSACAT00000026449	GNL3.2	G Protein Nucleolar 3 [Source:Hgnc Symbol;Acc:Hgnc:29931]
ENSACAT00000006564	GRB2	Growth Factor Receptor-Bound Protein 2 [Source:Hgnc Symbol;Acc:4566]
ENSACAT00000016466	RAPGEF2	Rap Guanine Nucleotide Exchange Factor 2 [Source:Hgnc Symbol;Acc:Hgnc:16854]
ENSACAT00000013894	RAPGEF1	Rap Guanine Nucleotide Exchange Factor 1 [Source:Ncbi Gene;Acc:100558908]
ENSACAT00000029738	GSK3B.1	Glycogen Synthase Kinase 3 Beta [Source:Hgnc Symbol;Acc:Hgnc:4617] 201 Splice Variant
ENSACAT00000003712	GSK3B.2	Glycogen Synthase Kinase 3 Beta [Source:Hgnc Symbol;Acc:Hgnc:4617] 202 Splice Variant
ENSACAT00000007957	HSL	Hormone Sensitive Lipase
ENSACAT00000003820	IRS1	Insulin Receptor Substrate 1 [Source:Hgnc Symbol;Acc:6125]
ENSACAT00000012637	IRS4	Insulin Receptor Substrate 4 [Source:Hgnc Symbol;Acc:6128]
ENSACAT00000000408	MAP2K2	Mitogen-Activated Protein Kinase Kinase 2 [Source:Hgnc Symbol;Acc:6842]
ENSACAT00000001764	MAP2K3	Mitogen-Activated Protein Kinase Kinase 3 [Source:Hgnc Symbol;Acc:6843]
ENSACAT00000017532	MAP2K4	Mitogen-Activated Protein Kinase Kinase 4 [Source:Hgnc Symbol;Acc:6844]
ENSACAT00000010177	MAP2K5	Mitogen-Activated Protein Kinase Kinase 5 [Source:Hgnc Symbol;Acc:6845]
ENSACAT00000030866	MAP2K6	Mitogen-Activated Protein Kinase Kinase 6 [Source:Hgnc Symbol;Acc:6846]

ENSACAT00000009956	MAP2K7	Mitogen-Activated Protein Kinase Kinase 7 [Source:Hgnc Symbol;Acc:6847]
ENSACAT00000013773	MLST8	Mtor Associated Protein, Lst8 Homolog (S. Cerevisiae) [Source:Hgnc Symbol;Acc:24825]
ENSACAT00000010374	MYC	Myc Proto-Oncogene, Bhlh Transcription Factor [Source:Hgnc Symbol;Acc:Hgnc:7553]
ENSACAT00000013790	NR3C1	Nuclear Receptor Subfamily 3, Group C, Member 1 (Glucocorticoid Receptor) [Source:Hgnc Symbol;Acc:7978]
ENSACAT00000017591	PDE3A	Phosphodiesterase 3A [Source:Hgnc Symbol;Acc:Hgnc:8778]
ENSACAT00000003554	PDPK1	3-Phosphoinositide Dependent Protein Kinase-1 [Source:Hgnc Symbol;Acc:8816]
ENSACAT00000016391	PCK1	Phosphoenolpyruvate Carboxykinase 1 [Source:Hgnc Symbol;Acc:Hgnc:8724]
ENSACAT00000001275	PCK2	Phosphoenolpyruvate Carboxykinase 2, Mitochondrial [Source:Hgnc Symbol;Acc:Hgnc:8725]
ENSACAT00000004827	PPARA	Peroxisome Proliferator Activated Receptor Alpha [Source:Hgnc Symbol;Acc:Hgnc:9232]
ENSACAT00000011918	PHKA2	Phosphorylase Kinase Regulatory Subunit Alpha 2 [Source:Hgnc Symbol;Acc:Hgnc:8926]
ENSACAT00000014131	PHKB	Phosphorylase Kinase Regulatory Subunit Beta [Source:Hgnc Symbol;Acc:Hgnc:8927]
ENSACAT00000004979	PIK3CA	Phosphatidylinositol-4,5-Bisphosphate 3-Kinase, Catalytic Subunit Alpha [Source:Hgnc Symbol;Acc:8975]
ENSACAT00000017770	PIK3R5.1	Phosphoinositide-3-Kinase, Regulatory Subunit 5 [Source:Hgnc Symbol;Acc:30035]
ENSACAT00000029838	PIK3R5.2	Phosphoinositide-3-Kinase, Regulatory Subunit 5 [Source:Hgnc Symbol;Acc:30035]
ENSACAT00000006498	PRKCH	Protein Kinase C, Eta [Source:Hgnc Symbol;Acc:9403]
ENSACAT00000015152	PTEN	Phosphatase And Tensin Homolog [Source:Hgnc Symbol;Acc:9588]
ENSACAT00000014006	PYG	Glycogen Phosphorylase
ENSACAT00000012973	RAC1	Rac Family Small Gtpase 1 [Source:Hgnc Symbol;Acc:Hgnc:9801]
ENSACAT00000016135	RAC2	Rac Family Small Gtpase 2 [Source:Hgnc Symbol;Acc:Hgnc:9802]
ENSACAT00000029270	RAF1.1	Raf-1 Proto-Oncogene, Serine/Threonine Kinase [Source:Hgnc Symbol;Acc:Hgnc:9829]
ENSACAT00000013316	RAF1.2	Raf-1 Proto-Oncogene, Serine/Threonine Kinase [Source:Hgnc Symbol;Acc:Hgnc:9829]
ENSACAT00000004483	RASD1	Ras, Dexamethasone-Induced 1 [Source:Hgnc Symbol;Acc:15828]
ENSACAT00000002273	Rheb	Ras Homolog, Mtorc1 Binding [Source:Hgnc Symbol;Acc:Hgnc:10011]
ENSACAT00000014310	RHO	Rhodopsin [Source:Hgnc Symbol;Acc:10012]
ENSACAT00000010084	RICTOR	Rptor Independent Companion Of Mtor, Complex 2 [Source:Hgnc Symbol;Acc:28611]
ENSACAT00000013049	RPS6KB1	Ribosomal Protein S6 Kinase B1 [Source:Hgnc Symbol;Acc:Hgnc:10436]
ENSACAT00000016838	RPS6KL1	Ribosomal Protein S6 Kinase-Like 1 [Source:Hgnc Symbol;Acc:20222]
ENSACAT00000015640	RPTOR	Regulatory Associated Protein Of Mtor, Complex 1 [Source:Hgnc Symbol;Acc:30287]
ENSACAT00000014553	SHBG	Sex Hormone-Binding Globulin [Source:Hgnc Symbol;Acc:10839]
ENSACAT00000015879	SHC1	Shc Adaptor Protein 1 [Source:Hgnc Symbol;Acc:Hgnc:10840]
ENSACAT00000012679	SHC2	Shc Adaptor Protein 2 [Source:Ncbi Gene;Acc:100553545]
ENSACAT00000005997	SHC4	Shc Adaptor Protein 4 [Source:Hgnc Symbol;Acc:Hgnc:16743]

ENSACAT00000014599	SOCS1	Suppressor Of Cytokine Signaling 1 [Source:Hgnc Symbol;Acc:Hgnc:19383]
ENSACAT00000012617	SOCS2	Suppressor Of Cytokine Signaling 2 [Source:Hgnc Symbol;Acc:Hgnc:19382]
ENSACAT00000016743	SOCS3	Suppressor Of Cytokine Signaling 3 [Source:Hgnc Symbol;Acc:Hgnc:19391]
ENSACAT00000016330	SOCS4	Suppressor Of Cytokine Signaling 4 [Source:Hgnc Symbol;Acc:Hgnc:19392]
ENSACAT00000004217	SOCS5	Suppressor Of Cytokine Signaling 5 [Source:Hgnc Symbol;Acc:Hgnc:16852]
ENSACAT00000011543	SOCS6	Suppressor Of Cytokine Signaling 6 [Source:Hgnc Symbol;Acc:Hgnc:16833]
ENSACAT00000007427	SOCS7	Suppressor Of Cytokine Signaling 7 [Source:Hgnc Symbol;Acc:Hgnc:29846]
ENSACAT00000006394	SOS1	Sos Ras/Rac Guanine Nucleotide Exchange Factor 1 [Source:Hgnc Symbol;Acc:Hgnc:11187]
ENSACAT00000001643	SOS2	Sos Ras/Rho Guanine Nucleotide Exchange Factor 2 [Source:Hgnc Symbol;Acc:Hgnc:11188]
ENSACAT00000006298	STAT1	Signal Transducer And Activator Of Transcription 1, 91Kda [Source:Hgnc Symbol;Acc:11362]
ENSACAT00000025425	STAT2	Signal Transducer And Activator Of Transcription 2, 113Kda [Source:Hgnc Symbol;Acc:11363]
ENSACAT00000018021	STAT3	Signal Transducer And Activator Of Transcription 3 (Acute-Phase Response Factor) [Source:Hgnc Symbol;Acc:11364]
ENSACAT00000009792	STAT6	Signal Transducer And Activator Of Transcription 6, Interleukin-4 Induced [Source:Hgnc Symbol;Acc:11368]
ENSACAT00000014051	STK11	Serine/Threonine Kinase 11 [Source:Hgnc Symbol;Acc:11389]
ENSACAT00000001057	TGFB1	Transforming Growth Factor, Beta-Induced, 68Kda [Source:Hgnc Symbol;Acc:11771]
ENSACAT00000001108	TGFB2	Transforming Growth Factor, Beta 2 [Source:Hgnc Symbol;Acc:11768]
ENSACAT00000017101	TGFB3	Transforming Growth Factor, Beta 3 [Source:Hgnc Symbol;Acc:11769]
ENSACAT00000025616	TGFBP3L	Transforming Growth Factor, Beta Receptor Iii-Like [Source:Hgnc Symbol;Acc:44152]
ENSACAT00000009230	TGFBR1	Transforming Growth Factor, Beta Receptor 1 [Source:Hgnc Symbol;Acc:11772]
ENSACAT00000014316	TGFBR2	Transforming Growth Factor, Beta Receptor Ii (70/80Kda) [Source:Hgnc Symbol;Acc:11773]
ENSACAT00000001424	TGFBR3	Transforming Growth Factor, Beta Receptor Iii [Source:Hgnc Symbol;Acc:11774]
ENSACAT00000004260	TSC1	Tuberous Sclerosis 1 [Source:Hgnc Symbol;Acc:12362]
ENSACAT00000008992	TSC2	Tuberous Sclerosis 2 [Source:Hgnc Symbol;Acc:12363]
ENSACAT00000013230	PRKAB2	Protein Kinase Amp-Activated Non-Catalytic Subunit Beta 2 [Source:Hgnc Symbol;Acc:Hgnc:9379]
ENSACAT00000006834	PRKAA2	Protein Kinase Amp-Activated Catalytic Subunit Alpha 2 [Source:Hgnc Symbol;Acc:Hgnc:9377]
ENSACAT00000002435	PRKAG2	Protein Kinase Amp-Activated Non-Catalytic Subunit Gamma 2 [Source:Hgnc Symbol;Acc:Hgnc:9386]
ENSACAT00000010286	PRKAA1	Protein Kinase Amp-Activated Catalytic Subunit Alpha 1 [Source:Hgnc Symbol;Acc:Hgnc:9376]
ENSACAT00000012952	PRKAG3	Protein Kinase Amp-Activated Non-Catalytic Subunit Gamma 3 [Source:Ncbi Gene;Acc:100564629]
ENSACAT00000008189	PRKAG1	Protein Kinase Amp-Activated Non-Catalytic Subunit Gamma 1 [Source:Hgnc Symbol;Acc:Hgnc:9385]

ENSACAT00000003404 PRKAB1 Protein Kinase Amp-Activated Non-Catalytic Subunit Beta 1
[Source:Hgnc Symbol;Acc:Hgnc:9378]

Table 2.4 A priori growth genes in mechanistic target of rapamycin pathway. Gene IDs ending in “.1” and “.2” reflect the 201 splice variant and 202 splice variant of the gene, respectively.

Ensembl ID	Gene ID	Ensembl description
ENSACAT00000011634	AKT1	Akt Serine/Threonine Kinase 1 [Source:Hgnc Symbol;Acc:Hgnc:391]
ENSACAT00000016563	IGF1	Insulin-Like Growth Factor 1 (Somatomedin C) [Source:Hgnc Symbol;Acc:5464]
ENSACAT00000003820	IRS1	Insulin Receptor Substrate 1 [Source:Hgnc Symbol;Acc:6125]
ENSACAT00000000480	MTOR	Mechanistic Target Of Rapamycin (Serine/Threonine Kinase) [Source:Hgnc Symbol;Acc:3942]
ENSACAT00000004979	PIK3CA	Phosphatidylinositol-4,5-Bisphosphate 3-Kinase, Catalytic Subunit Alpha [Source:Hgnc Symbol;Acc:8975]
ENSACAT00000017770	PIK3R5.1	Phosphoinositide-3-Kinase, Regulatory Subunit 5 [Source:Hgnc Symbol;Acc:30035]
ENSACAT00000029838	PIK3R5.2	Phosphoinositide-3-Kinase, Regulatory Subunit 5 [Source:Hgnc Symbol;Acc:30035]
ENSACAT00000015152	PTEN	Phosphatase And Tensin Homolog [Source:Hgnc Symbol;Acc:9588]
ENSACAT00000010084	RICTOR	Rptor Independent Companion Of Mtor, Complex 2 [Source:Hgnc Symbol;Acc:28611]
ENSACAT00000015640	RPTOR	Regulatory Associated Protein Of Mtor, Complex 1 [Source:Hgnc Symbol;Acc:30287]
ENSACAT00000004260	TSC1	Tuberous Sclerosis 1 [Source:Hgnc Symbol;Acc:12362]
ENSACAT00000008992	TSC2	Tuberous Sclerosis 2 [Source:Hgnc Symbol;Acc:12363]
ENSACAT00000015594	RPS6KA2	Ribosomal Protein S6 Kinase A2 [Source:Hgnc Symbol;Acc:Hgnc:10431]
ENSACAT00000006193	RPS6KC1	Ribosomal Protein S6 Kinase C1 [Source:Hgnc Symbol;Acc:Hgnc:10439]
ENSACAT00000008356	RPS6KB2	Ribosomal Protein S6 Kinase B2 [Source:Hgnc Symbol;Acc:Hgnc:10437]
ENSACAT00000013230	PRKAB2	Protein Kinase Amp-Activated Non-Catalytic Subunit Beta 2 [Source:Hgnc Symbol;Acc:Hgnc:9379]
ENSACAT00000006834	PRKAA2	Protein Kinase Amp-Activated Catalytic Subunit Alpha 2 [Source:Hgnc Symbol;Acc:Hgnc:9377]
ENSACAT00000002435	PRKAG2	Protein Kinase Amp-Activated Non-Catalytic Subunit Gamma 2 [Source:Hgnc Symbol;Acc:Hgnc:9386]
ENSACAT00000010286	PRKAA1	Protein Kinase Amp-Activated Catalytic Subunit Alpha 1 [Source:Hgnc Symbol;Acc:Hgnc:9376]
ENSACAT00000012952	PRKAG3	Protein Kinase Amp-Activated Non-Catalytic Subunit Gamma 3 [Source:Ncbi Gene;Acc:100564629]
ENSACAT00000008189	PRKAG1	Protein Kinase Amp-Activated Non-Catalytic Subunit Gamma 1 [Source:Hgnc Symbol;Acc:Hgnc:9385]
ENSACAT00000003404	PRKAB1	Protein Kinase Amp-Activated Non-Catalytic Subunit Beta 1 [Source:Hgnc Symbol;Acc:Hgnc:9378]
ENSACAT00000014051	STK11	Serine/Threonine Kinase 11 [Source:Hgnc Symbol;Acc:Hgnc:11389]
ENSACAT00000012470	STRADA	Ste20-Related Kinase Adaptor Alpha [Source:Hgnc Symbol;Acc:Hgnc:30172]
ENSACAT00000001329	STRADB	Ste20-Related Kinase Adaptor Beta [Source:Hgnc Symbol;Acc:Hgnc:13205]
ENSACAT00000005087	RAG1	Recombination Activating 1 [Source:Hgnc Symbol;Acc:Hgnc:9831]

ENSACAT00000005084	RAG2	Recombination Activating 2 [Source:Hgnc Symbol;Acc:Hgnc:9832]
ENSACAT00000011317	BRAF	B-Raf Proto-Oncogene, Serine/Threonine Kinase [Source:Hgnc Symbol;Acc:Hgnc:1097]
ENSACAT00000011021	HIF1AN	Hypoxia Inducible Factor 1 Subunit Alpha Inhibitor [Source:Hgnc Symbol;Acc:Hgnc:17113]
ENSACAT00000005963	VEGFC	Vascular Endothelial Growth Factor C [Source:Hgnc Symbol;Acc:Hgnc:12682]
ENSACAT00000001649	VEGFA	Vascular Endothelial Growth Factor A [Source:Hgnc Symbol;Acc:Hgnc:12680]
ENSACAT00000012033	EIF4B	Eukaryotic Translation Initiation Factor 4B [Source:Hgnc Symbol;Acc:Hgnc:3285]
ENSACAT00000029358	EIF4EBP1	Eukaryotic Translation Initiation Factor 4E Binding Protein 1 [Source:Hgnc Symbol;Acc:Hgnc:3288]
ENSACAT00000006498	PRKCH	Protein Kinase C, Eta [Source:Hgnc Symbol;Acc:9403]

Table 2.5 A priori-selected growth genes that exhibit sex-biased expression in the liver at one, four, eight, and twelve months of age. Negative log₂ fold change (log₂FC) indicates male-biased expression while positive indicates female-biased expression. Bold font indicates genes that experienced sex-biased expression across multiple age points. Within each age group, genes are sorted from most male-biased to most female-biased.

Age	Sex-bias	Gene	log ₂ FC	log ₂ CPM
4 months	<i>Male</i>	Insulin-like growth factor 1 (IGF1)	-3.26609	5.068586
		MTOR Associated Protein, LST8 Homolog (MLST8)	-1.44021	2.567336
		Insulin-like growth factor binding protein 5 (IGFBP5)	-1.32059	3.071516
		Insulin-like growth factor 2 (IGF2)	-1.09368	7.1934
	<i>Female</i>	TSC complex subunit 2 (TSC2)	0.582462	4.076259
		Insulin receptor substrate 1 (IRS1)	1.605095	4.679922
		SHC adaptor protein 4 (SHC4)	2.639907	1.325526
		Transforming growth factor beta 1 (TGFB1)	2.723285	6.311321
8 months	<i>Male</i>	Insulin-like growth factor 1 (IGF1)	-4.06143	5.068586
		SHC adaptor protein 4 (SHC4)	-3.41342	1.325526
		Insulin-like growth factor binding protein 5 (IGFBP5)	-2.49348	3.071516
		Insulin-like growth factor 2 (IGF2)	-2.11091	7.1934
		Insulin-like growth factor binding protein 2 (IGFBP2)	-1.73827	3.948268
		Insulin-like growth factor binding protein 4 (IGFBP4)	-1.47126	5.304117
		MTOR Associated Protein, LST8 Homolog (MLST8)	-1.32475	2.567336
		Eukaryotic translation initiation factor 4E binding protein 1 (EIF4EBP1)	-1.0943	6.694943
	<i>Female</i>	Insulin-like growth factor 2 mRNA binding protein 2 (IGF2BP2)	-0.80176	3.199163
		Transforming growth factor beta receptor 2 (TGFB2)	-0.56924	5.489862
		Flotillin 1 (FLOT1)	-0.55335	6.685024
		SOS Ras/Rac guanine nucleotide exchange factor 1 (SOS1)	-0.50361	4.844445
		Insulin-like growth factor 2 mRNA binding protein 3 (IGF2BP3)	0.560268	6.098526
		Signal transducer and activator of transcription 3 (STAT3)	0.641014	5.483781
		3-phosphoinositide dependent protein kinase 1 (PDPK1)	0.703481	5.291527
		Phosphorylase kinase regulatory subunit alpha 2 (PHKA2)	0.825086	5.702679
Transforming growth factor beta 1 (TGFB1)	3.530401	6.311321		
12 months	<i>Male</i>	Insulin-like growth factor 1 (IGF1)	-3.81765	5.068586
		Insulin-like growth factor 2 (IGF2)	-1.79678	7.1934
		Insulin-like growth factor binding protein 4 (IGFBP4)	-1.64652	5.304117
		Insulin-like growth factor binding protein 2 (IGFBP2)	-1.30289	3.948268
		Glycogen synthase 2 (GYS2)	-1.23066	4.886695

	Eukaryotic translation initiation factor 4E binding protein 1 (EIF4EBP1)	-1.22552	6.694943
	Transforming growth factor beta 2 (TGFB2)	-1.11422	2.970851
	SHC adaptor protein 2 (SHC2)	-1.02022	2.377493
	Peroxisome proliferator activated receptor alpha (PPARA)	-0.92378	4.404665
	Vascular endothelial growth factor C (VEGFC)	-0.77444	3.577911
	Fructose-bisphosphatase 1 (FBP1)	-0.72086	7.541905
	Ribosomal protein S6 kinase C1 (RPS6KC1)	-0.66652	5.81934
	Glycogen phosphorylase (PYG)	-0.6587	6.118753
	Insulin-like growth factor 2 mRNA binding protein 2 (IGF2BP2)	-0.57099	3.199163
	Mitogen-activated protein kinase kinase 3 (MAP2K3)	-0.5619	5.286363
	STE20-related kinase adaptor alpha (STRADA)	-0.50406	4.171097
	AKT serine/threonine kinase 1 (AKT1)	-0.37438	7.162062
<i>Female</i>	Insulin-like growth factor 2 mRNA binding protein 3 (IGF2BP3)	0.537954	6.098526
	Protein kinase AMP-activated non-catalytic subunit beta 1 (PRKAB1)	0.807365	2.107514 4
	Protein inhibitor of activated STAT 3 (STAT3)	0.886875	5.483781
	Protein kinase AMP-activated non-catalytic subunit beta 2 (PRKAB2)	0.902312	5.004255
	Glycogen synthase 1 (GYS1)	1.05015	6.797076
	Fatty acid synthase (FASN)	2.947725	8.495907
	Sex hormone-binding globulin (SHBG)	3.703496	3.502142
	Transforming growth factor beta 1 (TGFB1)	3.706043	6.311321

Table 2.6 A priori-selected growth genes that exhibit sex-biased expression in femoral muscle at ages one, four, eight, and twelve months. Negative \log_2 fold change (\log_2FC) indicates male-biased expression while positive indicates female-biased. Bold font indicates genes that experienced sex-biased expression across multiple ages. Within each age group, genes are sorted from most male-biased to most female-biased.

Age	Sex-bias	Gene name	\log_2FC	\log_2CPM
4 months	<i>Male</i>	Phosphoenolpyruvate carboxykinase 1 (PCK1)	-1.40236	4.456375
	<i>Female</i>	Protein kinase AMP-activated non-catalytic subunit gamma 3 (PRKAG3)	0.737703	5.866955
		Transforming growth factor beta receptor 3 (TGFB3)	1.267989	4.075512
		Cyclin dependent kinase inhibitor 1B (CDKN1B)	2.601503	7.172727
8 months	<i>Male</i>	Suppressor of cytokine signaling 2 (SOCS2)	-2.95466	2.762381
		Insulin-like growth factor 1 (IGF1)	-2.06985	5.068586
		Insulin-like growth factor binding protein 2 (IGFBP2)	-1.45219	3.948268
	<i>Female</i>	TSC complex subunit 2 (TSC2)	0.72961	4.076259
		Protein kinase AMP-activated non-catalytic subunit gamma 3 (PRKAG3)	0.762862	5.866955
		Protein kinase AMP-activated non-catalytic subunit beta 1 (PRKAB1)	0.834485	2.107514
		Ribosomal protein S6 kinase B2 (RPS6KB2)	0.92198	2.720488
		Transforming growth factor beta receptor 3 like (TGFB3L)	0.995106	2.685145
		Eukaryotic translation initiation factor 4E binding protein 1 (EIF4EBP1)	1.194363	6.694943
12 months	<i>Male</i>	Cyclin dependent kinase inhibitor 1B (CDKN1B)	-2.7931	7.172727
		Eukaryotic translation initiation factor 4E binding protein 1 (EIF4EBP1)	-1.86076	6.694943
		Insulin receptor substrate 4 (IRS4)	-1.14339	4.88699
		SOS Ras/Rac guanine nucleotide exchange factor 1 (SOS1)	-0.69663	4.844445
		Ribosomal protein S6 kinase B1 (RPS6KB1)	-0.57022	3.665018
	<i>Female</i>	Eukaryotic translation initiation factor 4E (EIF4E)	0.458095	6.099981
		Mitogen-activated protein kinase kinase 6 (MAP2K6)	0.486653	5.867802
		Phosphoenolpyruvate carboxykinase 2, mitochondrial (PCK2)	0.662378	9.479602
		Phosphodiesterase 3A (PDE3A)	1.050874	2.750514
		Transforming growth factor beta 2 (TGFB2)	1.072561	2.970851
		Insulin-like growth factor binding protein 4 (IGFBP4)	1.082546	5.304117
		Insulin-like growth factor binding protein 7 (IGFBP7)	1.251951	3.201967
		Glucose-6-phosphatase catalytic subunit 2 (G6PC2)	1.95452	0.695295
		Sex hormone binding globulin (SHBG)	4.853266	3.502142

Table 2.7 The results of general linear models testing for sex, age, and tissue effects on mean expression level of the growth hormone/insulin-like growth factor (GH/IGF), insulin, and mechanistic target of rapamycin (mTOR) growth networks within liver, femoral muscle, and brain of brown anoles. We performed three tests and utilized a Bonferroni-corrected alpha level of 0.01667 to assess significance. Factors with significant p-values are bolded.

Growth Network	Factor	Degrees of freedom	F-value	P-value
GH-IGF1	Sex	1,72	1.709022563	0.191310998
	Age	3,72	1.378532682	0.24762889
	Tissue	2,72	42.57839534	< 0.0001
	Sex:Age	3,72	0.369295381	0.775180239
	Sex:Tissue	2,72	1.135102212	0.321662986
	Age:Tissue	6,72	0.51634094	0.79632685
	Sex:Age:Tissue	6,72	0.141520743	0.990665279
	Residuals	72		
Insulin	Sex	1,72	0.060586276	0.805577558
	Age	3,72	1.243771517	0.292047657
	Tissue	2,72	40.09893007	< 0.0001
	Sex:Age	3,72	0.131025711	0.941666011
	Sex:Tissue	2,72	0.044832051	0.956158277
	Age:Tissue	6,72	1.272038271	0.266432665
	Sex:Age:Tissue	6,72	0.034718432	0.999825685
	Residuals	72		
mTOR	Sex	1,72	1.624251024	0.202591457
	Age	3,72	0.938977373	0.420849429
	Tissue	2,72	25.28729728	< 0.0001
	Sex:Age	3,72	0.458433299	0.711353383
	Sex:Tissue	2,72	1.004560267	0.366319662
	Age:Tissue	6,72	0.263583759	0.953856164
	Sex:Age:Tissue	6,72	0.131756156	0.992314701
	Residuals	72		

Table 2.8 The results of general linear models testing for sex and age effects on mean expression level of target growth genes within liver, femoral muscle, and brain of brown anoles. We performed 15 tests and utilized a Bonferroni-corrected alpha level of 0.0033 to assess significance. Significant p-values are bolded.

Gene	Factor	Degrees of freedom	F-value	P-value
IGF1	Sex	1,72	66.80991	< 0.0001
	Age	3,72	0.431348	0.731177
	Tissue	2,72	85.17288	< 0.0001
	Sex:Age	3,72	1.570839	0.20388
	Sex:Tissue	2,72	62.22524	< 0.0001
	Age:Tissue	6,72	0.800266	0.572909
	Sex:Age:Tissue	6,72	1.655884	0.144427
	Residuals	72		
IGF2	Sex	1,72	33.24968	< 0.0001
	Age	3,72	6.04856	0.000988
	Tissue	2,72	112.1735	< 0.0001
	Sex:Age	3,72	2.605883	0.05827
	Sex:Tissue	2,72	33.11659	< 0.0001
	Age:Tissue	6,72	6.078545	< 0.0001
	Sex:Age:Tissue	6,72	2.949206	0.01514
	Residuals	72		
GHR	Sex	1,72	0.026388	0.87141
	Age	3,72	14.69438	< 0.0001
	Tissue	2,72	307.1242	< 0.0001
	Sex:Age	3,72	2.565761	0.061183
	Sex:Tissue	2,72	1.600401	0.208911
	Age:Tissue	6,72	4.893104	< 0.0001
	Sex:Age:Tissue	6,72	0.97317	0.44969
	Residuals	72		
IGFBP1	Sex	1,72	0.581925	0.448051
	Age	3,72	0.349068	0.789923
	Tissue	2,72	87.48913	< 0.0001
	Sex:Age	3,72	0.989221	0.402837
	Sex:Tissue	2,72	0.290594	0.748692
	Age:Tissue	6,72	0.396578	0.878916
	Sex:Age:Tissue	6,72	0.975052	0.448445
	Residuals	72		
IGFBP2	Sex	1,72	68.85054	< 0.0001

	Age	3,72	5.561551	0.001727
	Tissue	2,72	347.0924	< 0.0001
	Sex:Age	3,72	1.303807	0.279835
	Sex:Tissue	2,72	58.23178	< 0.0001
	Age:Tissue	6,72	5.597962	< 0.0001
	Sex:Age:Tissue	6,72	1.261543	0.285967
	Residuals	72		
IGFBP3	Sex	1,72	1.310838	0.256035
	Age	3,72	0.251323	0.860144
	Tissue	2,72	28.30902	< 0.0001
	Sex:Age	3,72	0.385727	0.7636
	Sex:Tissue	2,72	1.409482	0.250928
	Age:Tissue	6,72	0.321237	0.923852
	Sex:Age:Tissue	6,72	0.351155	0.906999
	Residuals	72		
IGFBP4	Sex	1,72	56.97257	< 0.0001
	Age	3,72	9.670478	< 0.0001
	Tissue	2,72	261.5358	< 0.0001
	Sex:Age	3,72	4.284489	0.007708
	Sex:Tissue	2,72	59.02825	< 0.0001
	Age:Tissue	6,72	9.498694	< 0.0001
	Sex:Age:Tissue	6,72	4.999205	0.000248
	Residuals	72		
IGFBP5	Sex	1,72	13.11801	0.000541
	Age	3,72	4.818883	0.004099
	Tissue	2,72	388.3431	< 0.0001
	Sex:Age	3,72	2.344726	0.080045
	Sex:Tissue	2,72	7.598672	0.001014
	Age:Tissue	6,72	5.944202	< 0.0001
	Sex:Age:Tissue	6,72	2.313792	0.042419
	Residuals	72		
IGFBP6	Sex	1,72	0.109208	0.742008
	Age	3,72	0.149	0.93001
	Tissue	2,72	20.7183	< 0.0001
	Sex:Age	3,72	0.153907	0.92685
	Sex:Tissue	2,72	0.362619	0.697115
	Age:Tissue	6,72	0.46904	0.829084
	Sex:Age:Tissue	6,72	1.188918	0.321994
	Residuals	72		
IGFBP7	Sex	1,72	0.085435	0.770903
	Age	3,72	0.533129	0.661027
	Tissue	2,72	157.0725	< 0.0001

	Sex:Age	3,72	0.207693	0.89076
	Sex:Tissue	2,72	10.29629	0.000117
	Age:Tissue	6,72	1.29245	0.271666
	Sex:Age:Tissue	6,72	1.845839	0.102194
	Residuals	72		
IGF1R.1	Sex	1,72	1.245963	0.268036
	Age	3,72	2.603406	0.058446
	Tissue	2,72	32.76004	< 0.0001
	Sex:Age	3,72	1.373364	0.25781
	Sex:Tissue	2,72	0.219316	0.803602
	Age:Tissue	6,72	2.076334	0.066525
	Sex:Age:Tissue	6,72	0.507129	0.801027
	Residuals	72		
IGF1R.2	Sex	1,72	0.006295	0.936982
	Age	3,72	1.442279	0.237608
	Tissue	2,72	11.61282	< 0.0001
	Sex:Age	3,72	0.951515	0.420434
	Sex:Tissue	2,72	3.651515	0.03087
	Age:Tissue	6,72	1.622886	0.153231
	Sex:Age:Tissue	6,72	1.2796	0.277539
	Residuals	72		
IRS1	Sex	1,72	0.086976	0.768906
	Age	3,72	1.102839	0.353672
	Tissue	2,72	439.6721	< 0.0001
	Sex:Age	3,72	0.861962	0.464897
	Sex:Tissue	2,72	0.670339	0.514698
	Age:Tissue	6,72	0.983989	0.442558
	Sex:Age:Tissue	6,72	0.773228	0.593503
	Residuals	72		
IRS4	Sex	1,72	2.31104	0.132838
	Age	3,72	6.465274	0.000616
	Tissue	2,72	62.05655	< 0.0001
	Sex:Age	3,72	5.030416	0.003199
	Sex:Tissue	2,72	3.072526	0.052422
	Age:Tissue	6,72	5.383692	0.000122
	Sex:Age:Tissue	6,72	3.684442	0.003009
	Residuals	72		
MTOR	Sex	1,72	0.024247	0.876694
	Age	3,72	8.928516	< 0.0001
	Tissue	2,72	53.05153	< 0.0001
	Sex:Age	3,72	0.033843	0.991577
	Sex:Tissue	2,72	0.896263	0.412595

Age:Tissue	6,72	6.936055	< 0.0001
Sex:Age:Tissue	6,72	1.800405	0.111091
Residuals	72		

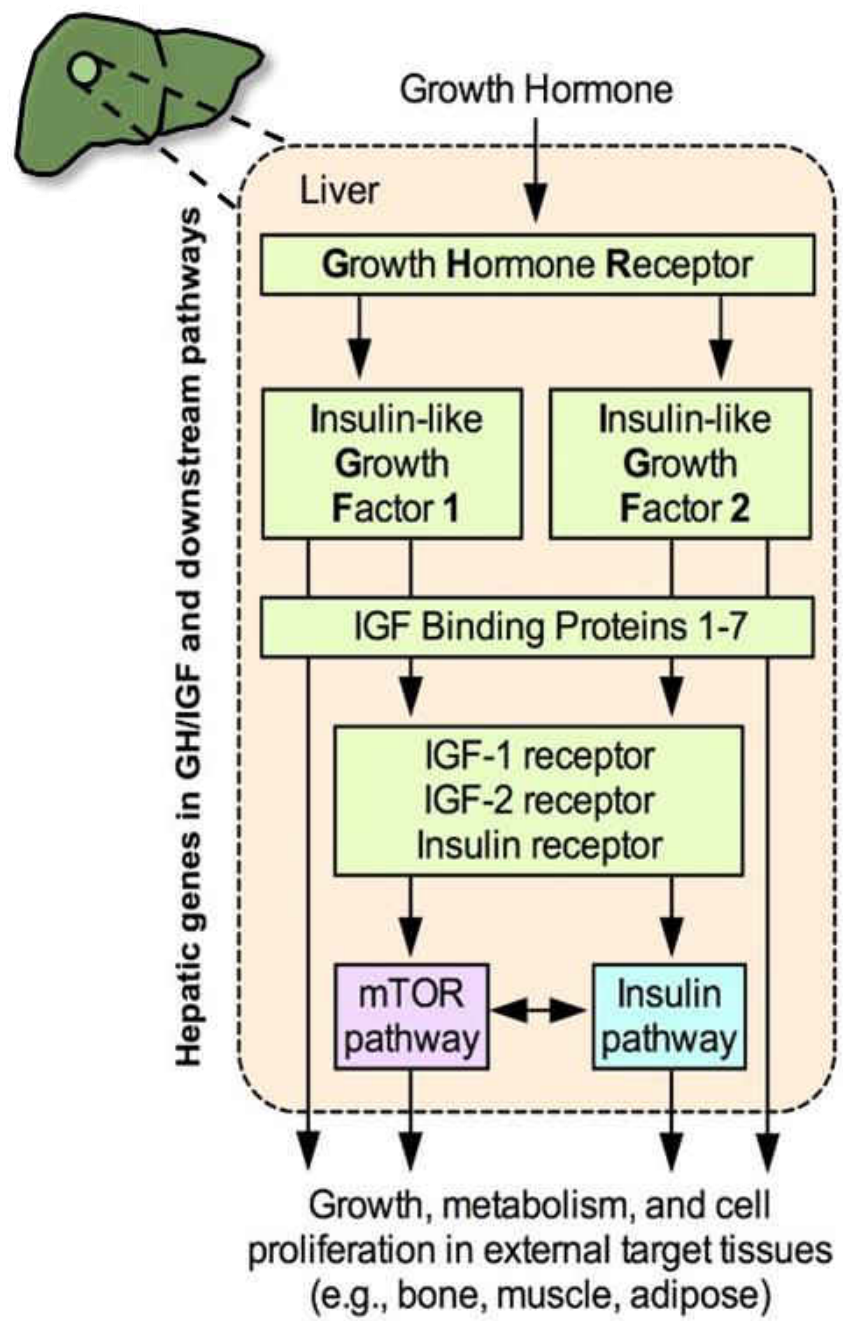


Figure 2.1 A flow chart of the growth hormone/insulin-like factor, insulin signaling, and mechanistic target of rapamycin growth regulatory signaling pathways interact to direct growth in vertebrates, specifically in the liver.

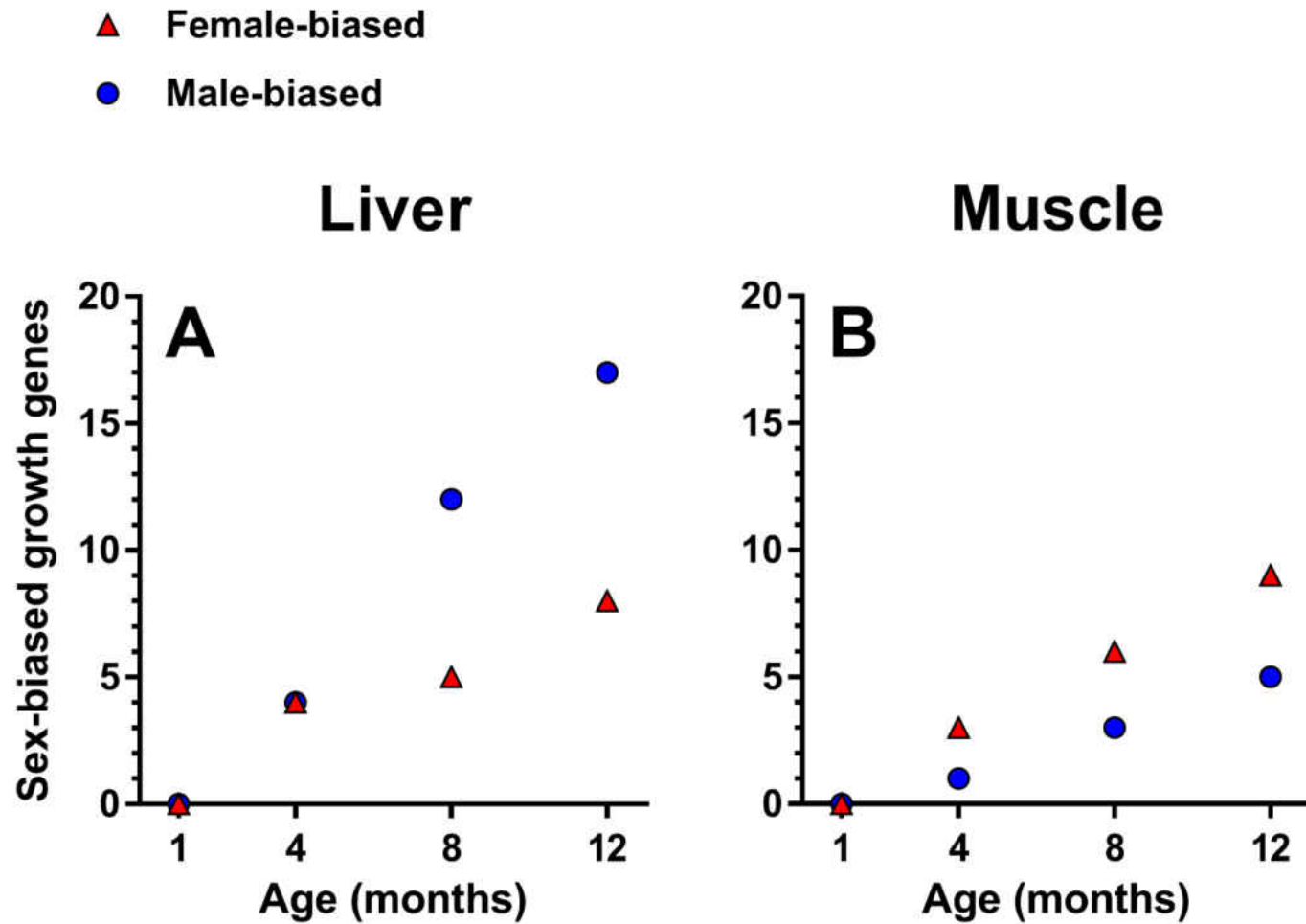


Figure 2.2 Male and female brown anoles increase and diverge in number of growth genes that exhibit sex-biased expression in the (A) liver and (B) femoral muscle across ontogeny.

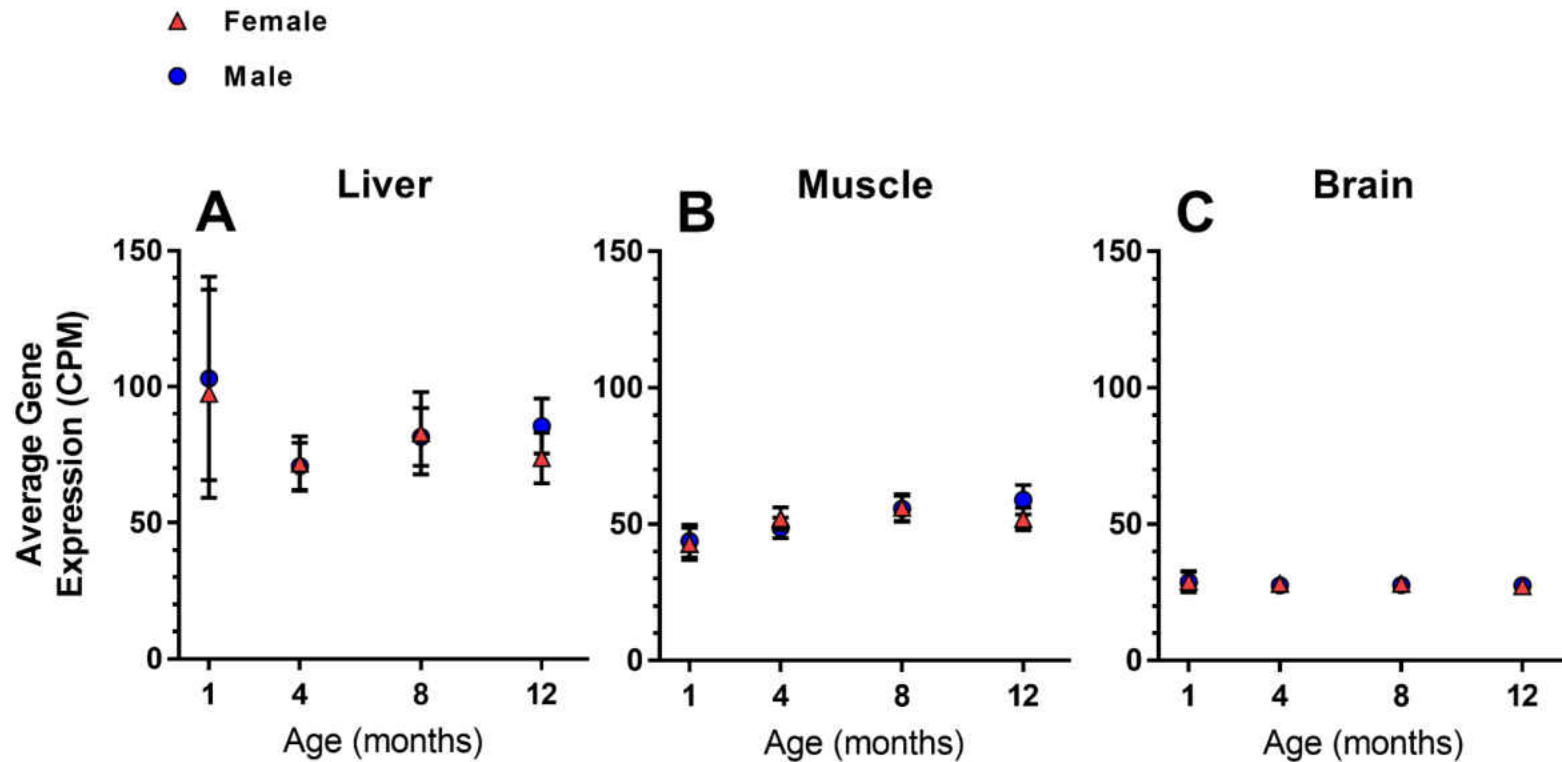


Figure 2.3 Male and female brown anoles express growth genes at similar levels across ontogeny within tissues. Data are the average expression, in counts per million (CPM), of all a priori selected growth genes plotted against age in the A) liver, B) femoral muscle, and C) brain. Data are expressed as means (symbols) with standard error bars (error bars shorter than the height of the symbol are not depicted).

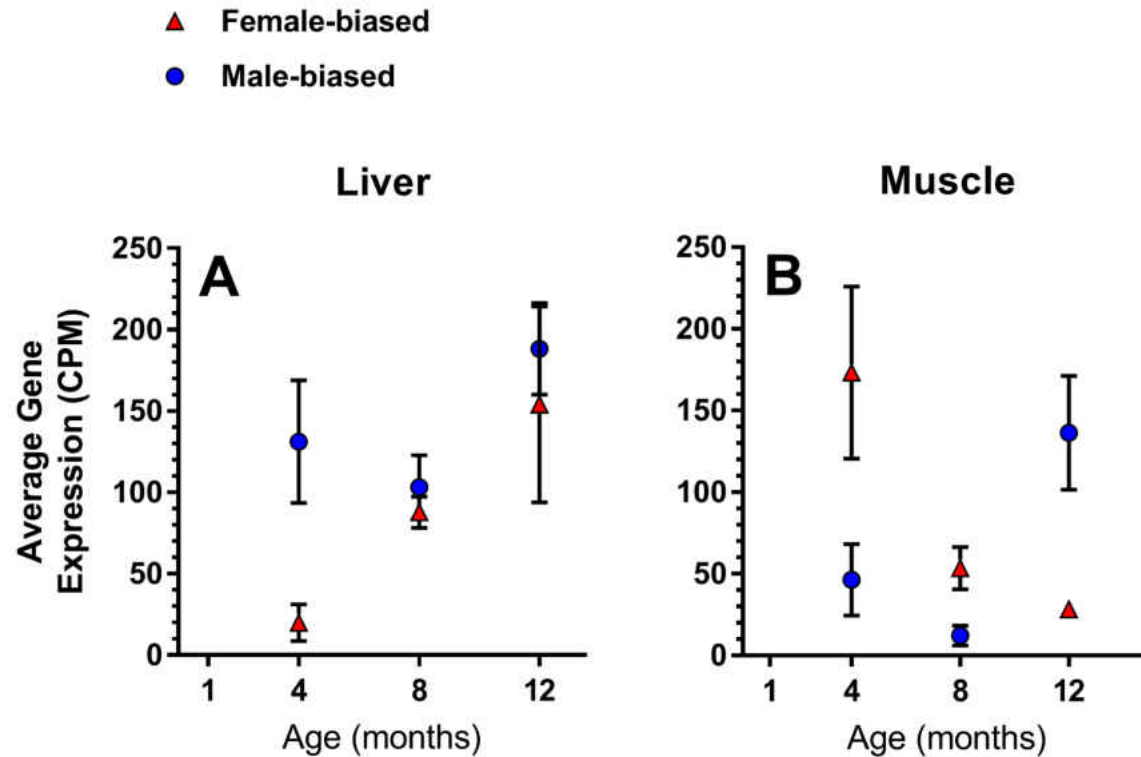


Figure 2.4 Male and female brown anoles diverge in growth gene sex-biased gene expression in the liver and muscle across ontogeny. Data are the average expression, in counts per million (CPM), of a priori selected growth genes that exhibit sex-biased expression plotted against age in the A) liver and B) femoral muscle. We did not find sex-biased growth gene expression in the brain for either sex at any age point. Data are expressed as means (symbols) with standard error bars (error bars shorter than the height of the symbol are not depicted).

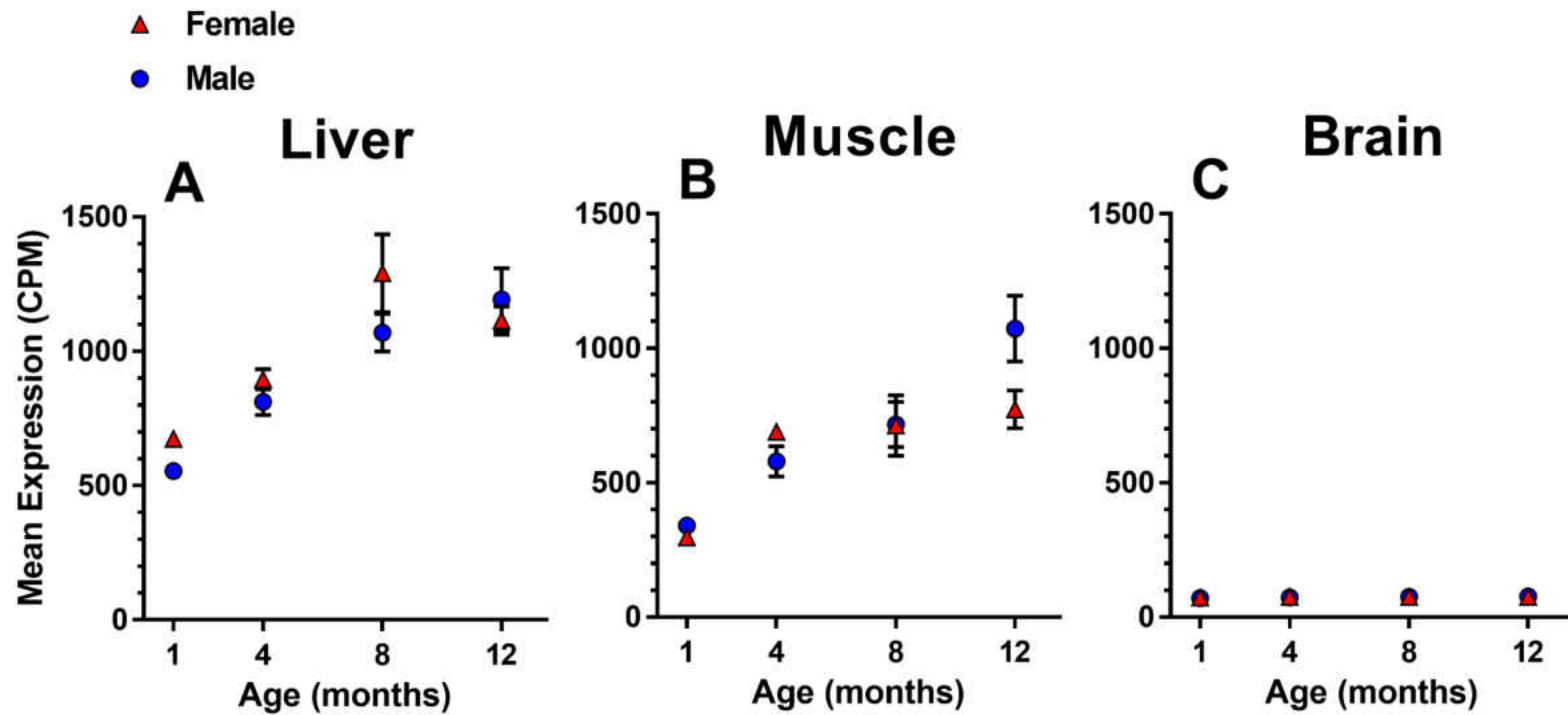


Figure 2.5 Expression of growth hormone receptor (GHR) increases in the liver and muscle for both male and female brown anoles across ontogeny. Data are the mean expression of growth hormone receptor, in counts per million (CPM), plotted against age in the liver, femoral muscle, and brain. Data are expressed as means (symbols) with standard error bars (error bars shorter than the height of the symbol are not depicted).

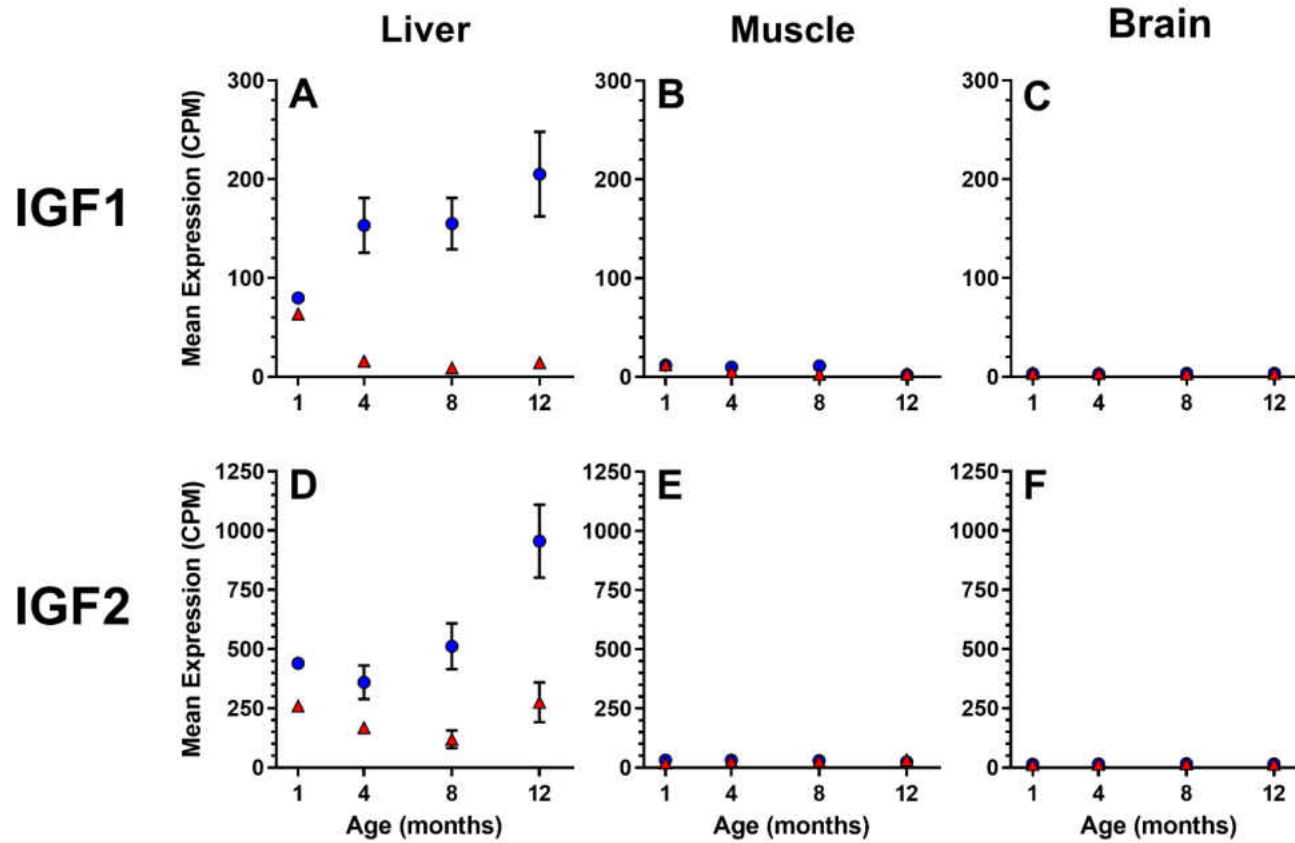


Figure 2.6 Male and female brown anoles diverge in expression of insulin-like growth factor 1 (IGF1) and insulin-like growth factor 2 (IGF2) in the liver across ontogeny. Data are the mean expression of IGF1 and IGF2, in counts per million (CPM), plotted against age in the liver, femoral muscle, and brain. Data are expressed as means (symbols) with standard error bars (error bars shorter than the height of the symbol are not depicted).

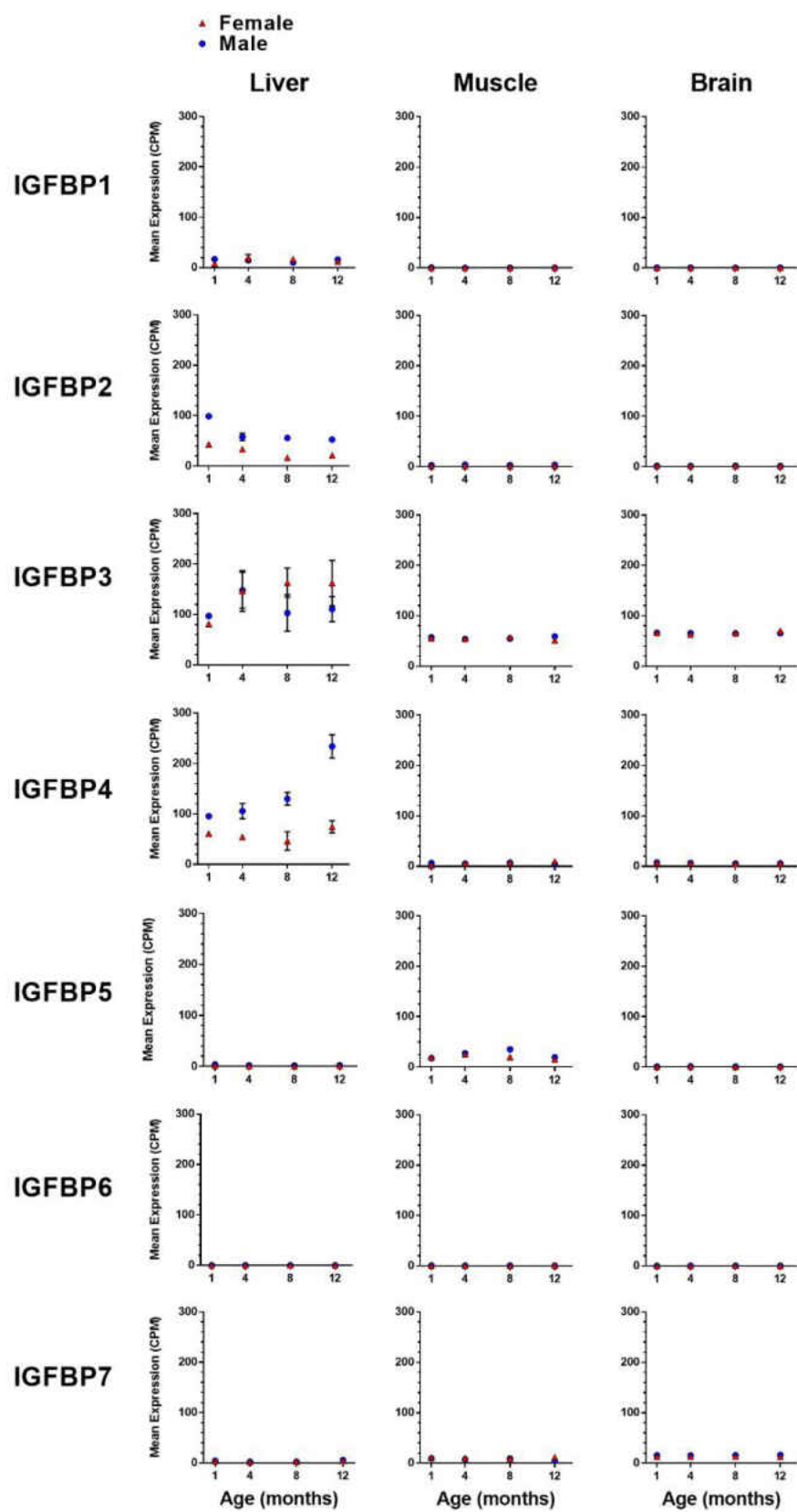


Figure 2.7 Male and female brown anole expression of the insulin growth factor binding proteins varies across tissues and ontogeny. Data are the mean expression of the IGFbps, in counts per million (CPM), in male and female brown anoles at one, four, eight, and twelve months in the liver, femoral muscle, and brain. Data are expressed as means (symbols) with standard error bars (error bars shorter than the height of the symbol are not depicted).

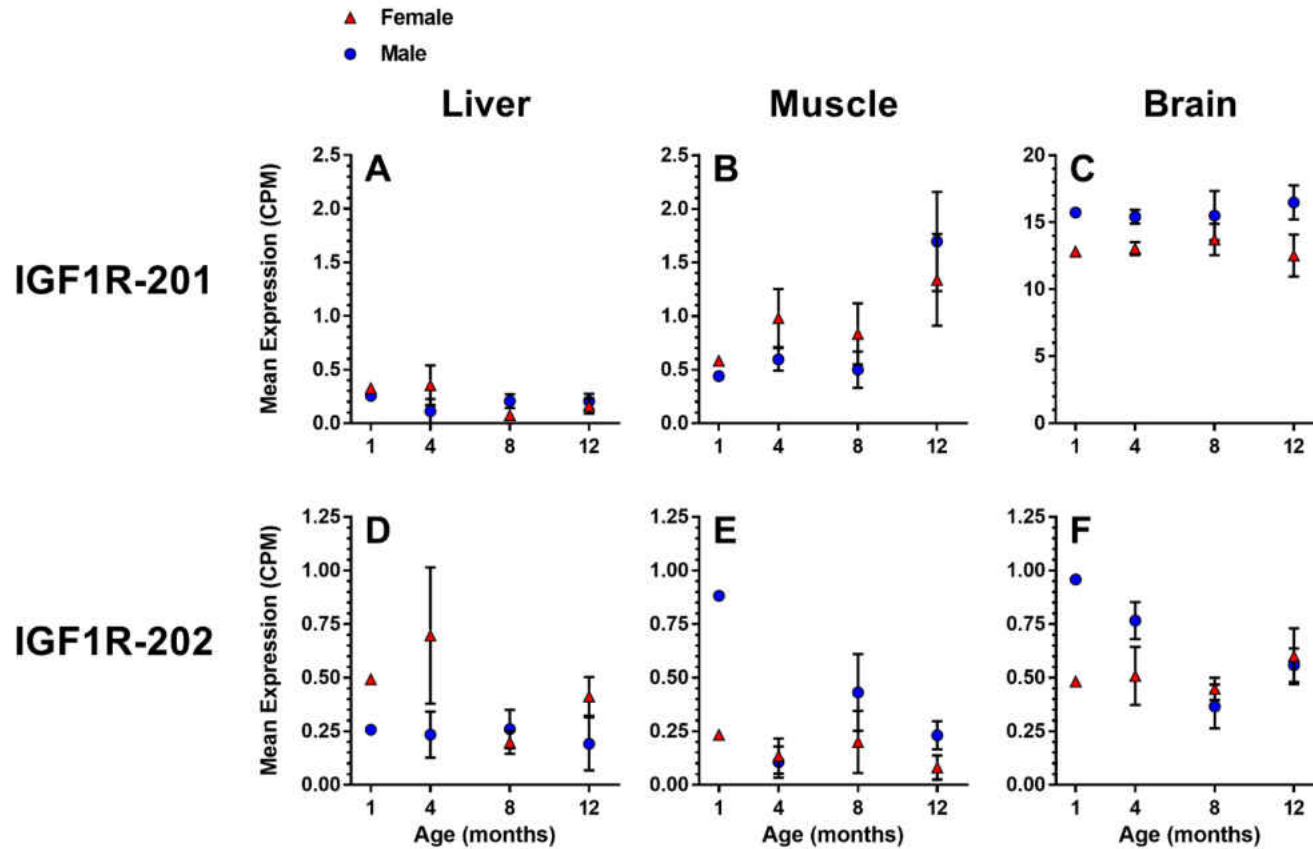


Figure 2.8 Male and female brown anoles diverge in their expression of the insulin-like growth factor 1 receptor across tissues and ontogeny. Data are the mean expression of insulin-like growth factor 1 receptor, expressed as the IGF1R-201 and IGF1R-202 splice variants, in counts per million (CPM) plotted against age in the liver, femoral muscle, and brain. Data are expressed as means (symbols) with standard error bars (error bars shorter than the height of the symbol are not depicted).

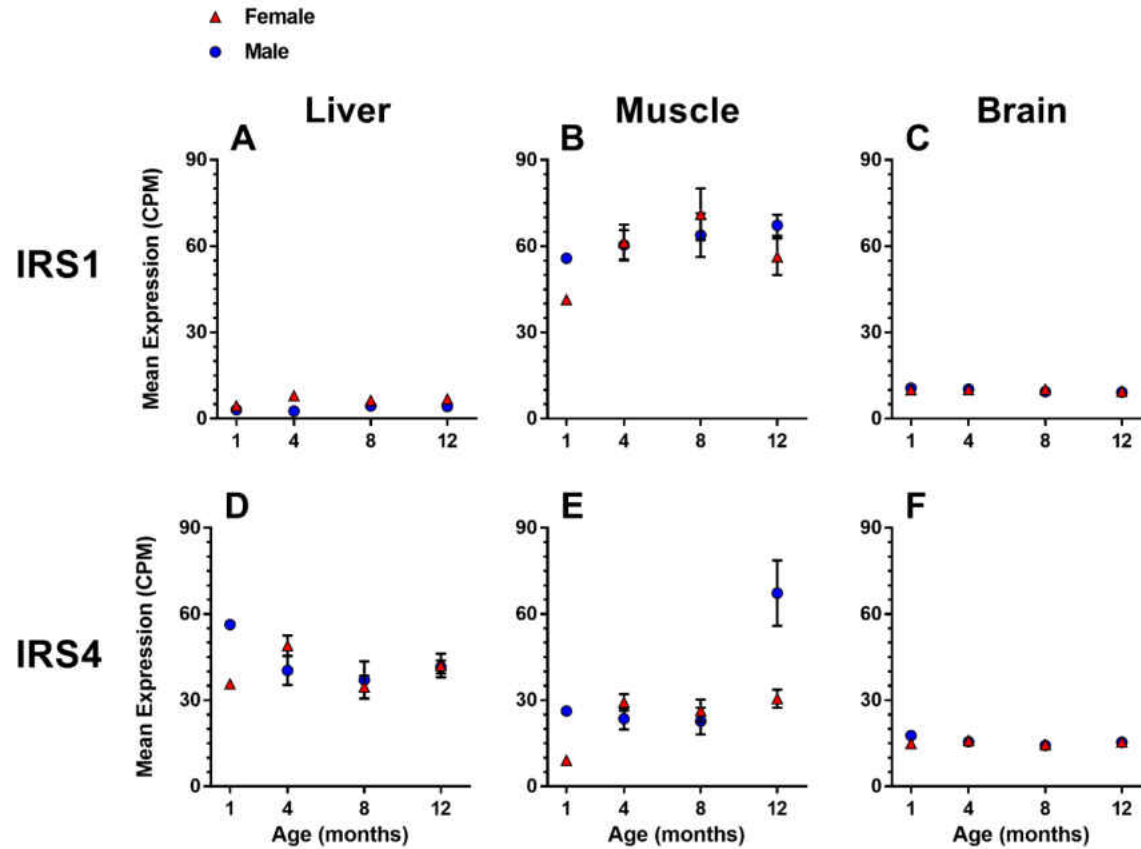


Figure 2.9 Male and female brown anoles diverge in their expression of insulin receptor substrate 1 (IRS1) and insulin receptor substrate 4 (IRS4) across tissues and ontogeny. Data are the mean expression of IRS1 and IRS4, in counts per million (CPM), plotted against age in the liver, femoral muscle, and brain. Data are expressed as means (symbols) with standard error bars (error bars shorter than the height of the symbol are not depicted).

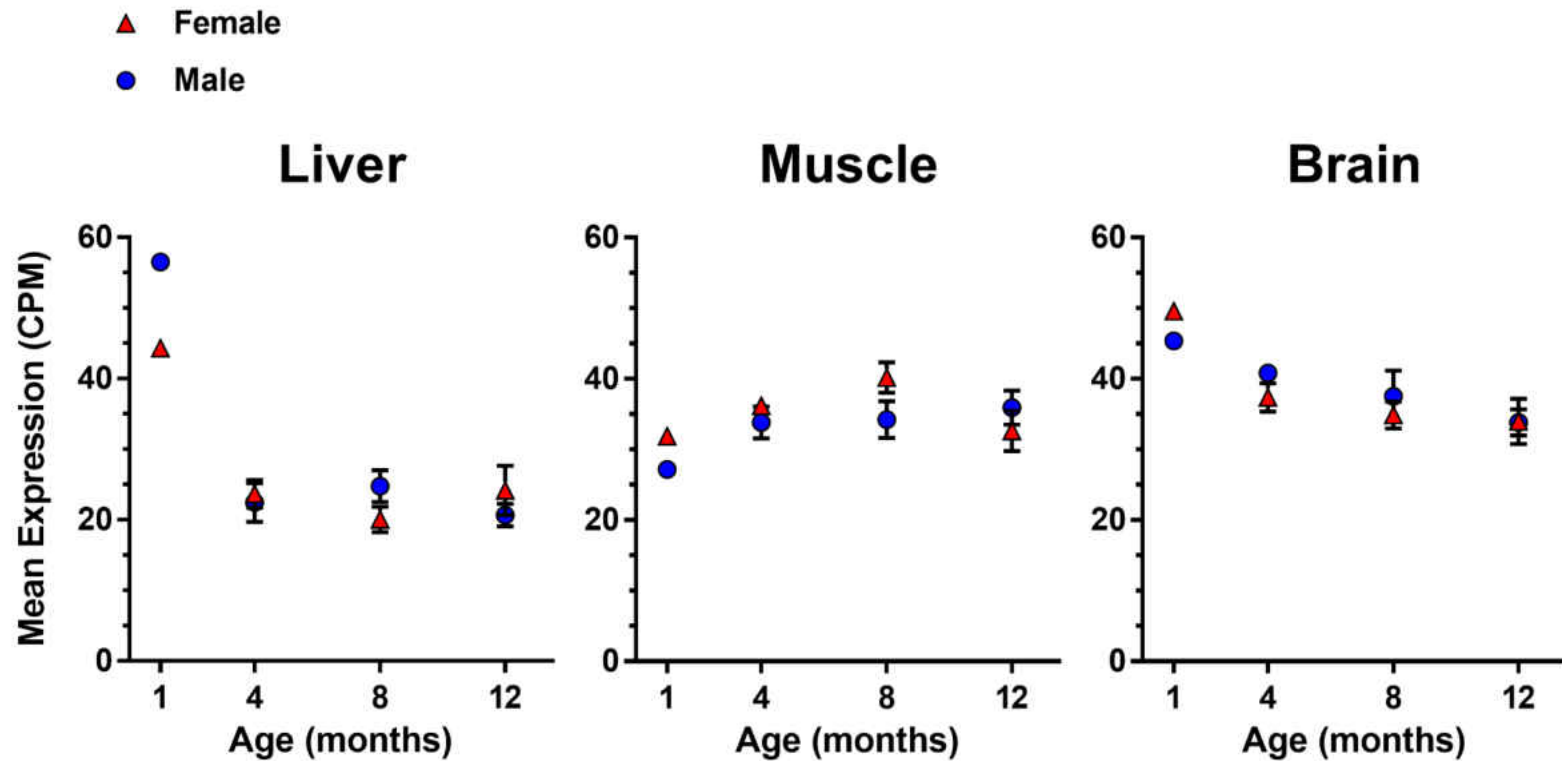


Figure 2.10 Male and female brown anoles express the mechanistic target of rapamycin (mTOR) at similar levels across tissues and ontogeny. Data are the mean expression of mTOR, in counts per million (CPM), plotted against age in the liver, femoral muscle, and brain. Data are expressed as means (symbols) with standard error bars (error bars shorter than the height of the symbol are not depicted).

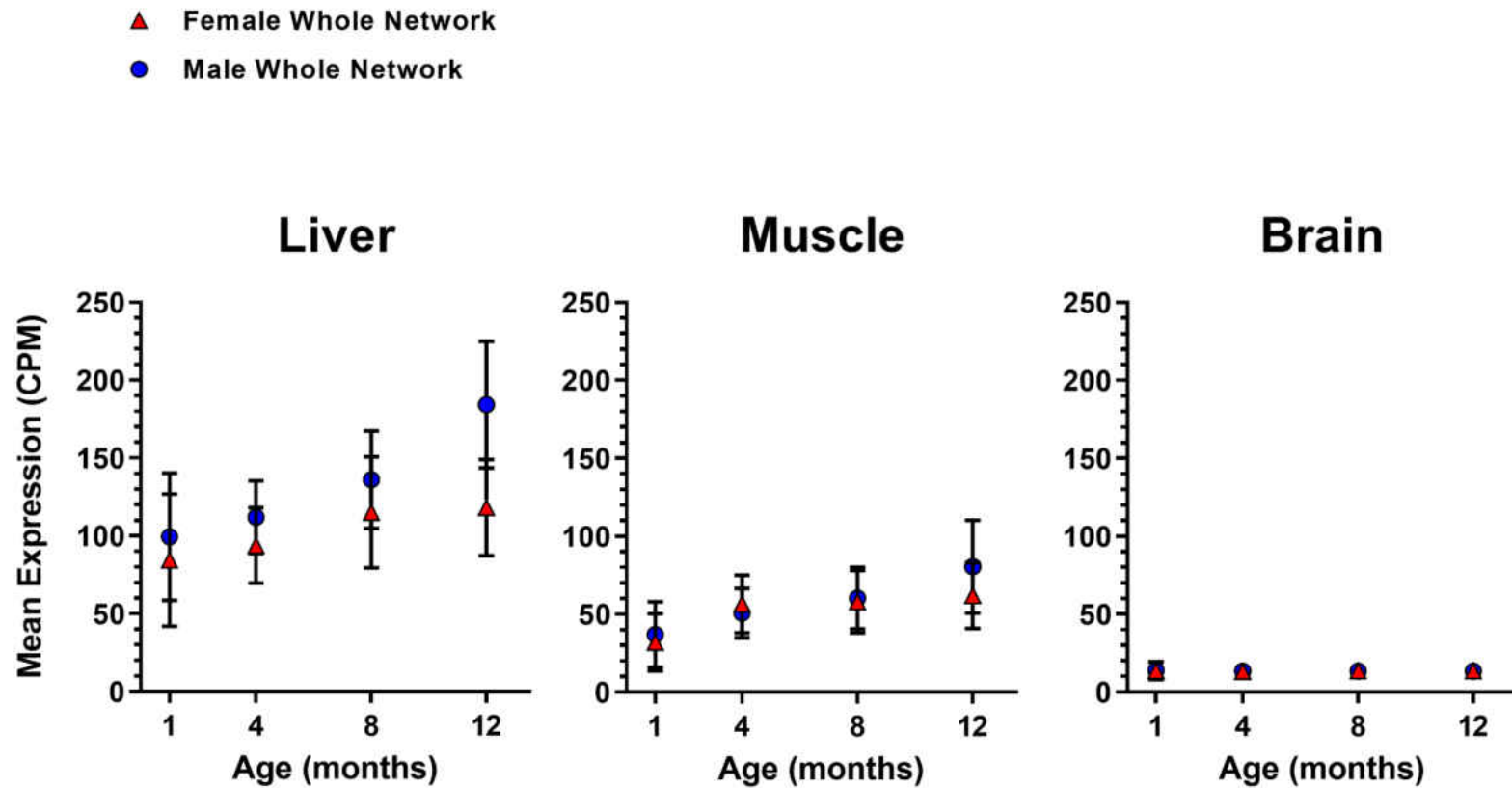


Figure 2.11 Male and female brown anoles have similar levels of expression of all growth genes in the growth hormone/insulin-like growth factor 1 signaling network within tissues across ontogeny. Data are the average expression, in counts per million (CPM), of all growth genes in the network plotted against age. Data are expressed as mean expression of genes in the network (symbols) with standard error bars (error bars shorter than the height of the symbol are not depicted).

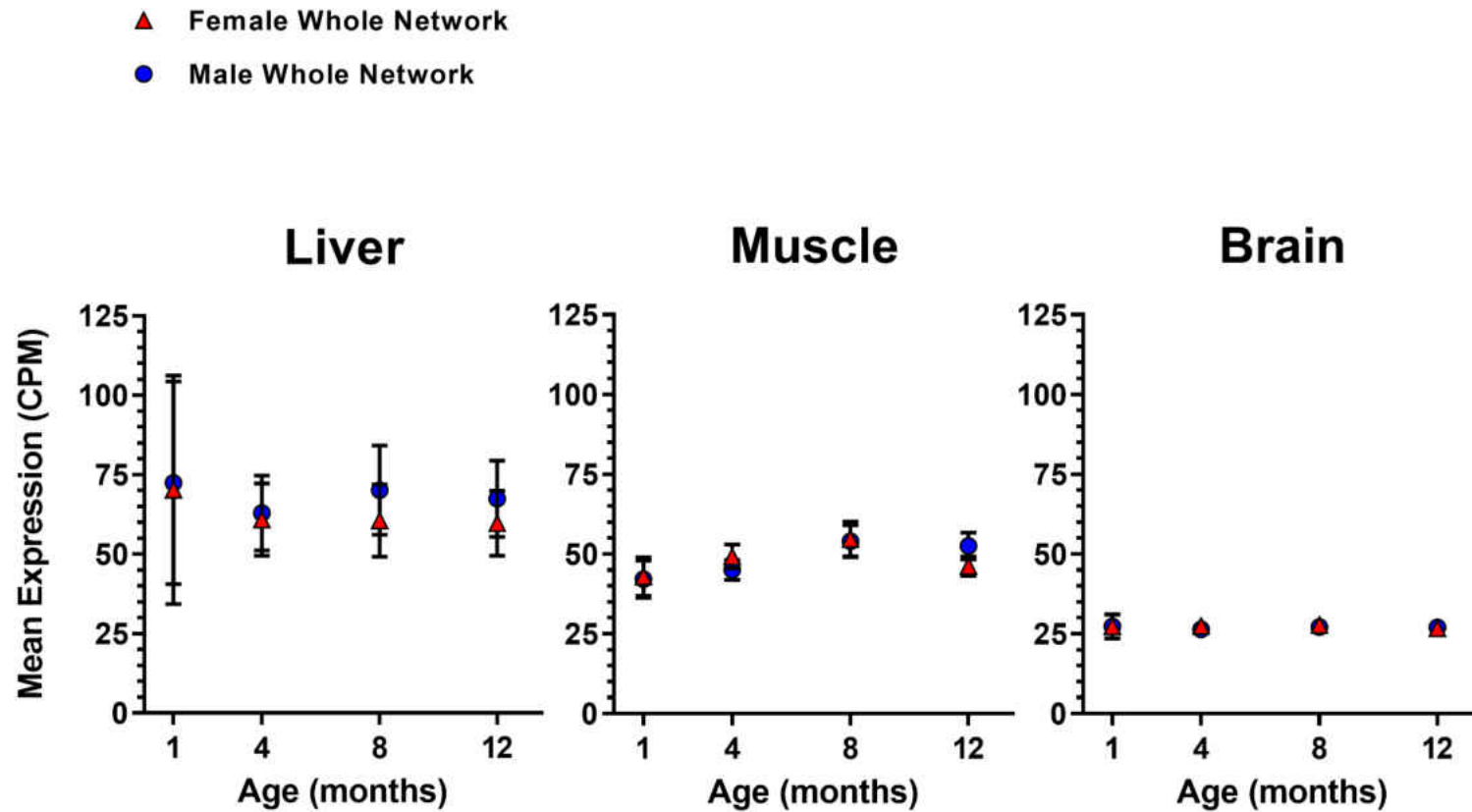


Figure 2.12 Male and female brown anoles have similar levels of expression of growth genes in the insulin-signaling network across tissues and ontogeny. Data are the average expression, in counts per million (CPM), of all growth genes in the insulin-signaling network plotted against age. Data are expressed as mean expression of genes in the network (symbols) with standard error bars (error bars shorter than the height of the symbol are not depicted).

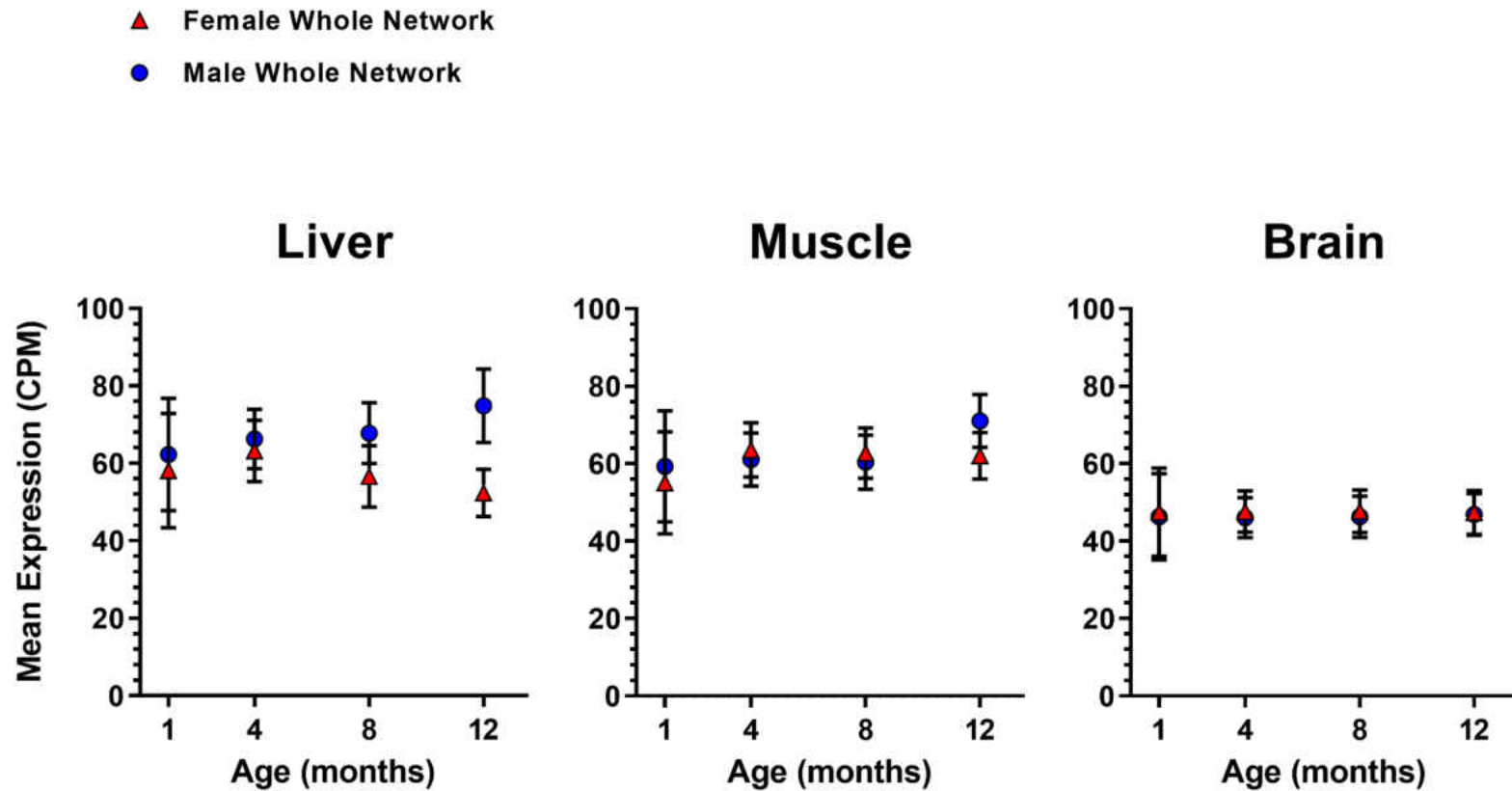


Figure 2.13 Male and female brown anoles have similar levels of expression of growth genes in the mechanistic target of rapamycin network across tissues and ontogeny. Data are the average expression, in counts per million (CPM), of all growth genes in the mechanistic target of rapamycin network plotted against age. Data are expressed as mean expression of genes in the network (symbols) with standard error bars (error bars shorter than the height of the symbol are not depicted).